

**DIFFERENTIAL EQUATIONS AND APPLICATIONS**

**STUDIES ON NONLINEAR DYNAMICS OF  
CERTAIN REACTION SYSTEMS**

**THESIS SUBMITTED FOR THE DEGREE OF  
DOCTOR OF PHILOSOPHY**

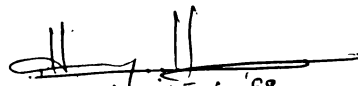
by  
**MERCY MANI P.**

**DEPARTMENT OF MATHEMATICS AND STATISTICS  
Cochin University of Science and Technology  
COCHIN - 682 022**

1988

## DECLARATION

This thesis contains no material which has been accepted for the award of any other Degree or Diploma in any University and, to the best of my knowledge and belief, it contains no material previously published by any other person, except due reference is made in the text of the thesis.

  
15.6.68.  
MERCY MANI P.

## CERTIFICATE

Certified that the work reported in the present thesis is based on the bona fide work done by Miss. Mercy Mani P, under my guidance in the Department of Mathematics and Statistics, Cochin University of Science and Technology and has not been included in any other thesis submitted previously for the award of any degree.

*M. Kaimal*

Dr. M. Ramachandra Kaimal  
(Former Lecturer,  
Dept. of Mathematics and  
Statistics,  
Cochin University of Science  
and Technology)  
Head, Dept. of Computer Science,  
University of Kerala,  
Trivandrum 695 034.

## ACKNOWLEDGEMENT

Words are few to express my heartfelt gratitude to my guide Dr.M.Ramachandra Kaimal, Head of the Department of Computer Science, University of Kerala, Trivandrum, for all help, guidance and encouragement given to me. It was an exhilarating experience to be guided by him.

I am deeply indebted to Prof. T. Thrivikraman, Head of the Department of Mathematics and Statistics, Cochin University of Science and Technology, for the keen interest, valuable advice and encouragement he has given during the course of this work.

I am grateful to Dr.N.Ramanujam who has lent me a hand to enter the research track at the initial stage of this work. My thanks also goes to the faculty members of the Department of Mathematics and Statistics, Cochin University of Science and Technology, for their kind hospitality in making me feel at home during the three year tenure of my research in the Department.

I feel obliged to all members of the faculty, especially to Prof. R. Pratap as well as to Prof. V.P. Narayanan Namboodiri, Prof. Babu Joseph of Department of Physics and Prof. K.L.Sebastian of Department of Applied Chemistry, Cochin University of Science and Technology, for the several valuable discussions I had with them.

I express my heartfelt thanks to Prof.A.K.Menon, Head of the Department of Computer Science, Cochin University of Science and Technology, for providing me with the computer facilities to carry out this research programme and to Prof. K.G. Nair, Head of the Department of Electronics, Cochin University of Science and Technology for the same.

I owe my gratitude to Prof.J. Pasupathy, Director, Centre for Theoretical Studies, I.I.Sc. , Bangalore, for helping me to use the computer in the Computer Centre, I.I.Sc Bangalore and also for the financial assistance given to me. The fruitful discussions I have had with Prof. P.L.Sachdev, Department of Applied Mathematics and Dr. N. Joshy, Centre for Ecological Studies, I.I.Sc. Bangalore, has inspired me a lot.

I am grateful to all the administrative and library staff of the Cochin University of Science and Technology, for their courtesy and help. I thank my colleagues and friends, especially Mr. A.K. Nandakumar, T.I.F.R as well as Miss. Sreekumary K.R., Miss. Rani Maria Thomas and Mr. Janardhan Pillai, I.I.Sc. for the great interest shown by them in my work.

I am grateful to Rev. Sr. Mary Savio, Principal, who has kindly helped me to continue my studies after joining the Department of Mathematics, B.C.M. College, Kottayam.

I wish to place on record my gratitude to the Cochin University of Science and Technology, for awarding me Junior Research Fellowship.

I am also thankful to Mr. Joseph Kuttikal for the excellent typing of this thesis.

My parents have been my great pillars of strength whose constant support has lead me to draw this work to an end. I also thank my brothers and sisters, who have offered their prayers for the grand success of my research work.

Above all, I praise and thank the Lord who has been an unfailing source of strength, comfort and inspiration to me throughout my work.

MERCY MANI P

Cochin 22 ॥  
June, '88 ॥

# C O N T E N T S

		Page
		..
CHAPTER 1	INTRODUCTION	.. 1
CHAPTER 2	METHODS OF NONLINEAR DYNAMICS	.. 18
2.1	Systems Involving Chemical Reactions	.. 18
2.2	Stability in Nonlinear Systems	.. 22
2.3	Limit Cycles	.. 33
2.4	Dependence of Steady State Solutions on a Parameter	.. 40
2.5	Bifurcation	.. 45
2.6	Numerical Methods	.. 56
CHAPTER 3	A MODEL FOR CHEMICAL REACTING SYSTEMS	.. 69
3.1	Introduction	.. 69
3.2	Chemistry of the B-Z Reaction	.. 70
3.3	Mathematical Modelling	.. 74
3.4	Two-Variable Oregonator Model	.. 77
3.5	Three-Variable Model	.. 91
3.6	Discussion	.. 98
CHAPTER 4	MODEL STUDIES ON A CUBIC AUTOCATALYTIC SYSTEM	.. 101
4.1	Introduction	.. 101
4.2	MNS Model	.. 103
4.3	A Modified Model	.. 111
4.4	Stationary States and Oscillations	.. 114
4.5	Numerical Results	.. 118
4.6	Discussion	.. 125
CHAPTER 5	CONCLUSION	.. 131
	BIBLIOGRAPHY	.. 136

# Chapter 1

## INTRODUCTION

Many phenomena that occur in nature are described by nonlinear dynamical systems. Mathematical models which describe these systems are usually formed by complicated systems of algebraic or differential equations [23, 56]. Such systems possess interesting properties such as oscillatory (periodic) solutions [45], travelling wave solutions [43, 79], spiral wave solutions [10, 31] and the like. These systems of equations very often include a number of characteristic parameters as well. The solution structures of these systems depend heavily on these parameters. If the values of some of these parameters change, the system may exhibit many new phenomena such as the birth of a family of limit cycles (oscillations) or new stationary states or chaotic structures etc.

The space-time structural organization of biological systems starting from the subcellular levels upto the level of ecological systems, behaviour of electrical net works[12] and complicated patterns produced by chemical reactions make good examples described by such nonlinear systems.



Periodic phenomena or oscillations are one of the fundamental characteristics observed in nonlinear dynamical systems. In biological, ecological, social, physical and chemical systems we find the oscillatory behaviour. Several mathematical models such as Lotka, Volterra, Brusselator [11], Oregonator [19] etc. are investigated to explain these periodicities. Most of these models are nonlinear and their analysis is based on the theory of nonlinear differential equations.

The chemical oscillators, whose mathematical properties have much in common with the physical and biological oscillators are less complicated, at least in modelling them. After introducing the concept of 'open system' the studies on oscillators began seriously. A brief discussion on the mathematical modelling of an open system is given below:

Consider a general reaction mixture containing  $n$  species  $\{X_i\}$ ,  $i = 1, 2, \dots, n$  in a volume  $v$ , which satisfies the local equilibrium conditions. The system is open to the flow of chemicals from outside which react with  $\{X_i\}$ ,  $i = 1, 2, \dots, n$  in the reaction volume. However, it may be assumed that the boundary conditions remain time independent and that the system is in mechanical equilibrium.

Under these conditions the instantaneous state will be described by the composition variables  $\{X_i\}$ ,  $i=1,2,\dots,n$  and by the internal energy density  $\rho e$ , where,

$$\rho = \sum_{i=1}^n X_i \quad (1.1)$$

and  $e$  is the specific energy per unit mass. These quantities satisfy the conservation equations,

$$\frac{\partial X_i}{\partial t} = v_i(X_i, T) - \nabla \cdot J_i^d \quad (1.2)$$

$$\frac{\partial(\rho e)}{\partial t} = -\nabla \cdot J^{th} + \mathcal{I} \cdot E \quad (i=1,2,\dots,n) \quad (1.3)$$

$J_i^d$  and  $J^{th}$  are respectively the diffusion and the heat flow vector and  $T$  is the temperature.  $v_i$ s describe the production of component  $i$  by the chemical reactions. These will be in general nonlinear functions of  $X_i$ s.  $\sum v_i \neq 0$ , characterises the open system.  $E$  is the electric field and  $\mathcal{I}$  the current density, which is given by

$$\mathcal{I} = \sum_{i=1}^n z_i J_i^d \quad (1.4)$$

with  $z_i$ , the charge per unit mass of  $i$ . It is assumed that  $i$  and  $E$  vary slowly enough to neglect.  $J_i^d$  and  $J^{th}$  can be expressed as follows,

$$J_i^d = -D_i X_i [ \nabla \mu_i(X,T) ] T - D_i^! \frac{\nabla T}{T^2} \quad (1.5)$$

$$J^{th} = -\lambda \nabla T - \sum_i D_i^! \frac{(\nabla \mu_i) T}{T} \quad (1.6)$$

assuming a diagonal diffusion coefficient matrix

$\{ D_i \delta_{ij}^{kr} \}$ ,  $\mu_i$ , the electrochemical potential of constituent  $i$ ,  $\lambda$  the thermal conductivity of the mixture, and  $D_i^!$  the thermal diffusion coefficient of  $i$ .

As (1.5) and (1.6) are introduced into (1.2) and (1.3), one obtains a closed system of nonlinear partial differential equations for  $\{ X_i \}$ ,  $i=1,2,\dots,n$  and  $T$ , provided one also uses the constitutive relation

$$e = e(X_i, T), \quad i = 1, 2, \dots, n \quad (1.7)$$

Their form is,

$$\frac{\partial X_i}{\partial t} = v_i(X_i, T) + \nabla \cdot [ D_i X_i (\nabla \mu_i) T + D_i^! \frac{\nabla T}{T^2} ] \quad (1.8)$$

$i = 1, 2, \dots, n.$

$$C \left( \frac{\partial T}{\partial t} \right) = \nabla \cdot \lambda \nabla T + (\text{diffusion and thermal diffusion terms}) + \dot{Q} \cdot E + \sum_{\rho} (-\Delta H)_{\rho} w_{\rho} \quad (1.9)$$

where  $C$  is the heat capacity of the mixture and  $\Delta H_{\rho}$  and  $w_{\rho}$  are respectively the heat and the velocity of reaction  $\rho$ . Equations (1.8) and (1.9) must of course be supplemented with appropriate boundary conditions.

In the case of homogeneous isothermal systems, we have the following simplified equations,

$$\frac{dX_i}{dt} = v_i(X_i), \quad i = 1, 2, \dots, n \quad (1.10)$$

They become nonlinear ordinary differential equations of the autonomous type. The mathematical theory of such equations has been developed extensively by several workers [8,24,33] beginning with Poincare. Convenience is not however, the only reason for taking up homogeneous cases as in (1.10). Many bio-chemical oscillators in homogeneous phase are known. In all these cases, oscillations can only be due to the chemical mechanism, since ~~all~~ additional causes, such as, the presence of surfaces,  $i$  macroscopic inhomogeneities, electric effects etc. have been removed. Thus the study of nonlinear system of ordinary differential equations ( 1.10 ) will reveal

conditions under which a chemical mechanism can by itself generate an oscillatory behaviour.

Let  $X_i(t)$  be a solution of the system (1.10). It is assumed that, the motion is defined in the open time interval  $(0, \infty)$  and that  $X_i(t)$  exists in this interval. Then any  $X_i(t+t_0)$ , where  $t_0$  is an arbitrary constant (phase) is still a solution of this system. These infinitely many solutions define in the  $n$ -dimensional space of  $X_i$ s a trajectory  $C$  (or orbit) of the system. Applying the techniques of the stability theory of Poincare, Liapunov and Laplace (see [53, 69] ), the oscillatory behaviour of the reaction system can be studied.

A system is structurally stable if the topological structure of its trajectories in the  $X_n$  space is unaffected by small disturbances modifying the form of the evolution equations (1.10). If a solution of the system (1.10), once near another solution, remains near together for all the future time, then that solution is stable in the sense of Liapunov. Usually, the behaviour of a chemical system described by (1.10) depends on the values of a set of parameters, say  $\{\mu\}$  describing, eg. the rate of entry of substances from outside or the initial composition of the mixture. The solutions of the differential equations thus, become functions of  $\{\mu\}$ . For certain critical

values of the parameter (or bifurcation value) say,  $\mu = \mu_c$ , the structure of the trajectories changes qualitatively (structural instability). Certain solutions (steady state) or trajectories of (1.10) become at this point (Liapunov) unstable. Thus the transition from a steady state to an oscillatory behaviour is accompanied by a bifurcation phenomenon which occurs for some critical values of a set of parameters influencing the system. The system has then to evolve to a new type of regime, the sustained oscillations. The theory of nonlinear oscillations, both in two-dimensional and three-dimensional systems are discussed in chapter two.

The oscillators are mainly classified here into two types, viz. biological and non-biological. From a mathematical point of view, a biological oscillator is any biological system which undergoes regular periodic changes. In many biological phenomena, such as circadian clocks, the rhythmic activity of the central nervous system, the problem of development and morphogenesis, interaction between competing species, oscillations are the rule rather than the exception. Certain parts of the mammalian brain respond electrically to an impulse-like stimulation in the form of damped or even sustained oscillations, (see [64, 68]). The short term memory and

learning processes are related to the electric activity of the brain (see [57] ). The FHN Model is a modification of Van der Pol's relaxation oscillator and is proposed to describe the electrochemical activity in a nerve [37]. The competition between populations is a very general phenomenon, whether one deals with the biosphere, human societies, or even economics. It takes place as soon as the resources necessary for the survival are limited or are exhausted. Several examples of this phenomenon are known (see [57] ) in the biosphere, both for natural [70] and for artificial ecosystems.

The theoretical developments which were motivated essentially by the study of biological systems, were enriched by the discovery of several striking non-biological oscillators viz., the Bray reaction, Belousov-Zhabotinskii reaction, Bernard convection problem etc. The first two are chemical oscillators, while the third is a non-chemical oscillator. In the case of Bernard convection problem (see [57]) when a horizontal fluid layer initially at rest is heated from below, the convection patterns appear, at a critical temperature gradient. Examples of chemical oscillators are many. The earliest reported periodic chemical reaction in homogeneous solution is the Bray reaction (see [57]) which is the catalytic decomposition

of hydrogen peroxide by the iodic acid-iodine oxidation couple. The second case of an oscillatory chemical reaction in homogeneous solution was reported by Belousov [5], which is the oxidation of citric acid by potassium bromate catalyzed by the ceric-cerous ion couple. Zhabotinskii [81] demonstrated that the cerium catalyst could be replaced by manganese or ferroin and that the citric acid reducing agent could be replaced by a variety of organic compounds, such as malonic or bromo-malonic acid. Sustained oscillations in the concentration of chemicals appear spontaneously if the reaction is carried out in a well-stirred homogeneous medium. The periods and amplitudes are very sharp and reproducible. This reaction is discussed in detail in the third chapter of this thesis.

The discovery of B-Z reaction lead to the discovery of many other chemical oscillators. One of them is the Briggs-Raucher reaction (see[58]) which is a combination of B-Z and Bray reactions. This reaction involves hydrogen peroxide, malonic acid, potassium iodate, manganese sulphate and sulphuric acid. The colourless solution becomes golden yellow, then blue, then colourless, ... . The oscillations are in the order of seconds and life time is in the order of the hour. More details about the chemical oscillators can be obtained from the review feature article by Nicolis and Portnow [57].



The appearance of periodic spatial structures in purely chemical systems fascinates all. When the B-Z reaction is carried out in a thin long vertical tube [7], there appear horizontal bands corresponding to alternately high concentration regions of the chemicals. Further more, Zaikin and Zhabotinskii [80] have reported travelling two-dimensional waves and Winfree [78] reported spiral waves in such systems.

Apparently simple chemical systems and reaction mechanisms involving a small number of components may give rise to remarkable variety of dynamical phenomena of the systems, which are maintained sufficiently far from equilibrium. These include multiple stationary states, simple and complex periodic oscillation, aperiodic (chaos) structures, and the growth of travelling waves and spatial structures in initially homogeneous media.

These types of complex dynamical phenomena can occur only in systems which are sufficiently far from equilibrium. To explain this situation the example of CSTR (Continuous Stirred Tank Reactor) may be used. CSTR may be thought of as a well stirred beaker, augmented by a constant temperature bath, potentiometric, optical and/or thermal probes and most importantly tubes for the input of reactants and for the

inflow of reacted material. Ideally, then the system is open, homogeneous and at constant volume and external temperature.

We may tend to think of chemical systems as having a single stable mode of long time behaviour, generally the equilibrium state. Multiple stable states are often associated with biological (eg. asleep-awake, living-dead) rather than chemical systems. The fact is that many chemical reactions under appropriate conditions give rise to two or more different states at a single set of constraint values. (example, the 'bistable' situations).

Two types of bistability occur in a reaction system, the first one viz., two stationary states, and the second one viz., a stationary and an oscillatory state. An example of a two component system, which shows the first type of bistability is the arsenite-iodate reaction discovered by De Kepper et al. (1981), (see [11]). Bistability need not always involve the existence of two stable stationary states. One or both of the stable states may be oscillatory. For examples of chemical oscillators showing this type of bistability is given by Epstein [11].

The study of aperiodic oscillation or 'chemical chaos' is one of the fastest growing areas of nonlinear

chemical dynamics. It is tedious to construct a simple model of chemical chaos. Chaos represents an inherently more complex phenomenon in the sense that at least three independent first order differential equations are required to generate chaos, whereas two equations will suffice for periodic oscillation and one for bistability. In an experimental study of the B-Z reaction in the CSTR, Turner et al.[72] observed a sequence of alternating periodic and chaotic states. In addition to the periodic-chaotic sequence described above, the B-Z system displays several other well known phenomena. These include the transition from simple periodicity to chaos via a period doubling sequence [67], intermittency [62] and the observation of the so-called U-sequence of periodic states bordering the chaotic region in constrained space. Many researchers reported about the spiral and travelling wave solutions of B-Z reaction [13, 21, 26, 40, 55, 61, 77].

A number of nonmonotonic behaviours appear where the B-Z reaction is run in a flow system (CSTR) which are not observed when the reaction is run in a closed system. One among these behaviours is the CDO (Composite Double Oscillation) in which nearly identical bursts of oscillation are separated by regular periods of quiescence. The CDO occur as the system is carried back-and-forth across the area of co-existence by the new slowly moving variable, whose concentration grows during the oscillatory phase, when the

system is on the LSLC (Locally Stable Limit Cycle) and decays during the quiescent phase, when the system is on the LSSS (Locally Stable Steady State) [41]. The transition from excitable steady state to the oscillatory state results in the SNIPER (Stable Node Infinite Period) bifurcation phenomena [3].

Autocatalysis is a necessary prerequisite for the existence of stable sustained oscillations, as we examine the reaction mechanism of oscillators. The earliest chemical model for sustained oscillations is that suggested by Lotka (1920). The Lotka scheme contains two quadratic autocatalytic steps. The 'Brusselator', suggested by Prigogine and Lefever [63] is perhaps the simplest oscillator obtainable from a chemical model based on the law of mass action. This scheme contains a cubic autocatalytic step. The reaction scheme of the Oregonator [19] model of the B-Z reaction contains a simple quadratic autocatalytic step. Many other models based on the cubic autocatalysis are known [52]. Elaborations of the cubic autocatalytic scheme in order to match experimental data from real systems have been made by Boiteux et al. (1975), (see [52]). This thesis consists of five chapters including this introductory chapter.

Chapter two presents the mathematical tools applied to analyse the nonlinear oscillations in nonlinear systems. The mathematical properties of reaction networks which can give rise to oscillations are schematically described here. Most of the reaction systems can be described in terms of a limited number of local variables, which can be connected by a relation, by the law of mass action. Once this is achieved, we can have the governing system of differential equations, describing the dynamics of the reaction systems under consideration. The steady state solutions, or the equilibrium states of the system can be found out. To study the behaviour of the solutions around critical points, apply perturbations to the system of nonlinear equations at these points the qualitative analysis of these points can be carried out using the stability theory due to Liapunov and Poincare. The techniques to check whether a system of nonlinear differential equations possess limit cycle behaviour are discussed here. The existence of limit cycles indicates the sustained oscillatory behaviour of the dynamical systems. A recipe to find whether a reaction system exhibits Hopf bifurcation is also given. Some numerical techniques to find the solutions, (both stationary and time dependent), bifurcation points, Hopf bifurcation points etc. of the system of nonlinear differential equations are mentioned.

Many methods to integrate systems of differential equations, to find bifurcation point, Hopf bifurcation points etc. can be cited in the literature [42, 46, 47, 49, 66].

Chapter three describes the oscillatory behaviour of a chemical reaction system, viz. the Belousov-Zhabotinskii reaction, which is not exactly biological, but whose mathematical properties have much in common with the physiology of electrically excitable tissues, including nerve, heart and smooth muscle. The oscillations occurring in B-Z reaction are explained using the chemical reaction steps in Section (3.2). The mathematical model studies to explain the oscillatory behaviour of the B-Z reaction mechanism are also given. The model we have studied is basically, the Oregonator model[19]. This model consists of a system of three ordinary differential equations, nonlinear and coupled in the concentrations of the three key substances  $[ \text{HBrO}_2 ]$  (X),  $[ \text{Br}^- ]$  (Y),  $2[ \text{Ce}^{4+} ]$  (Z). The evolution of X is very large compared to the evolution of the other two variables Y and Z. In section (3.2), a two variable model for the system (3.14) is studied. The equilibrium points, the oscillatory behaviour (or ~~limit~~ cycles) and the range of the controlling parameter  $f$ , for which the system exhibits oscillatory behaviour are found and discussed in detail. The numerical results obtained for this y-z system

are also displayed. The next section contains an elaborate analysis of the three dimensional model suggested by Field and Noyes [19]. This is a simple model of the Field-Körös-Noyes mechanism [17]. An attempt is made to study the oscillatory behaviour of the three-dimensional model for different values of the stoichiometric coefficient  $f$ . The analytic expression for the Hopf bifurcation value of the parameter  $f$  is obtained. The range of  $f$  at which the system has limit cycle behaviour is given. The numerical integration of the full model (3.14) results in one limit cycle in the  $y$ - $x$  phase plane for  $f = 1.0$  and for  $f = 1.1$ . These diagrams are shown at the end of the third chapter.

Considerable interest in oscillatory reaction systems has been generated by the large number of such processes observed in biological systems. The oscillatory reaction systems generally involve autocatalytic reactions. Chapter four describes an oscillatory model adopted from the MNS [52] cubic autocatalytic model. An elaborate system of three-variable nonlinear coupled differential equations represent the chemical reaction mechanism of ~~our~~ system. The physically realistic equilibrium states are investigated. Their qualitative behaviour is discussed here. The Hopf bifurcation points of the system are estimated both numerically and

analytically. The range of the parametric value  $\mathcal{K}$ , at which the system exhibits Hopf bifurcation phenomena is given in Section (4.4). The numerical results, obtained by integrating the model, by the Runge Kutta Method with the step doubling technique [25] is given. At the supercritical Hopf bifurcation point,  $\mathcal{K}_{2c}$  a stable limit cycle is obtained, the solution trajectory approaches it as time increases. The steady state is found to be unstable in the range  $\mathcal{K}_{1c} < \mathcal{K} < \mathcal{K}_{2c}$ . The values of  $\mathcal{K}_{1c}$  and  $\mathcal{K}_{2c}$  are obtained numerically.



## Chapter 2

### METHODS OF NONLINEAR DYNAMICS

In this chapter, we intend to discuss the mathematical techniques employed in understanding the nonlinear dynamics of the systems studied in this thesis.

#### 2.1. SYSTEMS INVOLVING CHEMICAL REACTIONS

A dynamical system in which the parameters vary in time is one type of system of evolution. We consider an open system at mechanical equilibrium involving  $n$  chemically reacting constituents  $X_1, X_2, \dots, X_n$ . The dynamical system is described by the composition variables (non dimensionalised concentrations of constituents)  $\{x_i\}$ ,  $i = 1, 2, \dots, n$ . Then we have the mass balance equations,

$$\frac{dx_i}{dt} = f_i(t, x_i), \quad t \in I, \quad i = 1, 2, \dots, n. \quad (2.1)$$

where the nonlinear functions  $f_i$  describes the overall rate of production of  $x_i$  from the chemical reactions and  $I$  is an interval of time. This is also known as the kinetic equations. When the right hand member of the equation (2.1) do not contain  $t$  explicitly, the system is autonomous. In the

vector form (2.1) becomes,

$$\dot{x} = f(x) \quad (2.2)$$

where  $x \in \mathbb{R}^n$  and  $f = (f_1, f_2, \dots, f_n)^T$ .

By the solution of (2.1) we mean a set of  $n$  functions  $\{\eta_i\}$  such that

- (i)  $\{\eta_i'(t)\}$ ,  $i = 1, 2, \dots, n$  exist
- (ii) the point  $(t, \eta_i(t))$  remains in  $D$ , the domain of  $f$ .
- (iii)  $\eta_i'(t) = f_i(t, \eta_i(t))$   
 $[t \in I, ' = \frac{d}{dt}; i = 1, 2, \dots, n]$

Geometrically, this is a curve in the  $n+1$  dimensional region  $D$  such that each point on the curve has co-ordinates  $(t, \eta_i(t))$ ,  $i=1, 2, \dots, n$ , where  $\eta_i'(t)$  is the  $i^{\text{th}}$  component of the tangent vector to the curve in the direction  $x_i$ .

Autonomous systems describing natural phenomena usually takes the form,

$$\dot{x}_i = f_i(x_i, \mu), \quad i = 1, 2, \dots, n \quad (2.3)$$

where  $\mu$  is a parameter appearing in the system. A reaction system that contains a parameter can be treated as a special case with one more state variables ( $x_i$ s). It is interesting to visualize what happens to the dynamical system, when we allow the parameter to vary in specified ways. This is discussed later in this chapter.

A more general form of (2.3),

$$\dot{x}_i = f_i(x_i, \mu_i), \quad i = 1, 2, \dots, n \quad (2.4)$$

where  $x_i \in \mathbb{R}^n$ , the system is known as the lumped parameter system or LPS, here  $\mu_i$ s also should belong to a finite dimensional space. When  $x_i$ s belong to an infinite dimensional space, the system is known as distributed parameter systems or DPS. The LPS are usually described by systems of ordinary differential equations, while the DPS are described by partial differential equations of the parabolic or hyperbolic type.

In a chemical reaction model, when the diffusion is also taken into consideration, we have,

$$\frac{\partial x_i}{\partial t} = f_i(x_i) + D_i \nabla^2 x_i \quad (2.5)$$

where the diffusion-coefficient matrix is diagonal and the

coefficients  $D_i$ s are constants. The  $f_i$ s has the same meaning as in equation (2.1). For a physico-chemical system obeying the law of mass action at equilibrium,  $f_i$ s will be nonlinear functions of  $\{x_i\}$ ,  $i=1,2,\dots,n$  of the polynomial type. This makes the differential system (2.5) a system of nonlinear partial differential equations. The presence of first order time derivatives and second order space derivatives makes the equation (2.5) parabolic. This will become the evolution equations describing dissipative systems (in which the dynamical parameter depends explicitly on time or energy absorbing or nonconservative).

Some boundary conditions can be applied to the system (2.5) such as Dirichlet conditions,

$$\{x_1, \dots, x_n\} = \{\text{const}\} \quad (2.6a)$$

or Neumann conditions,

$$\{n \cdot \nabla x_1, \dots, n \cdot \nabla x_n\} = \{\text{const}\} \quad (2.6b)$$

or a linear combination of both the conditions. The system is closed with respect to exchange of the corresponding chemical substance, if one of the constants in (2.6b) vanishes identically. This condition applies to some of the experiments of the Belousov-Zhabotinskii reaction, which is the well-known

chemical reaction giving rise to dissipative structures (structures maintained at the expense of energy flowing into the system from the outside).

## 2.2. STABILITY IN NONLINEAR SYSTEMS

Fixed points or equilibrium points are an important class of solutions of a system of differential equations. The steady state solution  $x_{i0}$  (or  $x_i(t_0)$ ) of the system(2.3) is defined by the equation

$$f_i(x_i, \mu) = 0, \quad i = 1, 2, \dots, n \quad (2.7)$$

where the values of the parameter  $\mu$  is known. This gives us a system of nonlinear algebraic equations. A nonlinear equation may have several singular points, all, none or some of which may be stable.

A fixed point  $x_{i0}$  is said to be stable if a solution  $x_i(t)$  based nearby remains close to  $x_i$  for all time. In addition, if  $x_i(t) \rightarrow x_{i0}$  as  $t \rightarrow \infty$ , then  $x_i(t)$  is said to be asymptotically stable.

There are basically three categories of the stability concept: Laplace, Liapunov and Poincare (see [69]). If all the solutions of the differential equations are bounded as

$t \rightarrow \infty$ , the system is stable in the sense of Laplace. Liapunov stability requires that solutions which are once near together remain near together for all the time. If for a given  $\eta > 0$ , there exists a  $\delta > 0$  such that any solution  $x_i(t)$ , satisfying  $|x_{i0} - x_i(t)| \leq \delta$  for  $t = 0$ , also implies  $|x_{i0} - x_i(t)| \leq \eta$  for every  $t \geq 0$ , we say the system is stable in the sense of Liapunov. But in some systems, eventhough the representative point on the path of the solutions does not satisfy the above criteria of Liapunov stability, they are considered to be stable. In this particular situation, Poincare introduced the orbital stability concept. A solution path is said to possess orbital stability, if the neighbouring half paths which are once near the solution path remains near for ever. The orbital stability need not imply the Liapunov stability.

The solutions of the system (2.4) depends on a number of parameters. As the system evolves and is continuously perturbed, some of the parameters change slightly or abruptly. New parameters can be appeared and hence increasing the number of interacting degrees of freedom. Thus the change of parameters generally changes the structure of the equations themselves. For

these new equations, we can have a new set of solutions. If this set of solutions remain in a neighbourhood  $O(\eta)$  [where  $\eta$  is the change in some representative parameter], we say that the system is structurally stable. If no such neighbourhood exists, the system is structurally unstable. Thus in a structurally stable system, the topological structure of the trajectories in phase space remains unchanged.

If  $x_{i0}$  is an equilibrium solution of the nonlinear system of differential equations (2.2), a new variable  $y_i$  is introduced as follows:

$$y_i = x_i - x_{i0}$$

and (2.2) can be transformed as

$$\dot{y}_i = f_i(y_i + x_{i0})$$

Then the right hand side of (2.2) can be expressed as,

$$f_i(x_i) = A(x_i - x_{i0}) + f_i^{(1)}(x_i) \quad (2.8)$$

where  $A$  is any constant matrix and  $f_i^{(1)}(x_i)$  is the difference  $f_i(x_i) - A(x_i - x_{i0})$ . Suppose a nonsingular matrix  $A$

can be so chosen that,

$$\lim_{x_i \rightarrow x_{i0}} \frac{|f_i^{(1)}(x_i)|}{|x_i - x_{i0}|} = 0, \quad i = 1, 2, \dots, n \quad (2.9)$$

Then the following system of equations,

$$\frac{dx_i}{dt} = A(x_i - x_{i0}) \quad (2.10)$$

is termed as the 'linear approximation'. The nonlinearity condition is given by (2.9). To check the stability of the solutions of (2.2), it is enough if we study the stability of the solutions of the linear approximation.

For the qualitative study of the solutions, it is not necessary to find all the characteristic roots of the linear matrix  $A$ . It is enough if we find the sign of the eigen values. If all the characteristic roots have negative real part, the solution is stable, since it decays exponentially and returns to its original position. If any one of the eigen values has a positive real part, the solution blows out as time increases. If all the eigen values are purely imaginary, we get the center and the solutions are stable. In certain systems, the variation of some controlling parameter results in changing the sign of the real part of the complex eigen value. This phenomenon is discussed in detail later.



We can study the qualitative behaviour of the solutions if we are able to represent the solution in a phase plane. We can represent the solution graphically only for the two dimensional systems. The general form of typical physical systems with one degree of freedom is,

$$\begin{aligned}\dot{x}_1 &= f_1(x_1, x_2) \\ \dot{x}_2 &= f_2(x_1, x_2)\end{aligned}\tag{2.11}$$

where  $f_1$  and  $f_2$  are analytic functions of  $x_1$  and  $x_2$  which vanish at the origin. It is possible to eliminate  $dt$  between the equations and write,

$$\frac{dx_2}{dx_1} = \frac{f_2(x_1, x_2)}{f_1(x_1, x_2)}, \quad f_1(x_1, x_2) \neq 0\tag{2.12}$$

which is a differential equation of the integral curves. The integral curves of (2.12) in the plane of variables  $(x_1, x_2)$  is called the phase plane. The asymptotic behaviour of the trajectories in the neighbourhood of a singular point determines the type of equilibrium represented by the singular point. According to Poincare, the singular points are classified as nodes, foci, centers and saddle points.

Also from the characteristic equation corresponding to (2.11), we can analyse the qualitative behaviour of the solutions. In some problems, it is very difficult to estimate the characteristic roots (eigen values). But from the coefficients of the characteristic polynomial we can find the sign and nature (ie. real or complex ) of the eigen values. The characteristic equation corresponds to the system (2.11) has the form,

$$\lambda^2 - T\lambda + \Delta = 0 \quad (2.13)$$

where

$$T = \frac{\partial f_1}{\partial x_1} + \frac{\partial f_2}{\partial x_2}$$

$$\Delta = \frac{\partial f_1}{\partial x_1} \cdot \frac{\partial f_2}{\partial x_2} - \frac{\partial f_1}{\partial x_2} \cdot \frac{\partial f_2}{\partial x_1}$$

are the trace and determinant of the coefficient matrix.

It is evident that, the roots are real when the discriminant  $T^2 - 4\Delta \geq 0$ . If in addition  $\Delta > 0$ , implies both the roots have the same sign and the singular point will be a stable or unstable node, according as the sign negative or positive. The characteristic roots are complex when  $T^2 - 4\Delta < 0$ . The two roots have non-vanishing real part  $T \neq 0$ .  $T < 0$  corresponds to a stable focus and  $T > 0$

corresponds to an unstable one. When  $\tau = 0$ , ( $\Delta < 0$ ), the roots are purely imaginary,  $\lambda_i = \pm i\omega$ . In this case, the trajectories are closed, surrounding the singular point viz. 'center'.

The reaction models consisting of three variables present a much more complicated structure. Let us discuss the characteristic equation of a three dimensional system of differential equations. It takes the form,

$$\lambda^3 - \tau\lambda^2 + \delta\lambda - \Delta = 0 \quad (2.14)$$

The necessary and sufficient conditions [1] for all the characteristic roots to have negative real parts are given by,

$$\tau < 0, \quad \Delta < 0, \quad \Delta - \tau\delta > 0 \quad (2.15)$$

The singular points, so far discussed belong to the class of 'simple' singular points. We consider the characteristic roots when  $\Delta \neq 0$ . The singular points, when  $\Delta = 0$  are referred to as multiple singular points. In fact, they are the points of contact of the curves defined by,

$$\frac{\partial f_1}{\partial x_1} \Big/ \frac{\partial f_2}{\partial x_1} = \frac{\partial f_1}{\partial x_2} \Big/ \frac{\partial f_2}{\partial x_2} \quad (2.16)$$

Multiple singular points splits up into more than one singular point, due to the slight variations of the functions  $f_1$  and  $f_2$ . The analysis of the trajectories in the vicinity of this point become more complex. New types of multiple singular points appear in systems involving several variables. As the system parameter crosses some 'critical' value, there occur coalescence of simple singular points and give rise to the multiple singular point.

The analytic approach (rather than the phase plane analysis) to the theory of stability develops from the so called variational equations (Poincare). Consider a dynamical system such as (2.1). If  $x_{i0} = x_{i0}(t)$  is a solution of the system (2.1), it is called the non-perturbed solution. The solution  $x_i(t)$ , corresponding to an initial value  $x_{i0} \neq 0$ , is called a perturbed solution. Between these two solutions, there exists a relation,

$$x_i(t) = x_{i0}(t) + \eta_i(t), \quad i = 1, 2, \dots, n \quad (2.17)$$

where the functions  $\eta_i(t)$  are called the perturbations and  $|\eta_i|$  are very small. When (2.17) is substituted in (2.1) and the functions  $f_i$ s are developed around the non-perturbed values  $x_{i0}(t)$  to the first order in  $\eta_i$ , the following system

of variational equations is obtained,

$$\dot{\eta}_i = \sum_{j=1}^n \frac{\partial f_i(x_{i0})}{\partial x_j} \eta_j, \quad i = 1, 2, \dots, n \quad (2.18)$$

If all the perturbation functions  $\eta_i(t) \longrightarrow 0$  as  $t \longrightarrow \infty$ , the perturbed solution tends to the nonperturbed solution (2.17). In this case, the stability is called the asymptotic stability. When  $x_{i0}(t) = 0$ , we have the position of equilibrium and which is referred to as the constant solution. Then from (2.17) we have,  $x_i(t) = \eta_i(t)$ . Then (2.18) can be read as,

$$\dot{x}_i = \sum_{j=1}^n \frac{\partial f_i}{\partial x_j} \cdot x_j \quad (2.19)$$

The variational equation of an autonomous system based on a constant solution is of the form,

$$\dot{x}_i = \sum_{j=1}^n a_{ij} x_j, \quad i = 1, 2, \dots, n \quad (2.20)$$

The characteristic roots of the above system are known as the characteristic exponents. If all the characteristic exponents have negative real parts, the identically zero solution of (2.20) is asymptotically stable. If at least one characteristic exponents has a positive real part, the identically zero solution is unstable.

From the above discussion, it is clear that, the stability of solutions of a system of differential equation is described by the sign of the characteristic roots or exponents. For this purpose, Hurwitz (see[53]) criterion is used. The necessary and sufficient conditions that the roots of a polynomial,  $a_0 x^n + a_1 x^{n-1} + \dots + a_n = 0$ ,  $a_i$ s are real and  $a_0 > 0$ , to have negative real part is,

$$a_1 > 0, \quad \begin{vmatrix} a_1 & a_3 \\ a_0 & a_2 \end{vmatrix} > 0, \quad \begin{vmatrix} a_1 & a_3 & a_5 \\ a_0 & a_2 & a_4 \\ 0 & a_1 & a_3 \end{vmatrix} > 0$$

$$\begin{vmatrix} a_1 & a_3 & a_5 & \dots & 0 \\ a_0 & a_2 & a_4 & \dots & 0 \\ 0 & a_1 & a_3 & \dots & 0 \\ \dots & \dots & \dots & \dots & \dots \\ \dots & \dots & \dots & \dots & a_n \end{vmatrix} > 0$$

By expanding the above determinants, we can make use of the conditions.

For systems involving many chemical variables,

Liapunov's second method (direct method) is used to study the qualitative behaviour of the solutions. The nonlinear system (2.2) is considered here. Let  $F = F(x_i)$ ,  $i=1,2,\dots,n$ . If  $F$  takes values having a single sign in  $D$ , ( $D: |x_i| < \eta$ ,  $\eta$  is a const) and  $F(x_i) = 0$  only for  $x_i = 0$  for every  $i$ , where  $i = 1,2, \dots, n$ , then  $F$  is said to be definite (Positive or Negative).  $F$  is semi-definite if it takes the same sign or vanishes in  $D$ .  $F$  is indefinite in any other case. The derivative of  $F$  (or the Eulerian derivative) along a solution of the system (2.1) is,

$$\dot{F} = \sum_i \left( \frac{\partial F}{\partial x_i} \right) \cdot \left( \frac{\partial x_i}{\partial t} \right), \quad i = 1,2, \dots, n \quad (2.21)$$

The three important results (Liapunov) about the stability of the system (2.1) are stated below without proof.

1. The steady state  $x_{i0} = 0$ ,  $i = 1,2,\dots, n$  is stable in a domain  $D$ , if there exists a definite function  $F$ , whose Eulerian derivative is either semi-definite of sign opposite to  $F$  or vanishes identically in  $D$ .

2. The steady state  $x_{i0} = 0$ ,  $i = 1,2, \dots, n$  is asymptotically stable if one can determine definite function, whose Eulerian derivative is definite and has a sign opposite to that of  $F$ .

3. The steady state  $x_{i0} = 0$ ,  $i = 1, 2, \dots, n$  is unstable if one can determine a function  $F$  whose Eulerian derivative is definite  $F$  assumes in  $D$  values such that,  
 $F \left( \frac{dF}{dt} \right) > 0$ .

These theorems only provide sufficient conditions for stability. The principal advantages of the direct method are:

- (i) independent of the integration of the linearized system,
- (ii) applicable to all initial solutions  $x_{i0}$  of all kinds including space and time dependent ones,
- (iii) applicable directly to nonlinear systems.

### 2.3. LIMIT CYCLES

The integral curves of the two-variable system (2.11) in the  $(x_1, x_2)$  plane in the parametric form is called a trajectory. Positive half path is that portion of trajectory for  $t \geq 0$ , while the negative half path is the portion of the trajectory for  $t \leq 0$ . The isolated closed trajectories are called limit cycles. The positive limit cycle of a trajectory is the set of those points which are near it for  $t \longrightarrow \infty$ .



If for large values of  $t$ , the trajectory intersects each neighbourhood of a point, then that point belongs to the positive limit cycle of the trajectory. A limit cycle could be a singular point or a closed trajectory, containing no singular point (corresponds to a periodic solution of the differential equations), or an empty set (ie. non existent), or a collection of singular points with the connecting paths (separatrices).

The limit cycles arise only in the theory of oscillations of nonlinear dissipative systems. The autonomous system of differential equations (2.11) some times gives rise to special type of solutions represented by closed curves in the phase plane, and are called limit cycles (Poincare). A limit cycle is stable if all the neighbouring trajectories tend to it as  $t \longrightarrow \infty$ , and unstable if they tend to it as  $t \longrightarrow -\infty$ . The limit cycle is said to be semistable (considered as unstable) if the trajectories are attracted to it from one side and are repelled from the opposite side. A stable limit cycle represents a stable stationary oscillation of a physical system in the same way that a stable singular point represents a stable equilibrium.

The existence of limit cycles (periodic solutions) in an autonomous system of differential equations is examined using several techniques. These techniques are discussed one by one in the remaining part of this section.

Converting the system (2.11) into the polar co-ordinates  $(r, \theta)$ , we have

$$\begin{aligned}\dot{r} &= \bar{\Phi}(r, \theta) \\ \dot{\theta} &= \bar{\Psi}(r, \theta)\end{aligned}\tag{2.22}$$

where  $r^2 = x_1^2 + x_2^2$ ,  $\theta = \arctan(x_2/x_1)$

and  $x_1 = r \cos \theta$ ,  $x_2 = r \sin \theta$ .

The system having self-sustained oscillations (limit cycle behaviour) has the form

$$\dot{r} = \bar{\Phi}(r), \quad \dot{\theta} = \text{const.}$$

Since the circular motion ( $\dot{r} = 0$ ) corresponds to the roots of the equation,  $\bar{\Phi}(r) = 0$  and these are to be positive, the problem reduces to the determination of real positive roots of  $\bar{\Phi}(r)$ . The roots are negative (real) or complex conjugate means the non-existence of the equilibrium. As  $\dot{\theta} = \text{const.}$ , to each positive root  $r_0$ ,

there corresponds a circle in the phase plane. The concentric circles corresponding to the positive roots of  $\bar{\Phi}(r) = 0$  are thus the limit cycles. The variational equation of  $\dot{r} = \bar{\Phi}(r)$ , corresponds to  $r = r_0$  is,

$$\delta \dot{r} = \bar{\Phi}_r(r_0) \cdot \delta r$$

and the root  $r_0$  is stable if  $\bar{\Phi}_r(r_0) < 0$ . But this direct approach is applicable only in a few isolated cases. Some established results for limit cycles in two-dimensional phase spaces [2] are stated below without proof.

(i) A limit cycle surrounds at least one singular point and this can only be a focus, a center or a node. It can be neither a saddle point nor a multiple singular point.

(ii) Stable limit cycles emerge from an unstable singular point (soft self-excitation).

(iii) Unstable limit cycles emerge from a stable singular point (hard self-excitation).

(iv) Stable limit cycles can emerge by the coalescence of a stable and an unstable limit cycle.

Around a singular point of certain systems, there can be infinite number of limit cycles [53]. In the configuration of limit cycles, the first limit cycle around an unstable critical point is stable, the second limit cycle will be unstable and so on. A stable critical point is surrounded by an unstable limit cycle, which is surrounded by a stable limit cycle and so on.

The limit cycles arise mainly from two situations, viz. soft self-excitation and hard self-excitation. The initial conditions do nothing in the stationary oscillatory state of the self-sustained oscillators, while the system parameters control the oscillatory behaviour. Self-starting or self-excitation means, the oscillatory phenomenon starts spontaneously from rest and reaches its stationary state on the limit cycle. This is known as the soft self-excitation. But in hard self-excitation a certain amount of impulse is needed to start the oscillation, and once this is obtained, the system attains the stationary oscillatory behaviour, ie. the limit cycle behaviour. Soft self-excitation corresponds to the ~~case~~ in which a system departs from an unstable singularity while the hard self-excitation corresponds to the situation in which the equilibrium is stable.

The concept of index (Poincare), just gives a necessary condition for the existence of limit cycles. This simply asserts the condition for the non-existence of the limit cycles. Consider a Jordan curve  $C$ , free of singular points in the phase plane of the system (2.11) and the vector field  $V$  of the trajectories. The Poincare index is defined as

$$I(C,V) = \frac{1}{2\pi} \int_C d \arctan \left( \frac{dx_2}{dx_1} \right) \quad (2.23)$$

This is the number of positive revolutions of the vector  $V$ , as the curve  $C$  is described once in the positive direction, and which is known as the index of  $C$  with respect to  $V$ .  $I(C,V) = 0$  indicates that  $C$  surrounds no singular points.  $I(C,V) = +1$ , implies that  $C$  contains either a focus or a node or a center. When  $I(C,V) = -1$ ,  $C$  surrounds the saddle point.

Poincare has indicated and Bendixson has completed a theorem that gives both necessary and sufficient condition for the existence of limit cycles. This is known as the Poincare-Bendixson theorem. Earlier, Bendixson established a condition for the non-existence of limit cycles and which is known as the negative criterion.

Bendixson theorem states that for the two dimensional system of differential equations (2.11), if the expression  $\left(\frac{\partial f_1}{\partial x_1} + \frac{\partial f_2}{\partial x_2}\right)$  does not change its sign (or vanish identically) within a region D of the phase plane, no closed trajectory can exist in D. It should be noted that, even though the expression  $\left(\frac{\partial f_1}{\partial x_1} + \frac{\partial f_2}{\partial x_2}\right)$  changes sign, it does not imply the existence of a limit cycle for the system (2.11). The powerful Poincare-Bendixson theorem defend this situation. If a half path C remains in a finite domain D without approaching any singularities, then C is either a limit cycle or approaches such a closed trajectory.

The principal drawback here is the determination of the domain D. Poincare suggested the following method to determine the P.B domain. In the case of a ring shaped domain D bounded by two concentric circles  $C_1$  and  $C_2$ , it is sufficient for the existence of atleast one closed trajectory that,

- (i) Trajectories enter (leave) D through every point of  $C_1$  and  $C_2$ .
- (ii) There are no singular points either in D or on  $C_1$  and  $C_2$ .

A topological method can be used to determine the existence of limit cycles in a system of nonlinear differential equations (2.2). A useful condition for proving the existence of oscillatory solutions of finite amplitude is that a surface  $S$  must exist on which every solution trajectory  $x_i$  of (2.2) must enter. Thus the condition required is,

$$\hat{n} \cdot \frac{dx_i}{dt} < 0, \quad x_i \text{ on } S, \quad i = 1, 2, \dots, n \quad (2.24)$$

and  $\hat{n}$  is the outward drawn unit normal to  $S$ . Hastings and Murray [36] used this method to discuss the limit cycle behaviour of the Oregonator model [19] of the B-Z reaction system.

A number of chemical systems exhibit limit cycle behaviour. Systems other than chemical systems exhibiting nonlinear behaviour are, Van der Pol oscillator, Harmonic oscillator etc.

#### 2.4. DEPENDENCE OF STEADY STATE SOLUTIONS ON A PARAMETER

If a dynamical system is represented by the system of differential equations (2.3) containing a parameter  $\mu$ , the solution (motion) becomes a function of  $\mu$ . If the

change in the parametric value does not give rise to any qualitative change in the topological structure of the solutions, such values of  $\mu$  are called ordinary values. If for some  $\mu = \mu_0$ , there arises a qualitative change in the topological configuration of solutions, then  $\mu_0$  is called a 'critical' or a 'bifurcation' value. In some systems, the total number of solutions varies as the parameter  $\mu$  crosses the critical value  $\mu_0$ . So it is necessary to study the dependence of steady state solutions of the system (2.3) on the values of the parameter  $\mu$ .

Consider the system of equations,

$$f_i(x_i(\mu), \mu) = 0 \quad (2.25)$$

The equilibrium points of the system (2.3) are given by the system (2.25). On differentiation of (2.25) with respect to  $\mu$ , the following set of differential equations is obtained.

$$J(x_i, \mu) \frac{dx_i}{d\mu} = \frac{-\partial f_i}{\partial \mu}, \quad x_i(\mu_0) = x_{i0} \quad (2.26)$$

where  $J(x_i, \mu)$  is the Jacobian matrix of (2.25). If  $\det J(x_i, \mu) \neq 0$ , we can have the following system of linear



algebraic equations  $\frac{dx_i}{d\mu}$ :

$$\frac{dx_i}{d\mu} = -J^{-1}(x_i, \mu) \frac{\partial f_i}{\partial \mu}, \quad x_i(\mu_0) = x_{i0} \quad (2.27)$$

For  $\mu = \mu_0$ , we shall assume that

$$f_i(x_{i0}, \mu_0) = 0 \quad (2.28)$$

If the Jacobian matrix  $J(x_i(\mu), \mu)$  is regular on the interval  $[\mu_0, \mu_1]$ , the dependence  $x_i(\mu)$  obtained by integrating (2.25) satisfies the following relation,

$$f_i(x_i(\mu), \mu) = 0, \quad \mu \in [\mu_0, \mu_1] \quad (2.29)$$

The Jacobian matrix is singular at a branch point and hence cannot be inverted at such points. In such cases, a parametrization, say, with respect to the arc length could provide a suitable method. Let us take arc length ( $y$ ) of the solution curve as a parameter. Differentiating (2.25) with respect to  $y$ , we get,

$$\frac{df_i}{dy} = \sum_{j=1}^n \left( \frac{\partial f_i}{\partial x_j} \frac{dx_j}{dy} \right) + \frac{\partial f_i}{\partial \mu} \frac{d\mu}{dy} = 0 \quad (2.30a)$$

$$i = 1, 2, \dots, n.$$

The initial conditions are,

$$y = 0, x_i = x_{i0}, \mu = \mu_0 \quad (2.30b)$$

The additional equation for the arc,

$$\left(\frac{dx_1}{dy}\right)^2 + \dots + \left(\frac{dx_n}{dy}\right)^2 + \left(\frac{d\mu}{dy}\right)^2 = 1 \quad (2.31)$$

determines  $y$  as the length of arc on the above mentioned curve of solutions. For each  $y$ , the equations (2.30a) form a system of  $n$  linear algebraic equations in  $n+1$  unknowns  $\frac{dx_i}{dy}$ ,  $i = 1, 2, \dots, n$  and  $\frac{d\mu}{dy}$ . Now let us assume that the matrix

$$J_k = \begin{bmatrix} \frac{\partial f_1}{\partial x_1} & \dots & \frac{\partial f_1}{\partial x_{k-1}}, \frac{\partial f_1}{\partial x_{k+1}}, & \dots & \frac{\partial f_1}{\partial x_{n+1}} \\ \vdots & & & & \\ \frac{\partial f_n}{\partial x_1} & \dots & \frac{\partial f_n}{\partial x_{k-1}}, \frac{\partial f_n}{\partial x_{k+1}}, & \dots & \frac{\partial f_n}{\partial x_{n+1}} \end{bmatrix} \quad (2.32)$$

is regular for some  $k$ ,  $1 \leq k \leq n+1$ , taking

$$x_{n+1} = \mu \quad (2.33)$$

The system (2.30) can be solved for the unknowns,

$\frac{dx_1}{dy}$ , ...,  $\frac{dx_{k-1}}{dy}$ ,  $\frac{dx_{k+1}}{dy}$ , ...,  $\frac{dx_{n+1}}{dy}$  in the form

$$\frac{dx_i}{dy} = \beta_i \frac{dx_k}{dy}, \quad i = 1, 2, \dots, k-1, k+1, \dots, n+1 \quad (2.34)$$

If (2.34) is substituted into (2.31), we obtain,

$$\left( \frac{dx_k}{dy} \right)^2 = \left( 1 + \sum_{\substack{i=1 \\ i \neq k}}^{n+1} \beta_i^2 \right)^{-1} \quad (2.35)$$

The sign of the derivative  $\frac{dx_k}{dy}$  is given by the orientation of the parameter  $y$  along the curve. The other derivatives can be computed from (2.34). The systems (2.34) and (2.35) can be solved by any numerical technique for the integration of initial value problems. Using this method, the solution can be obtained as a function of arc length. This method can take care of branch points. Thus the property that the solutions are dependent on parameter can be effectively made use in tracing solution curves of complex nature.

## 2.5. BIFURCATION

As mentioned earlier,  $x_{i_0}$  be the steady state solution of (2.3). By a branch of solutions, we mean a continuous and uniquely dependent  $x_i(\mu)$ , for every fixed  $\mu \in (\mu_0, \mu_1)$  such that

$$\| y_i(\mu) - x_i(\mu) \| < \eta, \text{ for a given } \eta,$$

the uniqueness fails. The branch of solutions can be continued in both directions upto certain values of  $\mu$ , where the uniqueness fails. Such critical points are called branch points. Mainly there are two types of branch points, viz. limit points and bifurcation points.

If all the eigen values of the Jacobian matrix  $J$  of the system (2.3) evaluated at the steady state solution,

$$J = \left\{ \frac{\partial f_i(x_0)}{\partial x_j} \right\} \quad (2.36)$$

have strictly negative real parts, the steady state solution is stable. Bifurcation theory is used to analyse what happens when a part of the Jacobian matrix  $J$  moves into the right half plane, where the steady state solution is unstable. The steady state solution of the one-dimensional

system [39] corresponds to the solution of

$$f(x, \mu) = 0 \quad (2.37)$$

where the function  $f$  is assumed to have continuous first and second derivatives. The solution state  $(x, \mu)$  may belong to one of the following seven categories.

1. The point  $(x, \mu)$  is regular if,

$$\frac{\partial f}{\partial x} \neq 0, \quad \frac{\partial f}{\partial \mu} \neq 0 \quad (2.38)$$

The unique curve  $x = x(\mu)$ , or  $\mu = \mu(x)$  (the branch of solutions) passes through this regular point  $(x, \mu)$ .

2. Limit point (regular turning point) is a point where  $\frac{\partial \mu}{\partial x}$  changes sign ( and  $\frac{\partial f}{\partial \mu} \neq 0$  ). ie. the two branches which are joined at this point have a limiting tangent  $\frac{d\mu}{dx} = 0$  while  $\frac{\partial \mu}{\partial x}$  has opposite sign on either side of this point. Clearly,

$$\frac{\partial f}{\partial x} = 0, \quad \frac{\partial f}{\partial \mu} \neq 0 \quad (2.39)$$

3. Singular point is a point where

$$\frac{\partial f}{\partial x} = 0, \quad \frac{\partial f}{\partial \mu} = 0 \quad (2.40)$$

4. Double point (bifurcation point) is a singular point at which two (and only two) curves possessing distinct tangents  $\frac{dx}{d\mu}$  cross. Four branches of solutions emanate from this point forming the two pairs, each of which has a common tangent  $\frac{dx}{d\mu}$ . Two such branches which have a common tangent at the double points are sometimes considered as one branch.

5. A singular turning point (bifurcation-limit point) of the curve (2.37) is a double point at which two of the four existing branches have a limiting tangent  $\frac{d\mu}{dx} = 0$  and different signs of  $\frac{d\mu}{dx}$  in the neighbourhood of the point.

6. A cusp point of the curve (2.37) is a point of second order contact between two curves (2.37). All four branches have the same limiting tangent at the cusp point.

7. A higher-order singular point of the curve (2.37) is a singular point at which all the three second derivatives  $\frac{\partial^2 f}{\partial x^2}$ ,  $\frac{\partial^2 f}{\partial \mu^2}$ ,  $\frac{\partial^2 f}{\partial x \partial \mu}$  of  $f(x, \mu)$ , vanish.

The limit points play an important role in determining the number of solutions to a specific problem for a given value of the parameter  $\mu$ . For particular values of  $\mu$ , sometimes we have multiplicity of solutions (or multiple solutions exist). A solution diagram is the pictorial representation

of the dependence of steady state solutions on the parameter  $\mu$ .

The relationship between the branch points and the loss of stability of the steady state solution is evident in the one-dimensional case (ie.  $x \in \mathbb{R}^1$ ). Here, the Jacobian matrix (2.36) contains only one element and therefore it has only one eigen value. A change of stability occurs (with the change of parameter  $\mu$ ), when the eigen value passes through the origin of the complex plane. In the Jacobian matrix, the element  $\frac{\partial f}{\partial x}$  vanishes at this instant. But exactly, this is the condition for the existence of the limit and bifurcation points. The stability of steady state solutions may change at these points only. As the parameter value increases beyond the critical value, the originally stable steady state solution becomes unstable. Branching of new solutions may occur in three ways viz. supercritical, subcritical and transcritical bifurcation.

By the term bifurcation point, we mean a point at which the branching of solutions occur. Generally, two types of bifurcations occur, the real and the complex bifurcation. When the branching is related to (branching of steady state solutions) the passage of the real eigen value of the Jacobian matrix  $J$  through the origin in the

complex plane, we get the 'Real' bifurcation. The loss of stability of the steady state solution, when a pair of complex conjugate eigen values crosses the imaginary axis corresponds to the complex bifurcation.

A method to evaluate the limit and bifurcation points is discussed briefly, as follows. Detailed discussion is given by Kubicek and Marek [48]. The determination of primary bifurcating points (branching from the trivial solution) is more easy than the determination of secondary bifurcating points (those occurring from nontrivial solutions). Consider the system of nonlinear algebraic equations,

$$f_i(x_i, \mu) = 0, \quad i = 1, 2, \dots, n \quad (2.41)$$

The necessary condition which determines the branch points is,

$$f_{n+1}(x_i, \mu) = \det J(x_i, \mu) = 0, \quad i = 1, 2, \dots, n \quad (2.42)$$

where J is the Jacobian matrix with the elements,

$$g_{ij} = \frac{\partial f_i(x_i, \mu)}{\partial x_j}, \quad i, j = 1, 2, \dots, n \quad (2.43)$$

Eigen values  $\lambda$  of the Jacobian matrix J satisfy the



characteristic equation,

$$| J(x_i, \mu) - \lambda I | = 0 \quad (2.44)$$

Equation (2.42) indicates that the Jacobian matrix  $J$  has a zero eigen value. This is another definition of point of real bifurcation. If the parameter  $\mu$  varies as, the eigen values move along the real axis and crosses from the left complex half plane into the right one or vice-versa, the stability of the solution can change.

Let,

$$f_{n+2}(x_i, \mu) = \det \bar{J}(x_i, \mu) = 0 \quad (2.45)$$

where

$$\bar{J} = \left\{ \bar{g}_{ij} \right\} = g_{ij} \quad \begin{array}{l} \text{for } i = 1, 2, \dots, n \\ \quad \quad \quad j = 1, 2, \dots, n-1 \end{array}$$

and

$$\bar{g}_{in} = \frac{\partial f_i}{\partial \mu}, \quad i = 1, 2, \dots, n$$

As the last column ie.  $\left( \frac{\partial f_i}{\partial x_n} \right)$  of  $J$  is replaced by the column  $\frac{\partial f_i}{\partial \mu}$ ,  $\bar{J}$  is obtained. A limit point  $(x_i^*, \mu^*)$  satisfies the inequality,

$$f_{n+2}(x_i^*, \mu^*) \neq 0 \quad (2.46)$$

Since a unique dependence  $\mu(x_n)$  exists in the neighbourhood

of this point from the implicit function theorem. On the other hand, a bifurcation point  $(x_i^0, \mu^0)$  satisfies the relation,

$$f_{n+2}(x_i^0, \mu^0) = 0 \quad (2.47)$$

because the dependence of  $\mu$  on  $x_n$  is not unique in the neighbourhood of  $(x_i^0, \mu^0)$ . Hence the limit and bifurcation points can be distinguished using the equations (2.46) and (2.47). The original equation (2.3) and the necessary condition (2.42) form a set of  $n+1$  equations in  $n+1$  unknowns  $(x_i, \mu)$ ,  $i = 1, 2, \dots, n$  corresponding to co-ordinates of the branch points (both limit and bifurcation points).

In the case of complex bifurcation, also known as Hopf bifurcation, a limit cycle (or periodic motion) surrounding an equilibrium point emerges from the equilibrium (steady state) solution. There arise two types of complex bifurcations in systems exhibiting nonlinear oscillations [53]. At the critical parameter value (say,  $\mu = \mu_0$ ), the steady state solution bifurcates to a stable limit cycle and an unstable singular point (soft self-excitation). In certain systems, two limit cycles, one stable and the other unstable coalesce and subsequently vanish at  $\mu = \mu_0$  (hard self-excitation).

Periodic phenomena, or oscillations are observed in many naturally occurring dissipative systems. Consider the autonomous system of nonlinear differential equations (2.3). The assumptions made are that (2.3) has an isolated stationary point say  $x_i = x_{i0}^*(\mu)$  and that the Jacobian matrix,

$$J(\mu) = \frac{\partial f_i}{\partial x_j} (x_{i0}^*(\mu), \mu), \quad i, j = 1, 2, \dots, n \quad (2.48)$$

has a pair of complex conjugate eigen values  $\lambda_1$  and  $\lambda_2$ ,

$$\lambda_1(\mu) = \overline{\lambda_2(\mu)} = \alpha(\mu) + i\omega(\mu) \quad (2.49)$$

such that, for some  $\mu = \mu_0$ ,

$$\omega(\mu_0) = \omega_0 > 0, \quad \alpha(\mu_0) = 0 \text{ and } \alpha'(\mu_0) \neq 0 \quad (2.50)$$

If the eigen values of  $J(\mu_0)$ , other than  $\pm i\omega_0$ , all have strictly negative real parts, the assumption (2.50) implies the loss of linear stability of the steady state  $x_{i0}^*(\mu)$ , as  $\mu$  crosses the threshold value  $\mu_0$ . The appearance of periodic solutions out of an equilibrium state, is examined by applying the Hopf bifurcation theorem in the system of equations (2.3). The periodic solutions exist in exactly one of the cases  $\mu > \mu_0$ ,  $\mu < \mu_0$ . The

classical Hopf bifurcation theorem may be stated as follows.

A steady state solution  $x_{i_0}(\mu)$  and a branch of steady state solution  $x_i(\mu)$  of (2.3) are considered at  $\mu = \mu_0$  and in the neighbourhood of  $\mu_0$  respectively. The  $f_i$ s are sufficiently smooth. It is assumed that all eigen values of the Jacobian matrix  $J$  are non-zero and that only two eigen values are purely imaginary viz.  $\lambda_1(\mu)$  and  $\bar{\lambda}_2(\mu)$  satisfying the conditions (2.49) and (2.50).

$$\text{ie. } \operatorname{Re} \left\{ \lambda_1(\mu_0) \right\} = \operatorname{Re} \left\{ \bar{\lambda}_2(\mu_0) \right\} = 0, \operatorname{Re} \left\{ \dot{\lambda}(\mu_0) \right\} \neq 0 .$$

Then there exists a branch of periodic solutions of (2.3) for  $\mu > \mu_0$  and  $\mu < \mu_0$ .

Hussard, Kazarinoff and Wan [35] have given a recipe to check whether a system exhibits Hopf bifurcation or not. The recipe is given below.

1. Select the bifurcation parameter  $\mu$ .  
Let  $\dot{x}_i = f_i(x_i, \mu)$ ,  $i = 1, 2, \dots, n$   
denote the system to be studied.
2. Locate  $x_{i^*}(\mu)$ , the stationary point of interest.  
Calculate the eigen values of the Jacobian matrix

$$J(\mu) = \frac{\partial f_i}{\partial x_j} (x_i^*(\mu), \mu) \quad i, j = 1, 2, \dots, n.$$

and order them according as

$$\operatorname{Re} \lambda_1 \geq \operatorname{Re} \lambda_2 \geq \dots \geq \operatorname{Re} \lambda_n.$$

3. Find a value  $\mu_0$  such that,  $\operatorname{Re} \lambda_1(\mu_0) = 0$

If (a)  $\lambda_1$  and  $\lambda_2$  are a conjugate pair

(ie.  $\lambda_1(\mu) = \overline{\lambda_2(\mu)}$ ) for  $\mu$  in an open interval including  $\mu_0$ .

(b)  $\operatorname{Re} \lambda_1'(\mu_0) \neq 0$

(c)  $\operatorname{Im} \lambda_1(\mu_0) \neq 0$

(d)  $\operatorname{Re}(\lambda_j, \mu_0) < 0$ , ( $j = 3, \dots, n$ .)

then a Hopf bifurcation occurs.

In the models presented in Chapters 3 and 4 we have observed the appearance of Hopf bifurcation.

Let us denote  $(x_i^0, \mu^0)$  as a complete bifurcation point of the system (2.3). At this point the Jacobian matrix  $J(x_i, \mu)$  has a pair of complex conjugate purely imaginary eigen values,

$$\text{ie.} \quad \operatorname{Re}\{\lambda_{1,2}\} = 0 \quad (2.51)$$

Let the characteristic polynomial  $J$  be

$$P(\lambda) = \lambda^n + a_1 \lambda^{n-1} + a_2 \lambda^{n-2} + \dots + a_{n-1} \lambda + a_n \quad (2.52)$$

The necessary condition for the occurrence of the Hopf bifurcation point is given by (2.51), ie. the polynomial (2.52) has two roots,

$$\lambda_{1,2} = \pm i\omega_0, \quad \omega_0 > 0 \quad (2.53)$$

The polynomial  $P(\lambda)$  can thus be decomposed into

$$P(\lambda) = (\lambda^2 + \omega_0^2) P_{n-2}(\lambda) \quad (2.54)$$

where  $P_{n-2}(\lambda)$  is a polynomial of degree  $n-2$ . For an estimate of  $\omega$ , (2.54) can be written using Lin-Bairstow method as,

$$P(\lambda) = (\lambda^2 + \omega) (\lambda^{n-2} + p_1 \lambda^{n-3} + \dots + p_{n-3} \lambda + p_{n-2}) + A \lambda + B \quad (2.55)$$

Coefficients  $p_i$ ,  $i = 1, 2, \dots, n-2$ ,  $A$  and  $B$  can be calculated recursively,

$$p_{-1} = 0, \quad p_0 = 1; \quad p_k = a_k - \omega p_{k-2}, \quad k=1, 2, \dots, n-2. \\ A = a_{n-1} - \omega p_{n-3}; \quad B = a_n - \omega p_{n-2} \quad (2.56)$$

The values  $p_k$ , A and B depend on  $x_i$ ,  $\mu$  and  $\omega$ .

For  $\omega = \omega_0^2$ , we can write (2.34) as

$$\begin{aligned} f_{n+1}(x_i, \mu, \omega) &= A(x_i, \mu, \omega) = 0 \\ f_{n+2}(x_i, \mu, \omega) &= B(x_i, \mu, \omega) = 0, \quad i=1, 2, \dots, n. \end{aligned} \tag{2.57}$$

As a result we have  $n+2$  equations; (2.3), (2.57) in  $n+2$  unknowns  $x_i, \mu, \omega$ ;  $i = 1, 2, \dots, n$ . The solution of these equations gives the Hopf bifurcation point  $(x_i^0, \mu^0, \omega^0)$ .

The above method is an indirect method used for the computation of Hopf bifurcation points. Hopf bifurcation points are obtained by solving the algebraic equation  $\alpha(\mu) = 0$  during a continuation process along the branch of steady state solutions.

## 2.6. NUMERICAL METHODS

The reaction models involving two intermediates can be handled mathematically without much difficulty. Powerful mathematical methods has been developed for limit cycle behaviour of differential equations, describing such two dimensional systems. As the state of a system can be

described by a point in a phase plane, the well known theorems of Poincare and Bendixson are applicable. The multivariable systems could be tackled only using numerical methods.

A number of numerical methods have been developed to get the approximate solution of a system of differential equations (2.1). When we think of approximating a solution numerically, we are concerned with the accuracy of it to the actual solution. At this point, we define the concept of convergence to mean that any described degree of accuracy can be achieved for any problem having a unique solution, by picking a small enough step size  $h$ . The discrete variable methods (difference methods) are used for the automatic computation of general nonlinear problems. This provides a rule for computing the approximation at step  $i$  to  $x_i(t_i)$  in terms of values of  $x_i$  at  $t_{i-1}$  and possibly preceding points.

Let an approximate solution at a point  $t_j$  ( $j = 0, 1, \dots, t_0 = 0, h_j = t_{j+1} - t_j > 0$ ), be  $x_i^j \sim x_i(t_j)$ . The methods of numerical integration can be classified into single-step and multi-step techniques. By means of the single-step methods, the approximation at the successive points  $t_{j+1}$  is constructed solely on the



basis of the known solution approximation at the point  $t_j$ ,

$$x_i^{j+1} = x_i^j + h_j \phi_i(t_j, x_i^j, h_j) \quad (2.58)$$

where the functions  $\phi_i$  do not depend on  $t_j$  for the autonomous systems (like 2.2). The function  $\phi_i$  characterizes the particular single-step method. When  $\phi_i$  depends on  $x^{j+1}$ , we say the method is implicit and explicit otherwise.

If in a method, the error behaves like  $O(h^r)$ , we call it an  $r^{\text{th}}$  order method. If the higher order derivatives of  $x_i$ s can be calculated, we have

$$x_i^{j+1} = x_i^j + hx_i' + \frac{h^2}{2!} x_i'' + \dots + \frac{h^r}{r!} x_i^{(r)}$$

The local truncation error will be  $\frac{h^{r+1} x_i^{(r+1)}}{(r+1)!}$ . Euler's

method (first order method) is not very useful in practical problems, because it requires a very small step size, for reasonable accuracy. Taylor series method of higher order is not appropriate, because of the need to obtain higher total derivatives of  $x_i$ s. The most important among the single step methods, the Runge-Kutta methods attempt to obtain greater accuracy and at the same time, avoid the need for higher derivatives, by evaluating the function  $f_i(x_i)$  at selected points on each subinterval.

The classical scheme for the fourth order Runge-Kutta method is as follows. For this the function  $\phi_i$  is expressed recursively in the form,

$$\begin{aligned}
 k_1 &= h \cdot f_i(x_i^j) \\
 k_2 &= h \cdot f_i(x_i^j + \frac{1}{2} k_1) \\
 k_3 &= h \cdot f_i(x_i^j + \frac{1}{2} k_2) \\
 k_4 &= h \cdot f_i(x_i^j + k_3) \\
 x_i^{j+1} &= x_i^j + \frac{1}{6} (k_1 + 2k_2 + 2k_3 + k_4)
 \end{aligned}
 \tag{2.59}$$

The local truncation error in this method is  $O(h^5)$ .

The disadvantage of this method is that, the four function evaluations, at each step provide much discretization error. This method has the important advantage that it is self starting.

The single-step method (2.58) is convergent if  $x_i^j \longrightarrow x_i(t)$ , for every  $0 \leq t \leq b$  as  $j \longrightarrow \infty$  and  $x_{i0} \longrightarrow x_i(0)$  with  $h = \frac{t}{n}$  for any differential equation like (2.1), which satisfies a Lipschitz condition. We note that errors are permitted in the starting value  $x_{i0}$  since in practice we cannot represent  $y(0)$  exactly in finite precision. Convergence assures that, the true solution can be approximated arbitrarily close by making  $h$  smaller and using greater precision.

Stability of a method is concerned with the effect of perturbations on the numerical solution. A single-step method is stable if for each differential equation satisfying a Lipschitz condition there exist positive constants  $h_0$  and  $k$  such that the difference between two different numerical solutions  $x_i$  and  $\tilde{x}_i$ , each satisfying (2.58) is such that

$$\| x_i - \tilde{x}_i \| \leq k \| y_0 - \tilde{y}_0 \|,$$

for every  $0 \leq h \leq h_0$ .

Some results in connection with the stability of single-step method [25] are stated below without proof.

1. If  $\phi(t,x,h)$  satisfies a Lipschitz condition in  $L$ , then the method given by (2.58) is stable.

2. If  $\phi(x,t,h)$  is continuous in  $y,t,h$  for  $0 \leq t \leq b$ ,  $0 \leq h \leq h_0$ , and all  $x$ , and if it satisfies a Lipschitz condition on  $y$  in that region, a necessary and sufficient condition for convergence is that,

$$\phi(x(t), t, 0) = f(x(t), t)$$

This is called the condition of consistency.

Applying the above result, we can show that the classical fourth order Runge-Kutta Method converges for a system of equations (2.2). Since the functions  $f_i$  satisfies a Lipschitz condition,

$$k_1 = h f_i(x_i) \text{ satisfies}$$

$$\| k_1(x_i) - k_1(x_i^*) \| \leq h L \| x_i - x_i^* \|$$

$$k_2(x_i) = h \cdot f_i(x_i + \frac{1}{2} k_1(x_i)) \text{ satisfies}$$

$$\begin{aligned} \| k_2(x_i) - k_2(x_i^*) \| &\leq h L \| x_i - x_i^* + \frac{1}{2} k_1(x_i) - \frac{1}{2} k_1(x_i^*) \| \\ &\leq h L (1 + \frac{1}{2} h L) \| x_i - x_i^* \| \end{aligned}$$

$$k_3(x_i) = h f_i(x_i + \frac{1}{2} k_2(x_i)) \text{ satisfies,}$$

$$\begin{aligned} \| k_3(x_i) - k_3(x_i^*) \| &\leq h L \| x_i - x_i^* + \frac{1}{2} k_2(x_i) - \frac{1}{2} k_2(x_i^*) \| \\ &\leq h L (1 + \frac{1}{2} h L + \frac{1}{4} (h L)^2) \| x_i - x_i^* \| \end{aligned}$$

and  $k_4(x_i) = h f_i(x_i + k_3(x_i))$  satisfies,

$$\begin{aligned} \| k_4(x_i) - k_4(x_i^*) \| &\leq h L \| x_i - x_i^* + k_3(x_i) - k_3(x_i^*) \| \\ &\leq h L (1 + h L + \frac{1}{2} (h L)^2 + \frac{1}{4} (h L)^3) \| x_i - x_i^* \| \end{aligned}$$

Therefore

$$\phi(x_i, t, h) = \frac{1}{6h} (k_1 + 2k_2 + 2k_3 + k_4) \text{ satisfies,}$$

$$\begin{aligned} \| \phi(x_i, t, h) - \phi(x_i^*, t, h) \| \\ \leq \frac{1}{6} (1 + \frac{1}{2} h L + \frac{1}{6} (h L)^2 + \frac{1}{24} (h L)^3) \| x_i - x_i^* \| \end{aligned}$$

Hence  $\phi$  satisfies a Lipschitz condition in  $x_i$ . It can also be seen to be continuous in  $h$  and hence we can conclude that the classical Runge-Kutta method converges for a system of differential equations.

To minimize the error in a single-step method, we have to choose the suitable step size and order of the method. Step doubling technique is one method used for the error control in the Runge-Kutta Method. Each basic step size  $h$  is done twice once as two steps of size  $\frac{h}{2}$  and once as one step of size  $h$ . Since the error has the form,

$$h^{r+1} \phi_i(x_i, t) + O(h^{r+2}) \quad (2.60)$$

the two results can be compared to estimate  $\|\phi\|$ . If the result of one step of size  $h$  is  $y_i$ , while the result of two steps of size  $\frac{h}{2}$  is  $x_i$ , we have,

$$\|y_i - x_i\| = h^{r+1}(1-2^{-r}) \|\phi_i(t)\| + O(h^{r+2}) \quad (2.61)$$

We have basically followed the typical fourth order Runge-Kutta method with the step doubling technique as suggested by Gear [25], to solve the reaction systems described here. The scaled error is restricted to be less

than  $10^{-8}$  (EPS), an input parameter. The value of  $h$  for the next step is computed to make  $h$  nearly as necessary to make the next scaled error equal to  $10^{-8}$ . If the scaled error is greater than EPS, the step is rejected and repeated with the newly recommended  $H$  subject to a minimum step size of HMIN. This method keeps the relative error approximately constant in the maximum norm.

The difference between the multi-step and single-step methods, lies in the fact that, in the former, the value of solutions (and the right hand sides of the differential equations to be solved) are used at more than one of the previous mesh points. In comparison with the single step methods, multi-step methods have higher efficiency. But the disadvantage is that the initial conditions are not sufficient to begin the integration. To begin the multi-step method, several steps of a single step method are usually used. The second disadvantage to multi-step method is the difficulty in implementing the automatic step-size control.

For a constant step size  $h$ , the general linear multi-step method can be written in the form

$$\begin{aligned} & \alpha_k x_i^{j+1} + \alpha_{k-1} x_i^j + \alpha_{k-2} x_i^{j-1} + \dots + \alpha_0 x_i^{j+1-k} \\ & = h[\beta_k f_i^{j+1} + \beta_{k-1} f_i^j + \dots + \beta_0 f_i^{j+1-k}] \end{aligned} \quad (2.62)$$

where  $\alpha_k \neq 0$ ,  $\alpha_0^2 + \beta_0^2 > 0$ .

This is called the  $k$ -step method. It is fully characterized by the elements  $\alpha_i$  and  $\beta_i$ . If  $\alpha_k = 1$ ,  $\alpha_{k-1} = -1$ , and  $\alpha_i = 0$ , for  $i = 0, 1, 2, \dots, k-2$  (2.62) are Adam's methods.

For  $\beta_k = 0$ , the method is explicit (Adams-Bashforth) because, we need not iterate to calculate  $x_i^{j+1}$ . In the Adams-Bashforth method, we have:

$$x_i^{j+1} = x_i^j + h(f_i^j + \frac{1}{2} \Delta f_i^{j-1} + \frac{5}{12} \Delta^2 f_i^{j-2} + \frac{3}{8} \Delta^3 f_i^{j-3} )$$

where

$$\begin{aligned} \Delta f_i^{j-1} &= f_i^j - f_i^{j-1} \\ \Delta^2 f_i^{j-2} &= f_i^j - 2f_i^{j-1} + f_i^{j-2} \\ \Delta^3 f_i^{j-3} &= f_i^j - 3f_i^{j-2} + 3f_i^{j-2} - f_i^{j-3} \end{aligned} \quad (2.63)$$

In this method, we should know four successive values of

$f_i$  at equally spaced points before this formula can be used. These starting values can be obtained by using either Taylor series or Runge-Kutta Methods.

For  $\beta_k \neq 0$  (2.62) gives an implicit multistep method (Adams-Moulton type). To obtain  $x_i^{j+1}$ , we have to use an iteration technique. If  $\alpha_k = 1$ ,  $\alpha_{k-2} = -1$  and  $\alpha_i = 0$  for  $i \neq k, k-2$ , we obtain the Nystrome and Milne-Simpson methods. Coefficients of these methods as well as coefficients of the Adams type are given by Henrici (1962), (see [48] ).

When some of the components  $x_i$  change rapidly with varying independent variable  $t$  (the derivative  $\frac{dx_i}{dt}$  is large), the method of integration along the solution arc may be used. Let  $y$  denotes the length of the arc and differentiating (2.1) formally with respect to  $y$ ,

$$\frac{dx_i}{dy} = \frac{dx_i}{dt} \frac{dt}{dy} \quad (2.64)$$

Then it follows from the Pythagorean theorem for the length of arc that,

$$\frac{dt}{dy} = \pm \left[ 1 + \left( \frac{dx_1}{dt} \right)^2 + \dots + \left( \frac{dx_n}{dt} \right)^2 \right]^{-\frac{1}{2}} \quad (2.65)$$



where the positive or negative sign denotes orientation along arc. The  $n+1$  differential equations (2.64) and (2.65) are integrated instead of integrating the  $n$  differential equations. Further,

$$\left| \frac{dx_i}{dz} \right| = | f_i(t, x_i) f_0(t, x_i) | \leq 1 \quad (2.66)$$

$$\left| \frac{dt}{dz} \right| = | f_0(t, x_i) | \leq 1 \quad (2.67)$$

where

$$f_0(t, x_i) = \left\{ 1 + [f_1(t, x_i)]^2 + \dots + [f_n(t, x_i)]^2 \right\}^{-\frac{1}{2}} \quad (2.68)$$

will not occur.

Stiff systems of ordinary differential equations are characterised by systems with real parts of the corresponding eigen values differ from each other by several orders of magnitude. The problem of 'stiffness' arises in solving system of differential equations describing reaction systems. The two aspects of problems connected with the stiff systems are the stability and the accuracy.

Let us consider a scalar equation,

$$\frac{dx}{dt} = \lambda x \quad (2.69)$$

for a general complex number  $\lambda$  with a negative real part. A numerical method of integration that produces a sequence  $x^j = x(t_j)$  with a constant integration step  $h$  is called A-stable (see [48] ) if in the recurrent relation,

$$x^{j+1} = p(h\lambda) \cdot x^j \quad (2.70)$$

the variable  $p$  (dependent on the product  $h\lambda$ ) satisfies the relation,

$$| p(h\lambda) | < 1 \quad (2.71)$$

for any integration step size  $h$ . Also the method is said to be L-stable if  $|p(h\lambda)| \longrightarrow 0$  as  $h \longrightarrow \infty$ .

If a method which is not A-stable is used, large negative numbers decrease the integration step  $h$ , so that the integration becomes ineffective. On the other hand, if an A-stable method is used, the problem arises in the aspect of accuracy in the solution, rather than the stability. Here, for certain step size  $h$ , the solution component corresponding to the eigenvalue with the largest absolute value is approximated inaccurately. Gear [25] gives a method (based on Multi-step Methods) to solve a system of stiff differential equations. Many of the chemical reaction systems exhibit stiffness property.

We have tried several numerical methods to study the systems. However, we found that the Runge-Kutta method with step doubling to be a more efficient method to study our systems. However, to trace points of bifurcation or points of branching continuation methods or the like are more suitable if one can afford for the computer time. We have used a continuation method [47] to study the dependence of steady state solution of the system (3.14).

## Chapter 3

### A MODEL FOR CHEMICAL REACTING SYSTEMS

#### 3.1. INTRODUCTION

The Belousov-Zhabotinskii (B-Z) reaction is probably the most widely studied oscillating reaction in recent years. Although it is chemically complicated, it is still very simple compared with biological oscillators. The oscillatory phenomenon in the oxidation of citric acid by potassium bromate in a sulphuric acid medium, catalyzed by the ceric-cerous ion couple was first reported by Belousov [5] and the necessary modification (citric acid is replaced by malonic acid) was done by Zhabotinskii [81]. Field, Körös and Noyes [17] produced a detailed reaction mechanism consisting of eleven complicated steps, widely known as the FKN mechanism. Many mathematical models are suggested for the study of B-Z reaction. The most well known among them is the Oregonator model [19] consisting of five steps.

The reaction mechanism and model are described below. In the earlier studies, the oscillatory behaviour of the Oregonator is explained mathematically by keeping the controlling parameter fixed, viz.  $f = 1.0$ . Both the two-dimensional and the three-dimensional systems were

studied [19] for  $f = 1.0$ . We have presented some results pertaining to both the two-dimensional and the three-dimensional approximations of B-Z reaction for various values of the stoichiometric parameter  $f$ . We have followed basically the kinetic model suggested by Field and Noyes[19] to explain the oscillations.

### 3.2. CHEMISTRY OF THE B-Z REACTION

A convenient recipe [73] for the B-Z reaction is as follows:

Ingredients ---	Initial concentrations ---	
150 ml 1M $H_2SO_4$	1 M	
0.175 g $Ce(NO_3)_6(NH_4)_2$	0.002 M	(3.1)
4.292 g $CH_2(COOH)_2$	0.28 M	
1.415 g $NaBrO_3$	0.063 M	

Dissolve malonic acid and cerium ammonium nitrate in sulphuric acid in a beaker equipped with stirring apparatus. This yellow solution turns clear after a few minutes. When sodium bromate is added to the clear solution, it will turn to yellow (corresponds to ceric ion), then clear (corresponds to cerous ion), ..., oscillating

with a period on the order of one minute, depending on the rate of stirring, whereas the life time of the phenomena of the order of the hour. Finally the oscillations die out as the system remains closed to mass transfer and the raw materials necessary for the reaction are exhausted.

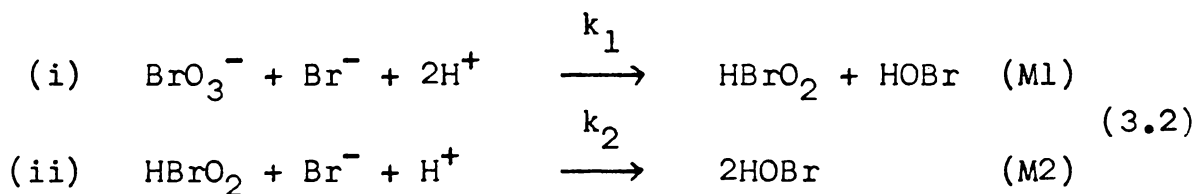
In 1972, Field, Körös and Noyes [17] proposed a detailed kinetic mechanism (FKN) of the reaction, comprising 11 steps. Later, in 1974, Field and Noyes [19] simplified the more complicated FKN, consisting only of five steps (referred to as the Oregonator in the literature) and interpret the oscillations in homogeneous solution, in terms of the properties of the key substances,

(i)  $\text{HBrO}_2$  (Bromous acid), seems to play the role of a switch intermediate.

(ii)  $\text{Br}^-$  (Bromide-ion), which seems to play the role of a control intermediate, and

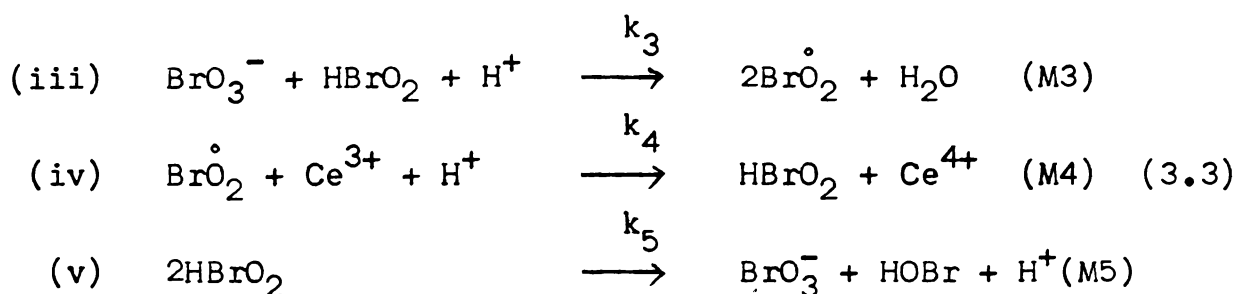
(iii)  $\text{Ce}^{4+}$  (ceric-ion), which seems to be a regeneration intermediate, in the sense that, it is rapidly produced when the system is switched in one direction and permits thereafter the formation of the control intermediate  $\text{Br}^-$ .

• With excess of  $\text{Br}^-$ .



• With small quantities of  $\text{Br}^-$  left,

Cerous-ion ( $\text{Ce}^{3+}$ ) is oxidized as follows.



Here  $k_i$ ,  $i = 1, 2, 3, 4, 5$  are the reaction constants. The superscripted '.' of  $\text{Br}\overset{\cdot}{\text{O}}_2$  indicates that it is more reactive.

By the law of mass action, in the first quasi-steady state, the rate of reaction of  $\text{HBrO}_2$  is given by,

$$[\text{HBrO}_2]_A = (k_1/k_2) [\text{BrO}_3^-] [\text{H}^+] \quad (3.4)$$

where  $k_1/k_2 \approx 10^{-9}$ .

Similarly, in the second quasi-steady state,

$$[\text{HBrO}_2]_B = (k_3/2k_5) [\text{H}^+] [\text{BrO}_3^-] \quad (3.5)$$

where  $k_3/k_5 \approx 10^{-4}$ ,  $k_3 = 10^4 \text{ M}^{-2} \text{ s}^{-1}$

From (ii) and (iii) it appears that  $\text{Br}^-$  and  $\text{BrO}_3^-$  compete with  $\text{HBrO}_2$ . Then at equilibrium,

$$k_2 [\text{Br}^-] = k_3 [\text{BrO}_3^-] \quad (3.6)$$

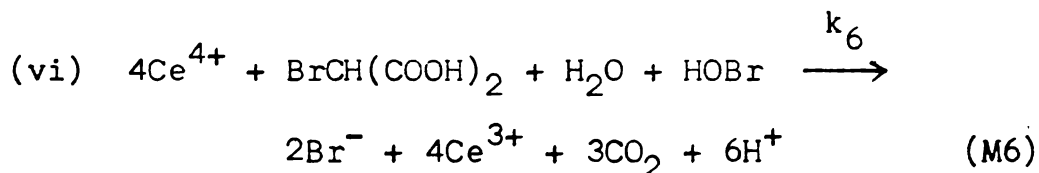
The autocatalytic production of  $\text{HBrO}_2$  ceases when

$$k_2 [\text{Br}^-] > k_3 [\text{BrO}_3^-] \quad (3.7)$$

Thus at the critical concentration value,

$$[\text{Br}^-]_c = (k_3/k_2) [\text{BrO}_3^-] \quad (3.8)$$

where  $k_3/k_2 \approx 5 \times 10^{-6}$ , the reaction switches from pathway (3.2) to pathway (3.3). As  $[\text{HBrO}_2]$  increases,  $\text{Br}^-$  is consumed and  $[\text{Br}^-]$  drops below the critical value. On the other hand, the produced ceric-ion ( $\text{Ce}^{4+}$ ), regenerates bromide-ion ( $\text{Br}^-$ ), according to the global reaction,



Hence the oscillation occurs.



### 3.3. MATHEMATICAL MODELLING

It has already noted that the most important phenomena associated with B-Z reaction is the oscillations. The occurrence of oscillations is explained [19,20] mathematically below. Let X,Y,Z represents the concentrations of the three key substances: Bromous acid, Bromide-ion and ceric-ion respectively. ie.

$$\begin{aligned} X &= [\text{HBrO}_2] \\ Y &= [\text{Br}^-] \\ Z &= 2 [\text{Ce}^{4+}] \end{aligned} \quad (3.9)$$

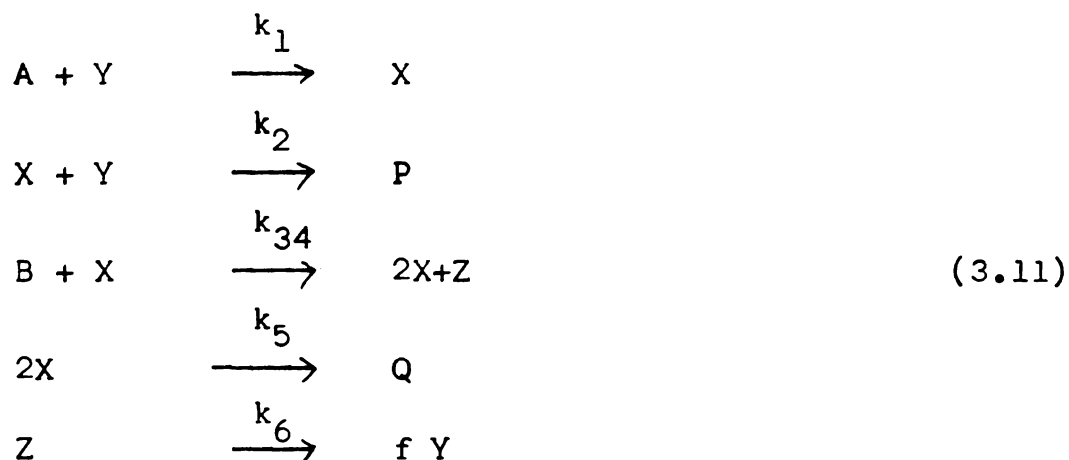
And also it is set

$$\begin{aligned} A &= B = [\text{BrO}_3^-] \\ P, Q &= \text{Waste product concentration} \end{aligned} \quad (3.10)$$

Then from the reactions (M1)-(M5), we can see that,

- (i) describes the conversion of Y to X,
- (ii) implies the simultaneous inactivation of X and Y,
- (iii) indicates the catalytic generation of X,
- (iv)
- (v) the bimolecular decomposition of X and the global reaction,
- (vi) indicates the transformation of Z into Y.

Hence we have the following scheme,



Here,  $f$  is a suitable stoichiometric coefficient, the rate constants  $k_1$  to  $k_{34}$  contain the effect of bromomalonic acid. A comparison with the detailed mechanism [15] suggests the following values for the rate constants [63].

$$\begin{array}{lcl}
 k_1 & = & 1.34 \text{ M}^{-1} \text{ S}^{-1} \\
 k_2 & = & 1.6 \times 10^9 \text{ M}^{-1} \text{ S}^{-1} \\
 k_{34} & = & 8 \times 10^3 \text{ M}^{-1} \text{ S}^{-1} \\
 k_5 & = & 11 \times 10^7 \text{ M}^{-1} \text{ S}^{-1}
 \end{array} \tag{3.12}$$

The values of  $k_6$  and the stoichiometric coefficient  $f$  are used as parameters in general [60]. But in our discussion we fix  $k_6 = 1$  and only  $f$  is used as the system parameter. Also in the region studied experimentally,  $A = B = [\text{BrO}_3^-] = 0.06\text{M}$ ,  $[\text{H}^+] = 0.8\text{M}$ .

The differential equations describing the dynamics of the model obtained by applying the law of mass action to the reactions (M1)-(M5) are as follows.

$$\begin{aligned}\frac{dX}{dt} &= k_1AY - k_2XY + k_3BX - 2k_4X^2 \\ \frac{dY}{dt} &= -k_1AY - k_2XY + k_6Z \\ \frac{dZ}{dt} &= k_3BX - k_6Z.\end{aligned}\tag{3.13}$$

The dimensionless scheme of (3.13) is given as

$$\begin{aligned}\frac{dx}{d\tau} &= s(y-xy+x-qx^2) \\ \frac{dy}{d\tau} &= \frac{1}{s}(-y-xy+fz) \\ \frac{dz}{d\tau} &= w(x-z)\end{aligned}\tag{3.14}$$

These equations represent a system of nonlinear coupled ordinary differential equations with  $x, y, z, \tau, q, s$  and  $w$  as,

$$\begin{aligned}x &= (k_2/k_1)X, & y &= (k_2/k_{34}^B)Y \\ z &= (k_2k_6/k_1k_{34}^{AB})Z, & \tau &= (k_1k_{34}^{AB})^{\frac{1}{2}}.t \\ q &= 2k_1k_5^A/k_2k_{34}^B, & s &= k_{34}^B/k_1^A \\ w &= k_6/k_1k_{34}^{AB}\end{aligned}\tag{3.15}$$

For the estimates given above, we have

$$q = 8.375 \times 10^{-6}, \quad s = 77.27 \quad \text{and} \quad w = 0.161 k_6$$

We notice that the system (3.14) involves two time scales, since the evolution of  $x$  is very large, whereas that of  $y$  and  $z$  by inverse time constants of order less than unity.

Since the three-variable model (3.14) is nonlinear, coupled and stiff in nature, it cannot be integrated directly. Therefore we first present a discussion of the two variable model,  $y$ - $z$  system which is more interesting than the  $x$ - $z$  system. Rinzel and Troy [65] have discussed the  $x$ - $z$  system in detail.

#### 3.4. TWO VARIABLE OREGONATOR MODEL

As mentioned earlier, the values of the constants  $s$ ,  $1/s$  and  $w$  in (3.14) suggest that the evolution of  $x$  is much faster than  $y$  or  $z$ . The pseudo-steady state hypothesis  $\dot{x} \equiv 0$ , ie.

$$y - xy + x - qx^2 \equiv 0 \tag{3.16}$$

provides a value of  $x$  as a function of  $y$ , say  $g(y)$ . When this value of  $x$ , viz.  $g(y)$  is introduced in the  $x$ - $y$ - $z$  model, the  $y$ - $z$  model is obtained. When we discuss this  $y$ - $z$  model, we restrict our attention to the parametric

values  $f > 1$ . The second half of this section describes the behaviour of the system for  $0 < f < 1$ .

The quadratic equation (3.16) gives,

$$x = g(y) = [1-y + [(1-y)^2 + 4yq]^{\frac{1}{2}}] / 2q \quad (3.1)$$

where  $y > 0$ .

Now, the  $y$ - $z$  model can be cast in the form,

$$\begin{aligned} \dot{y} &= [-y(1+g(y)) + fz] / s \\ \dot{z} &= w[g(y)-z] \end{aligned} \quad (3.1)$$

The model (3.18) exhibits oscillatory behaviour over an appropriate range of the controlling parameter  $f$ . Limit cycles for the system are obtained numerically for several values of  $f$  and some of them are given towards the end of this section.

The steady state solutions of the system is obtained by solving  $\dot{y} = \dot{z} = 0$ , we have  $g(y_0) = z_0$ . And  $\dot{y} = 0$ , implies  $y_0 = (f \cdot g(y_0)) / (1+g(y_0))$ .

$$\text{ie. } y_0 = fz_0 / (1+z_0) \quad (3.1)$$

From the complete model (3.14),  $\dot{z} = 0$ , implies,  $x_0 = z_0$ .

Then by using (3.19) and (3.16), we can have

$$qz_0^2(1+z_0) - z_0(1+z_0) - y_0(1+z_0) + fz_0^2 = 0$$

$$\text{ie. } qz_0^2 - (1-f-q)z_0 - (1+f) = 0 \quad (3.20)$$

$$\therefore z_0(f) = \frac{1}{2q} \left\{ (1-f-q) \pm [(1-f-q)^2 + 4q(1+f)]^{\frac{1}{2}} \right\} \quad (3.21)$$

Also from (3.16), we can have the following relation

$$qz_0^2 - z_0 + y_0(1+z_0) - 2y_0 = 0$$

$$\text{ie. } 2y_0 = qz_0^2 - z_0 + fz_0 \quad (3.22)$$

Applying (3.22) in (3.20) we have,

$$2y_0 = 1+f - qz_0$$

$$\therefore y_0(f) = \frac{f+1}{2} \text{ (approximately)} \quad (3.23)$$

We can expand  $y_0$  and  $z_0$  as powers of  $q$ , since  $q = O(10^{-5})$ .

Consider the discriminant of the equation (3.21), we have

$$[(1-f-q)^2 + 4q(1+f)]^{\frac{1}{2}} \approx (1-f-q) + 2q \left( \frac{1+f}{1-f} \right) + \frac{q^2}{2(1-f)}$$

$$\therefore z_0(f) \approx \frac{f+1}{f-1} + O(q)$$

$$\approx \frac{f+1}{f-1} \quad (3.24)$$

Thus the approximate value of the equilibrium solution is

$$[y_0(f), z_0(f)] = \left[ \frac{f+1}{2}, \frac{f+1}{f-1} \right]$$

The  $y$ - $z$  system (3.18) can be modified, by introducing the variable

$$\begin{aligned} z^*(y) &= \frac{y(1+g(y))}{f}, \text{ as} \\ \dot{y} &= (-z^*(y) \cdot f + fz)/s \\ \dot{z} &= w(g(y)-z) \end{aligned} \quad (3.25a)$$

Now applying the linear transformation  $Y = y - y_0$ ,  $Z = z - z_0$  and using Taylor series expansion, we have the linearized matrix,  $A$  as follows,

$$A = \begin{bmatrix} -\frac{f}{s} & \frac{dz^*(y_0)}{dy} & \frac{f}{s} \\ w \cdot \frac{dg(y_0)}{dy} & & -w \end{bmatrix} \quad (3.25b)$$

From (3.17), we can have the approximation for  $g(y)$  as

$$g(y) \approx \frac{y}{y-1} + O(q) \quad (3.26)$$

$$\therefore \frac{dg(y)}{dy} \approx \frac{-1}{(y-1)^2} < 0 \quad (3.27)$$

$$\frac{dz^*}{dy} = \frac{1}{f} [yg'(y) + 1 + g(y)]$$

$$\therefore \frac{dz^*(y)}{dy} = \frac{1}{f} \left[ \frac{2(y-1)^2 - 1}{(y-1)^2} \right] \quad (3.28)$$

The roots  $\lambda_1, \lambda_2$  of the  $\det (A-\lambda I)$ , determine the stability of  $(y_0, y_z)$  and satisfy the equations,

$$T = \lambda_1 + \lambda_2 = -\frac{f}{s} \frac{dz^*(y_0)}{dy} - w \quad (3.29)$$

$$\Delta = \lambda_1 \lambda_2 = \frac{wf}{s} \frac{dz^*(y_0)}{dy} - \frac{dg(y_0)}{dy} \quad (3.30)$$

From (3.27) and (3.28) we have

$$\frac{dz^*}{dy} > \frac{1}{f} \frac{dg}{dy} \quad (3.31)$$

Using the trace  $T$  (sum of the eigen values) and the determinant  $\Delta$  (product of the eigen values) of the matrix  $A$ , we can discuss the topological structure of the steady state  $(y_0, z_0)$ . Both the eigen values are real if  $T^2 > 4\Delta$ . Because the accessible phase plane is bounded and the uniqueness of steady state solution in the positive  $y$ - $z$  quadrant lead to the requirement that, for this model,  $\Delta > 0$ , and hence both real roots have the same sign.  $T < 0$  corresponds to the stable node, while  $T > 0$  gives the unstable node. When  $T^2 = 4\Delta$ , the two roots become equal. When  $T^2 < 4\Delta$ , the roots are complex conjugate and the steady state is a focus, which is stable or unstable depending upon the sign of  $T$ .



The steady state  $(y_0, z_0)$  is a stable node, when  $\frac{dz^*(y_0)}{dy} > 0$ . i.e. when  $f > 1 \pm \sqrt{2}$ . i.e. when  $f > 1 + \sqrt{2}$ . When  $\frac{dz^*(y_0)}{dy} < 0$ , with a small enough  $w$ , and  $\frac{dz^*(y_0)}{dy} - \frac{dg(y_0)}{dy} > 0$  implies the steady state is an unstable node. Hence the range of  $f$ , where the unstable node lies is

$$f < 1 + \sqrt{2} \quad \text{and} \quad f > 1.$$

$$\text{i.e.} \quad 1 < f < 1 + \sqrt{2} \quad (3.33)$$

As  $f$  crosses the critical value  $f = 1 + \sqrt{2}$ , unstable node becomes a stable one. Hence the real bifurcation occurs.

When the roots are complex conjugate, the steady state is a focus, which is stable or unstable depending upon the sign of  $T$ . Since the accessible phase plane is bounded, the Poincare-Bendixson theorem requires that an unstable node or focus is always surrounded by at least one stable limit cycle. When  $T = 0$ , the system undergoes a Hopf bifurcation as it makes a transition between stable and unstable foci. If that bifurcation is supercritical, the associated stable focus is globally attracting [3].

The value of  $f$  (say  $f = f_1$ ) at which a Hopf bifurcation occurs in our system satisfies,

$$\frac{dz^*(y_0)}{dy} = -\frac{ws}{f} \quad (3.34)$$

Using (3.28) we have

$$(2+ws) (y_0-1)^2 = 1$$

$$\therefore y_0 = \frac{1+(2+ws)^{1/2}}{(2+ws)^{1/2}} \quad (3.35)$$

From (3.23), for  $f = f_1$ , we can have

$$f_1 = 2y_0 - 1$$

$$\text{ie. } f_1 = 1 + \frac{2}{(2+ws)^{1/2}} \quad (3.36)$$

Then at  $f = f_1$ , the eigen values of  $A$  have zero real part (to first order in  $q$ ).

Let the eigen values have the form

$$\lambda_1 = \alpha_0 + i\omega_0, \quad \lambda_2 = \alpha_0 - i\omega_0$$

where  $\alpha_0 = 0$  and hence the eigen values are  $\pm i\omega_0$ .

Considering the characteristic equation of (3.25b)

with  $\lambda_1, \lambda_2 = \pm i\omega_0$ , we have

$$T = 0 \quad \text{and} \quad \Delta = \omega_0^2$$

Thus

$$\begin{aligned} \lambda_1, \lambda_2 &= \pm i \sqrt{\Delta} \\ &= \pm \left[ \frac{w}{s} \frac{(2(y_0-1)^2 - 1 + f_1)}{(y_0-1)^2} \right]^{\frac{1}{2}} \\ &= \pm i \left[ \frac{2w}{s} [1 + (2+ws)^{\frac{1}{2}}] \right]^{\frac{1}{2}} \end{aligned}$$

$\omega_0$  can be expressed in terms of  $f_1$  as follows,

$$\lambda_1, \lambda_2 = \pm i \left[ \frac{2w}{s} \left( \frac{f_1+1}{f_1-1} \right) \right]^{\frac{1}{2}} \quad (3.37)$$

Here, for sufficiently small  $|f-f_1| > 0$ ,  $\omega_0$  gives the frequency of oscillation of small perturbations from  $(y_0, z_0)$ . The condition for the existence of complex eigen values for the matrix A can be obtained in the form,

$$\left[ 1 - \frac{2}{(f-1)^2} + \frac{ws}{2} \right]^2 < \frac{4wsf}{(f-1)^2}$$

$$\therefore \left| 1 - \frac{2}{(f-1)^2} + \frac{ws}{2} \right| < \frac{2\sqrt{fws}}{f-1} \quad (3.38)$$

By the Hopf bifurcation theorem discussed in chapter two, we can test the behaviour of the steady state solution as  $f$  crosses the threshold value  $f_1$ .

$$\frac{d}{df} [\text{Re } \lambda]_{f=f_1} = - \frac{(2+ws)^{\frac{3}{2}}}{2s} \quad (3.39)$$

The loss of stability at  $f=f_1$  is thus a classical Hopf bifurcation in which

$$\alpha'(0) = \text{Re } \lambda'(f_1) \neq 0$$

and hence periodic solutions are observed out of the stationary state  $(y_0, z_0)$ .

For  $f \lesssim 1$ , the above mentioned approximations are not valid. In this range of  $f$ , the following approximations [19] for  $(y_0, z_0)$  are used.

$$\begin{aligned} z_0 &\approx \frac{1-f}{q}, \quad \text{when } f < 1 \\ &\approx \sqrt{\frac{2}{q}}, \quad \text{when } f \approx 1 \end{aligned} \quad (3.40)$$

The corresponding value for  $y_0$  can be obtained using (3.19). From (3.40), it is to be noted that  $z_0$  be of  $O(10^5)$  and we cannot proceed further in this direction analytically. But numerically, some results are obtained for the whole range,  $\frac{1}{2} < f < 1 + \sqrt{2}$ , which is discussed below.

To solve the two-variable system (3.18) numerically, we used a fourth order Runge-Kutta method with the step doubling technique (Section 2.6). Oscillation occurs only for  $0.5 < f < 1+\sqrt{2}$ . In this range of  $f$ , limit cycles are obtained for certain values of  $f$  in the  $y$ - $z$  plane. We have plotted  $\log z$  vs.  $\log y$ . The initial values set for the computation is  $(y_0, z_0) \approx (1.0, 488.8)$  and the values of the parameters as,  $s = 77.27$ ,  $q = 8.375 \times 10^{-6}$ , and  $w = 0.161$ .

At  $f = 0.5$  an 'L' shaped solution curve is obtained instead of closed trajectory, and the solution  $(y, z)$  blows out at the dimensionless time  $\tau = 30$  [Fig.1(a)]. But for a value of  $f$ , very near to 0.5, ie. at  $f = 0.5001$ , a limit cycle is formed and the trajectory just closes at  $\tau = 297.0$ . According to Bar Eli and Noyes [3], all limit cycles (stable and unstable) can occur in the range of  $0.50005 < f < 1.9475$ . Our results are in confirmatory with this observation. Fig.1(b) gives the limit cycle corresponding to  $f = 0.5001$  and it is in the shape of a pentagon.

An incomplete trajectory in the  $y$ - $z$  phase plane is obtained for  $f = 0.6$  and the solution blows out at  $\tau = 340.0$ , [Fig.2(a)]. The same behaviour is observed [Fig.2(b)] for the parametric value  $f = 0.7$  and the solution blows up at  $\tau = 235.0$ . But at  $f = 0.74$ , a complete limit cycle [Fig.3(a)] is obtained and it closes at  $\tau = 375.0$ . For the parametric

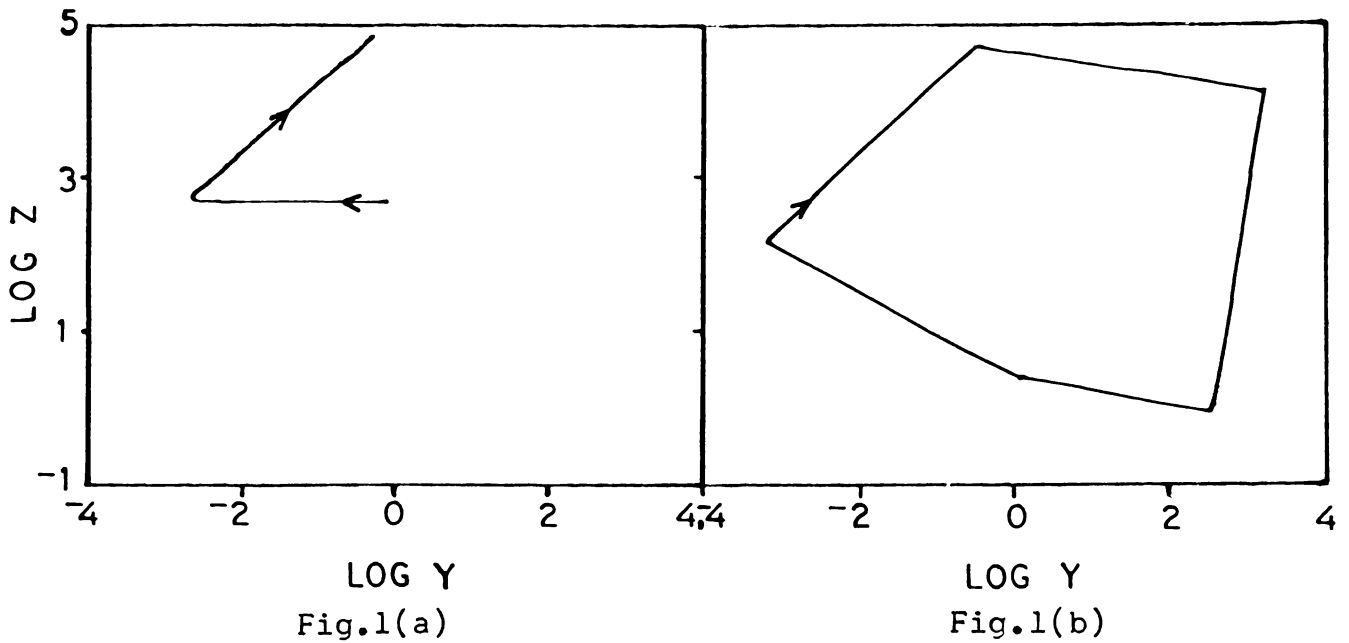


Fig.1(a). Phase plane plot of  $\log_{10}[\text{Ce}^{4+}](z)$  vs.  $\log_{10}[\text{Br}^{-}](y)$  obtained by the numerical integration of equations (3.18). The trajectory corresponds to the parametric value  $f=0.5$  and it blows out at  $\tau = 30$ . The steady state  $(y_0, z_0) = (1.0, 488.8)$  and the values for  $s = 77.27$ ,  $q = 8.375 \times 10^{-6}$ ,  $w = 0.161$  are used throughout this work. The arrow indicates the direction of time evolution.

Fig.1(b). Limit cycle obtained from the system (3.18), for  $f=0.5001$  which closes at  $\tau = 297.0$ .

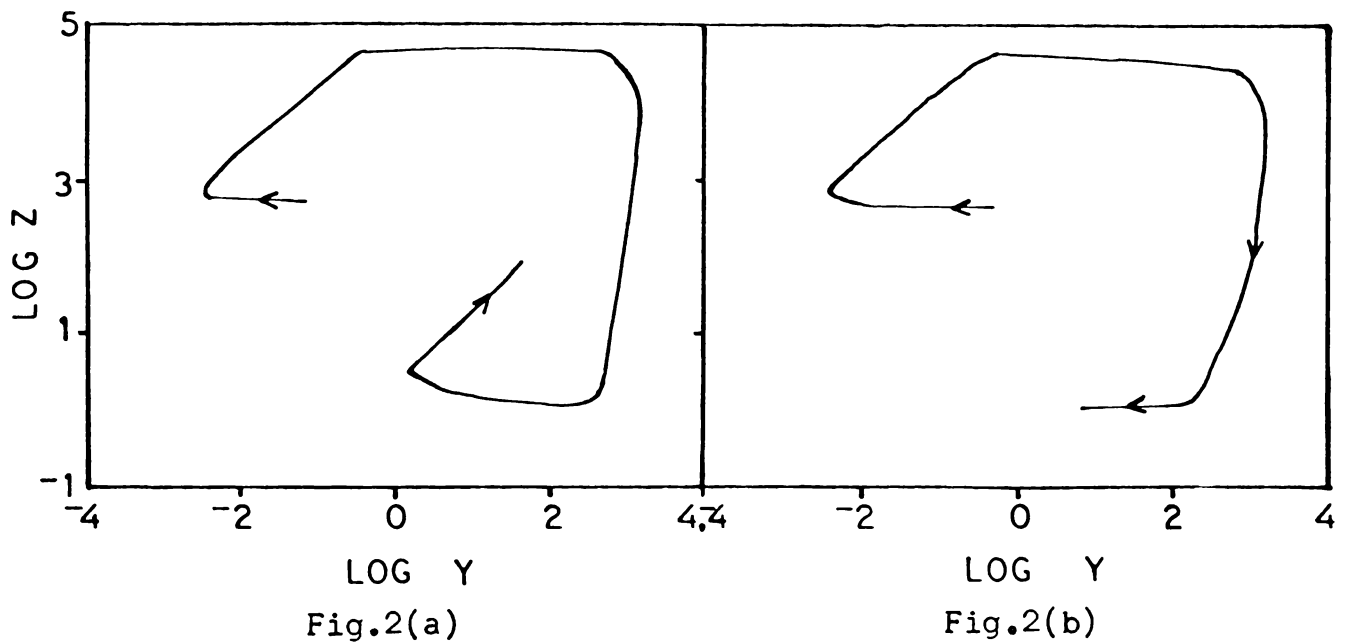


Fig.2(a). Phase plane diagram of  $\log_{10}z$  vs.  $\log_{10}y$  obtained by numerical integration of equations (3.18). The incomplete limit cycle corresponds to the parametric value  $f = 0.6$ , and the solution blows out at  $\tau = 340.0$ .

Fig.2(b). Phase plane plot of  $\log_{10}z$  vs.  $\log_{10}y$  obtained by the numerical integration of (3.18). The trajectory corresponds to the parametric value  $f = 0.7$ , and which blows up at  $\tau = 235.0$ .

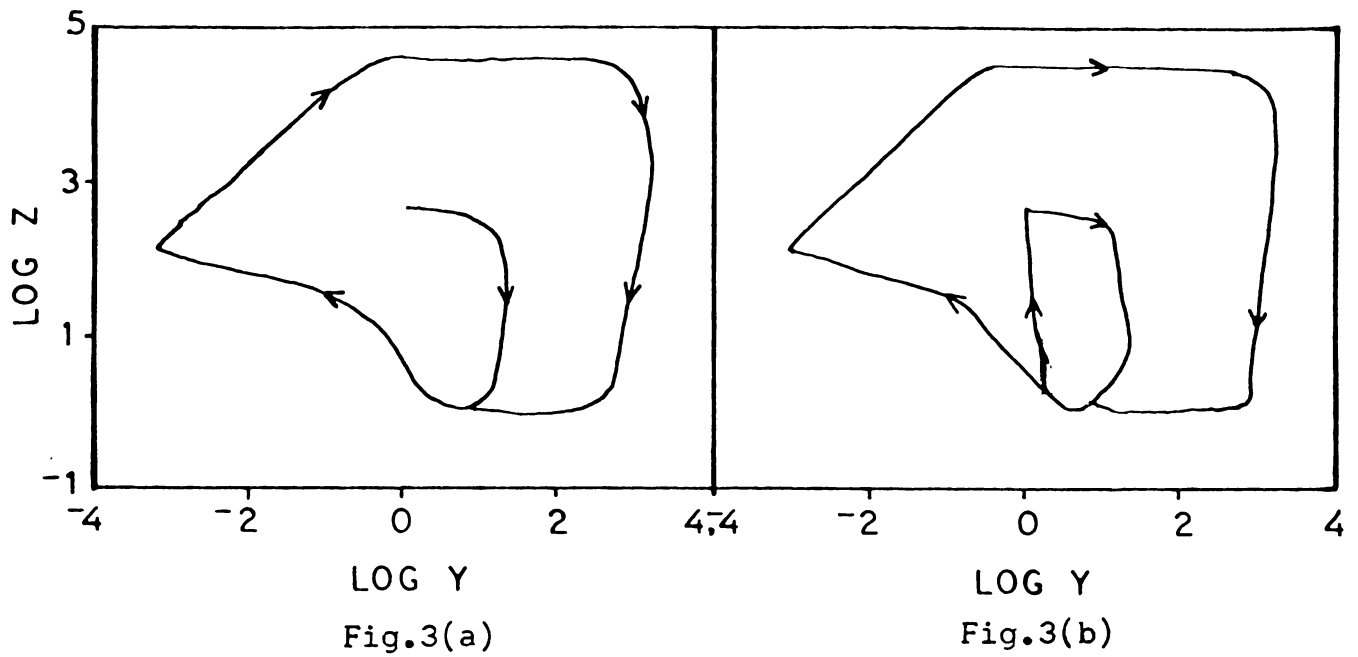


Fig.3(a). Limit cycle obtained for the system (3.18) for the parametric value  $f = 0.74$ , where  $\log_{10} z$  is plotted against  $\log_{10} y$ . The period is  $\tau = 375.0$ .

Fig.3(b). The unstable limit cycle surrounded by the stable one for the system (3.18) corresponds to  $f = 0.8$ .  $\log_{10} z$  is plotted against  $\log_{10} y$ . This leads to hard self excitation.



value  $f = 0.8$ , an unstable limit cycle surrounded by a stable limit cycle [Fig.3(b)] is obtained. The steady state is locally stable, then Fig. 4(a) illustrates the existence of an unstable periodic solution, surrounding the steady state and wholly inside the stable limit cycle. This situation is often called hard self-excitation because though there exists a self-excited oscillation (ie. an orbitally asymptotically stable limit cycle), it takes a hard (finite) perturbation to move the system out of the domain of attraction of the stable resting state. In the two-dimensional case, a separatrix may be an unstable limit cycle, which separates a locally stable steady state or limit cycle from a surrounding locally stable limit cycle.

Isolated limit cycles are observed [Fig.4(a) and (b)] at the parametric values, viz.  $f = 0.9$  and  $f = 1.0$  and the period of oscillation are  $\tau = 448.0$  and  $\tau = 395.0$ . More than one limit cycle is obtained for some values of  $f$  greater than 1.0. At  $f = 1.1$ , two limit cycles are formed simultaneously, in the sense that, the first one is formed from  $\tau = 0$  to  $\tau = 353.0$  and the next starts from  $\tau = 353.0$  and winds up at  $\tau = 743.9$  (ie. with a period 390.9). These two limit cycles are shown [Fig. 5(a) and (b)] separately.

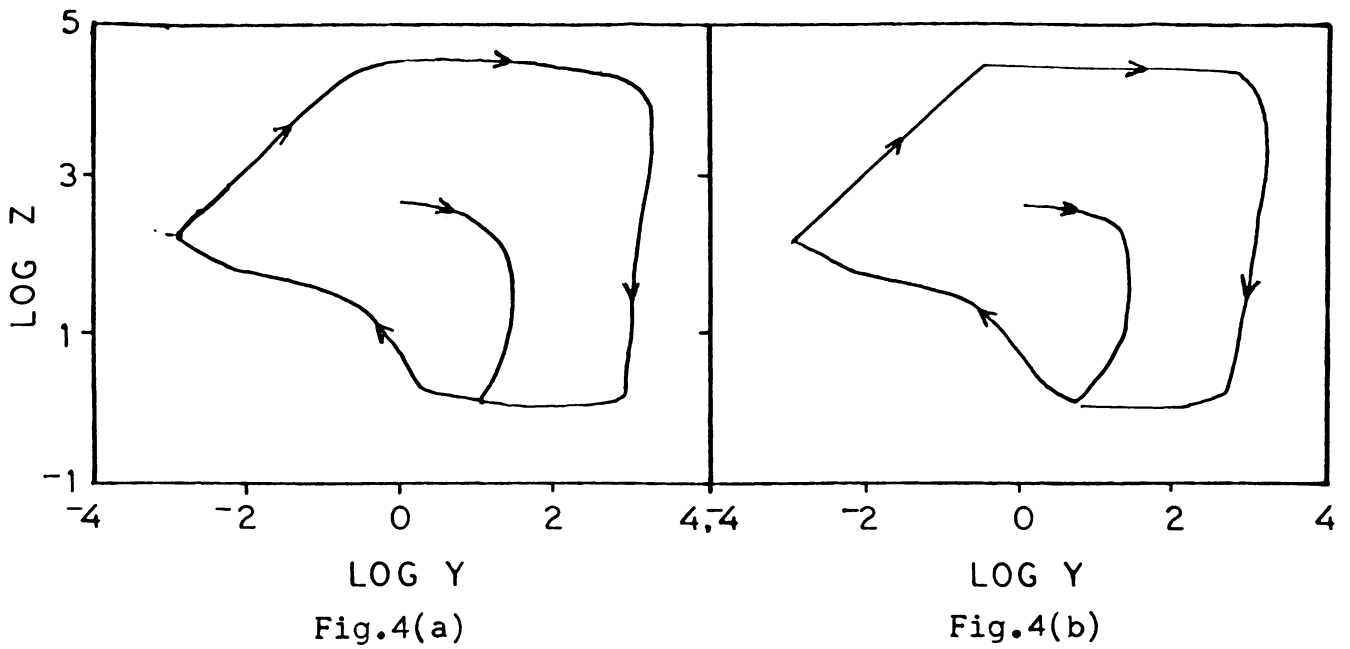


Fig.4(a). The isolated limit cycle of the system (3.18) corresponds to  $f = 0.9$ , when  $\log_{10}z$  is plotted vs.  $\log_{10}y$ . This limit cycle formed at  $\tau = 448.0$

Fig.4(b). The isolated limit cycle in the  $\log_{10}y - \log_{10}z$  plane of the system (3.18) corresponding to  $f = 1.0$ , which completes at  $\tau = 395.0$ . Field and Noyes [19] found their limit cycle closed at  $\tau = 302.9$ .

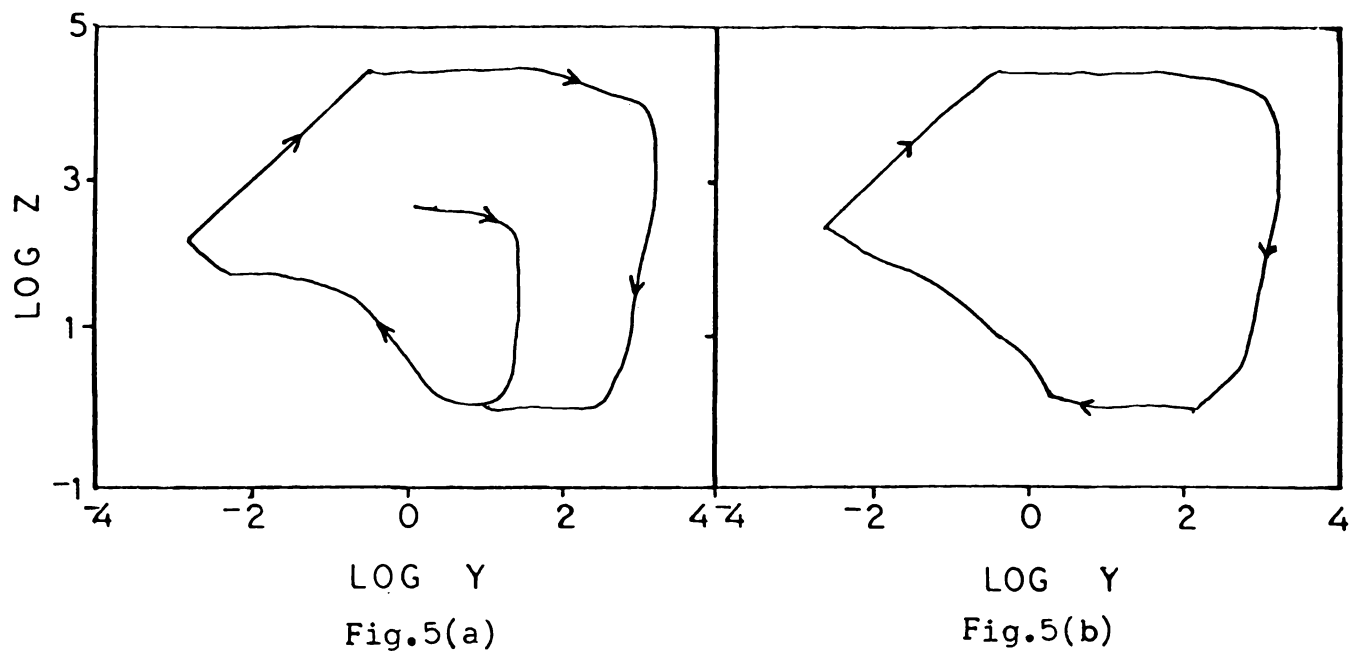


Fig.5(a). The limit cycle of the system (3.18) at  $f = 1.1$  in the  $\log_{10}Y - \log_{10}Z$  plane formed from  $\tau = 0$  to  $\tau = 353.0$ .

Fig.5(b). The second limit cycle for the Y-Z model at  $f = 1.1$ , from  $\tau = 353.0$  to  $\tau = 743.9$  (period = 390.9)  $\log_{10}Z$  is plotted against  $\log_{10}Y$ .

For  $f = 1.3$  [Fig.6(a)] and  $f = 1.4$  [Fig.6(b)], single closed trajectories are formed. Former closes at  $\tau = 425.0$ , while the latter closes at  $\tau = 432.3$ . The isolated limit cycle [Fig.7(a)] formed at  $f = 1.5$  closes at  $\tau = 458.6$ . It is very interesting to note that for  $f = 1.2$ , there are three limit cycles. First one forms with a period  $\tau = 376.16$ . The second one starts from  $\tau = 376.16$  to  $\tau = 736.9$ . The third starts from  $\tau = 736.9$  to  $\tau = 982.0$ .

It may be noted that for values, 0.74, 0.9, 1.0, 1.3, 1.4, 1.5, there arise only one limit cycle and for some other values of  $f$  like 1.2 there arise more than one limit cycle. This behaviour indicates that in this particular range of  $f$ , something more than the oscillatory behaviour of the system happens. We can expect excitability in this region. In the previous section, the qualitative analysis of the steady state solution  $(y_0, z_0)$  of (3.18) we have seen that  $(y_0, z_0)$  is an unstable node in the parameter range  $1 < f < 1 + \sqrt{2}$  and therefore by Poincare-Bendixson theorem, we can have limit cycle solutions for the system. Theoretically the Hopf bifurcation occurs at  $f_1$  and which is estimated as  $f_1 = 1.526$ , using the parameter values,  $s = 77.27$  and  $w = 0.161$ .

Three limit cycles [Fig.8 (a), (b) and (c)] are obtained for a parametric value  $f = 1.595288$ , which is very close to  $f_1$ .

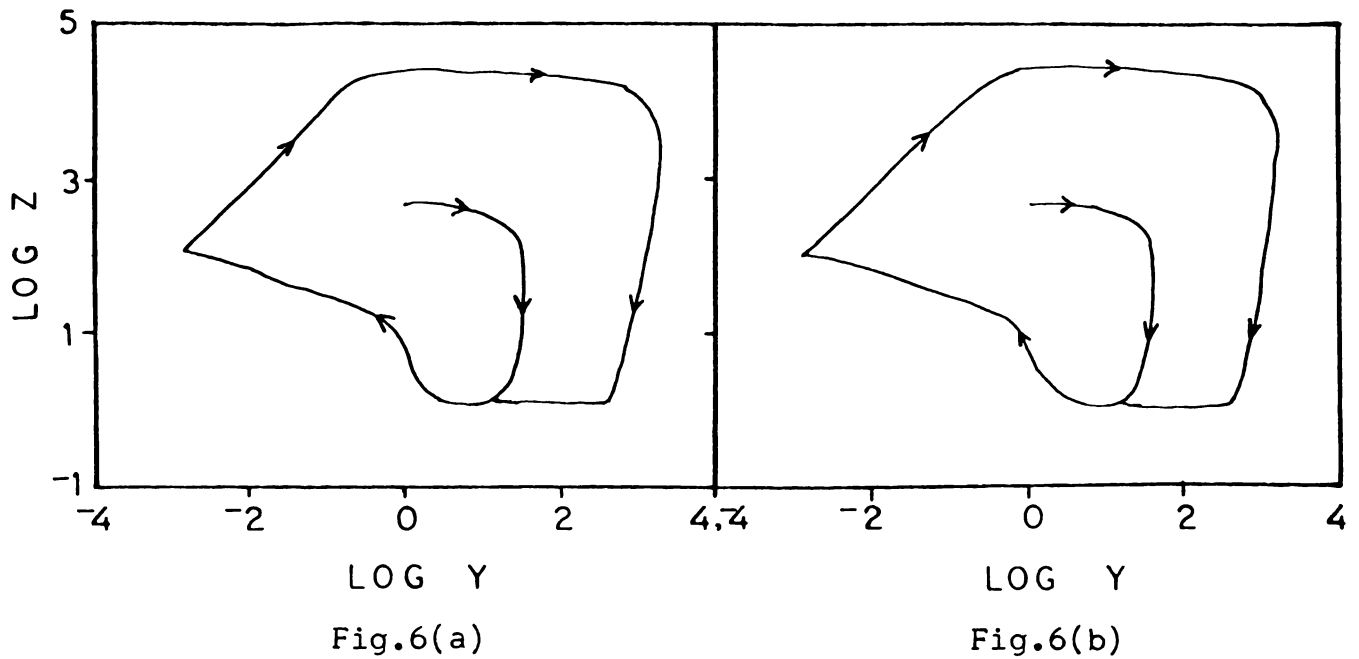


Fig.6(a). Phase plane plot of  $\log_{10}z$  vs.  $\log_{10}y$  obtained by the numerical integration of the system (3.18). The isolated closed trajectory corresponds to the parametric value  $f=1.3$ , with period 425.0.

Fig.6(b). Numerical solution of the system (3.18) is represented graphically by plotting  $\log_{10}z$  vs.  $\log_{10}y$ . The limit cycle corresponds to the parametric value  $f=1.4$ , with period 432.3.

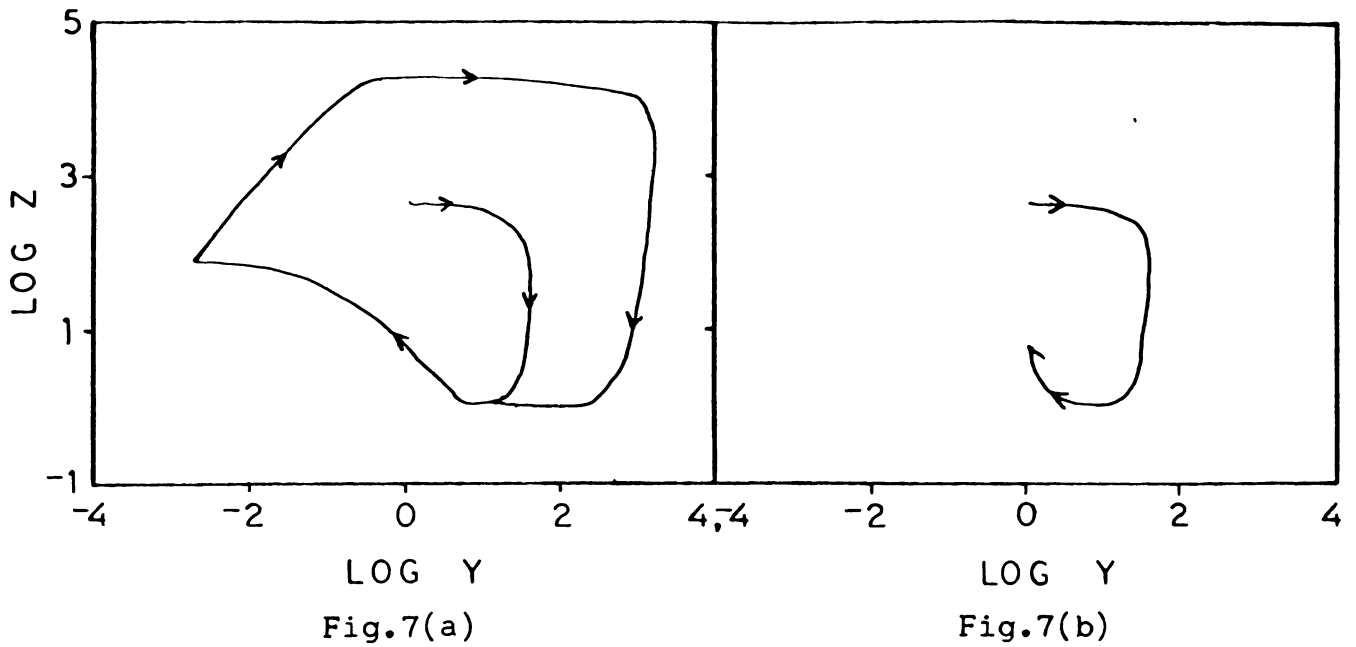
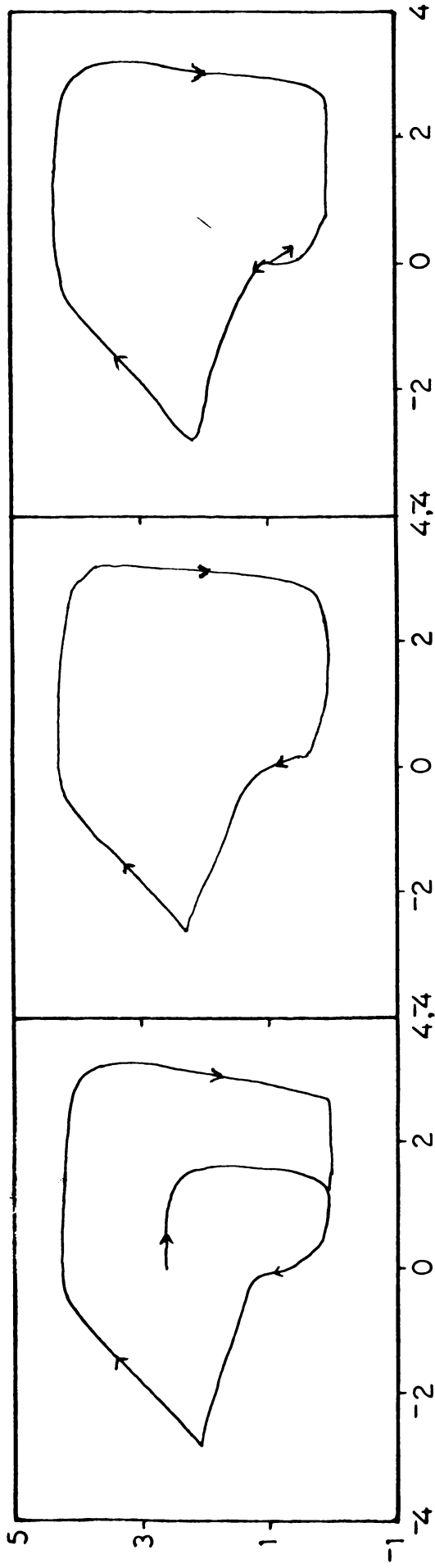


Fig.7(a). The isolated limit cycle corresponds to the parametric value  $f=1.5$  with period 458.6.  $\log_{10}z$  is plotted against  $\log_{10}y$ .

Fig.7(b). The phase plane plot of  $\log_{10}z$  vs.  $\log_{10}y$  obtained for the system (3.18) at  $f=1.6$ . After a time  $\hat{\tau}=381.0$ , the trajectory comes steady at a point  $(\log_{10}y, \log_{10}z) = (0.113, 0.639)$



LOG Y  
Fig.8(a)

LOG Y  
Fig.8(b)

LOG Y  
Fig.8(c)

Fig.8(a) The numerical solution of the system of equations (3.18), at  $f = 1.595288$  when  $\log_{10} z$  is plotted against  $\log_{10} y$ . The limit cycle forms from  $\hat{\tau} = 0$  to  $\hat{\tau} = 454.1$ .

Fig.8(b) The second limit cycle of the system (3.18) corresponds to the parametric value  $f = 1.595288$  forms from  $\hat{\tau} = 454.1$  to  $\hat{\tau} = 860.92$

Fig.9(c) The third limit cycle corresponds to the parametric value  $f = 1.595288$  forms from  $\hat{\tau} = 860.92$  to  $\hat{\tau} = 1265.0$

The first limit cycle is formed by taking a period  $\tau = 454.1$ , second one with period  $\tau = 406.82$  and the third with period 404.08. Then the trajectory continues to be steady at a point  $(\log_{10}y, \log_{10}z) = (0.113, 0.639)$ . The existence of more than one limit cycle at this point indicates the possibility of excitability in the region,  $1 < f < 1 + \sqrt{2}$ .

We have not come across any limit cycle behaviour for the system (3.18) in the parametric range,  $f < 0.5$  or  $f > 1.6$ .

We have presented here a series of figures obtained, explaining the behaviour of the system. The intermediate concentrations are clearly oscillatory in time and the plots qualitatively supports the experimental [19] observations in the B-Z reaction. The critical bromide ion concentration,  $[\text{Br}^-]_c$  can be read from the  $\log [\text{Br}^-]$  plot, at which the spikes form.  $\log_{10}y$  and  $\log_{10}z$  are plotted against the time  $\tau$ . The spikes corresponding to  $\log_{10}y$  and  $\log_{10}z$  form at the same time  $\tau$ . That is the bromide-ion concentration at which the concentration of the ceric-ion changes from one phase to another (ie. increases or decreases) at the same time. From the  $\log_{10}y$  vs. time plot, we can see that the concentration of bromide-ion was in plenty and it decreases till the  $[\text{Br}]_c$  and the concentration of bromide-ion shoots up again and this procedure continues. For the parametric



values,  $f = 0.74, 0.9, 1.0, 1.3, 1.4$  and  $1.5$  only one spike is obtained. This is depicted graphically in this chapter. At the point where the spikes are forming, the reaction switches from pathway (3.2) to the pathway (3.3).

More than one spike are seen for the parametric values viz.  $f = 1.1, f = 1.2$  and  $f = 1.595288$ . Two spikes are seen (Fig.10) at  $f = 1.1$ . Three spikes unequally spaced are seen [Figs. 11 and 12] for  $f = 1.2$  and  $f=1.595288$ . Obviously, the number of spikes indicates the number of limit cycles formed for the system.

For the parametric value  $f = 0.8$ , the spike forms at  $\tau = 130.0$  and at  $f = 0.9$ , the spike forms at  $\tau = 133.0$  [Fig.9(a)]. For  $f = 1.0$ , the spike appears at  $\tau = 139.0$  [Fig.9(b)]. At the parametric value  $f = 1.1$ , the first spike forms at  $\tau = 145.0$ , followed by the second one at  $\tau = 448.0$ . Figure 11 gives three spikes at  $\tau = 151.0, 457.0$  and  $762.0$  for the parametric value  $f = 1.2$ . Similarly the spikes of concentration profile of  $y$  and  $z$  for  $f = 1.595288$  are formed at  $\tau = 193.0, 530.0$  and  $865.0$ .

For  $f = 1.3$ , the spike forms at  $\tau = 158.0$ , for  $f = 1.4$ , the spikes forms at  $\tau = 165.0$  and for  $f = 1.5$ , the spike forms at  $\tau = 173.0$ . No spikes are observed for  $f = 0.5, 0.6, 0.7, 1.6, 1.7$  etc.

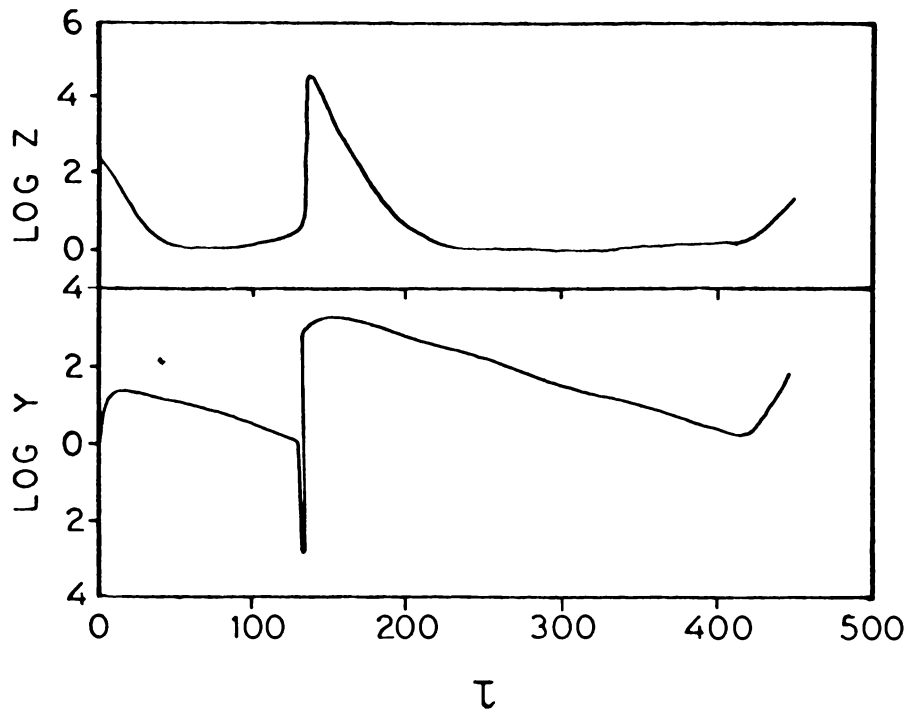


Fig.9(a)

Fig.9(a). Traces of  $\log_{10}z$ ,  $\log_{10}y$  vs. time( $\tau$ ). The integration used  $f=0.9$ . The Process I(3.2) is occurring during the long stretches when  $[\text{Br}^-]$  or ( $y$ ) is high and Process II (3.3) is occurring when the sharp spikes of  $[\text{Br}^-]$  or ( $y$ ) appear. The spikes corresponding to  $\log_{10}y$  and  $\log_{10}z$  are forming at  $\tau=133.0$ .

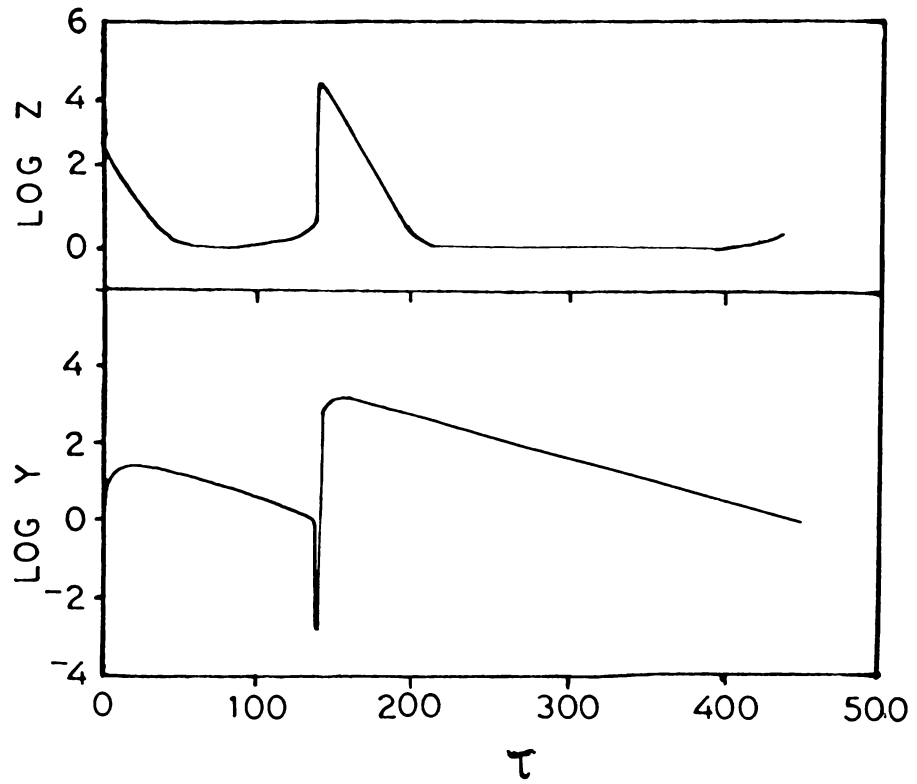


Fig.9(b)

Fig.9(b) Traces of  $\log_{10}z$ ,  $\log_{10}y$  vs. time( $\tau$ ) obtained by the numerical integration of (3.18) at  $f=1.0$ . The spikes corresponding to  $\log_{10}y$  as well as  $\log_{10}z$  are forming at  $\tau = 139.0$ .

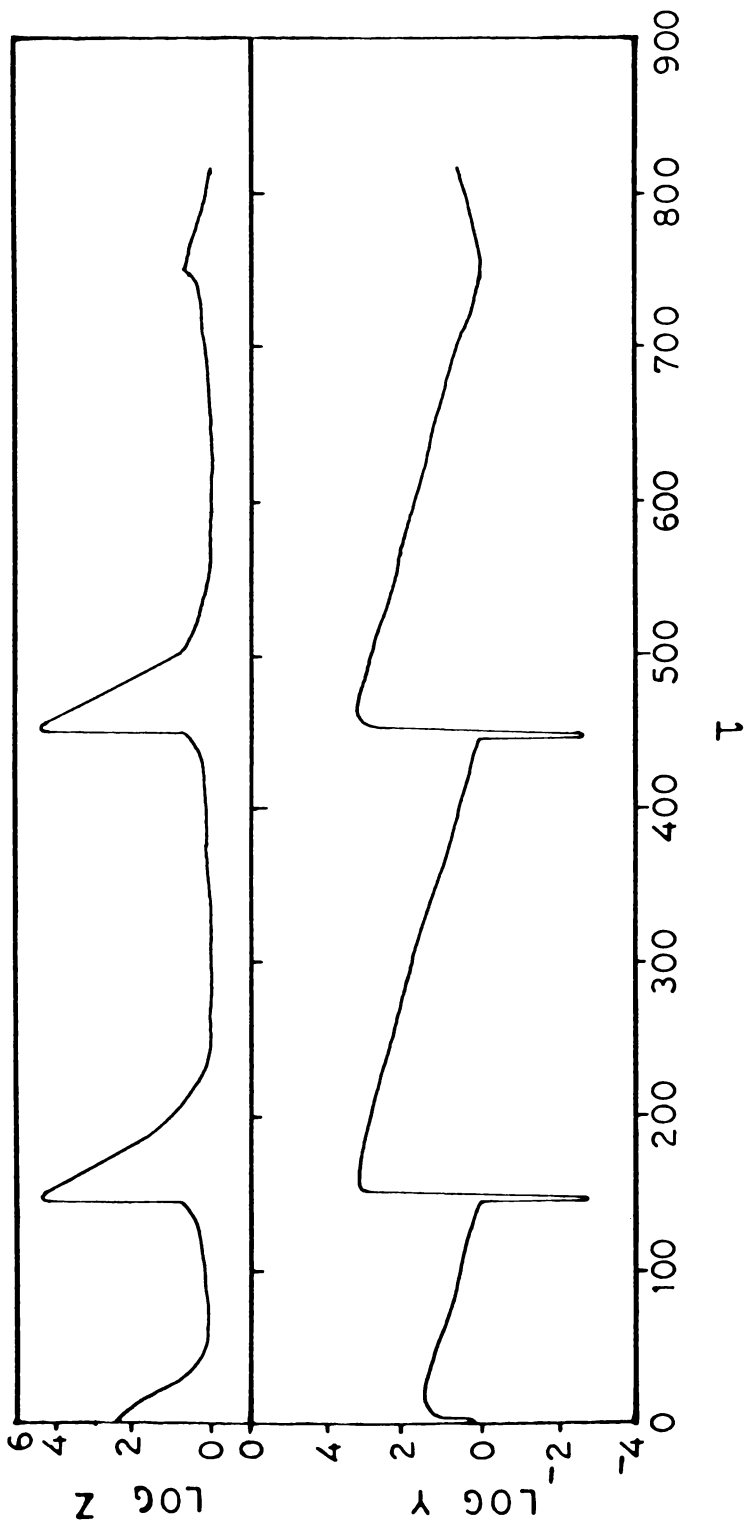


Fig.10

Fig.10. The two spikes corresponding to  $\log_{10} z$  and  $\log_{10} y$  obtained by tracing  $\log_{10} z$  and  $\log_{10} y$  vs.  $\text{time}(\tau)$  on integration of (3.18) at  $f=1.1$ . The first spike forms at  $\tau = 145.0$  and the second at  $\tau = 448.0$ .

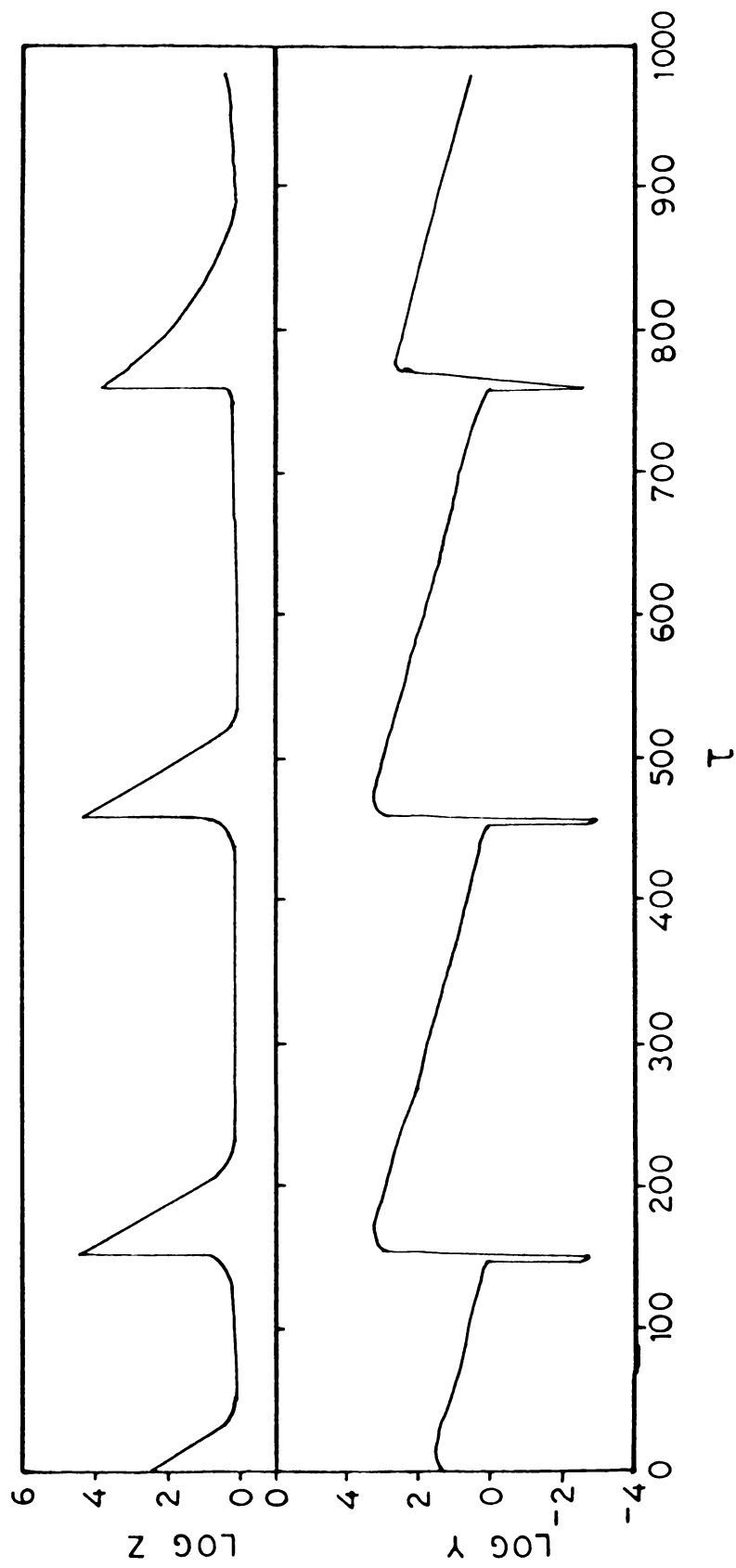


Fig.11.

The three spikes obtained by tracing  $\log_{10} z$  and  $\log_{10} \gamma$  vs. time ( $\tau$ ) at the parametric value,  $f=1.2$ . The first spike forms at  $\tau = 151.0$ , the second one at  $\tau = 457.0$  and the third at  $\tau = 762.0$ .

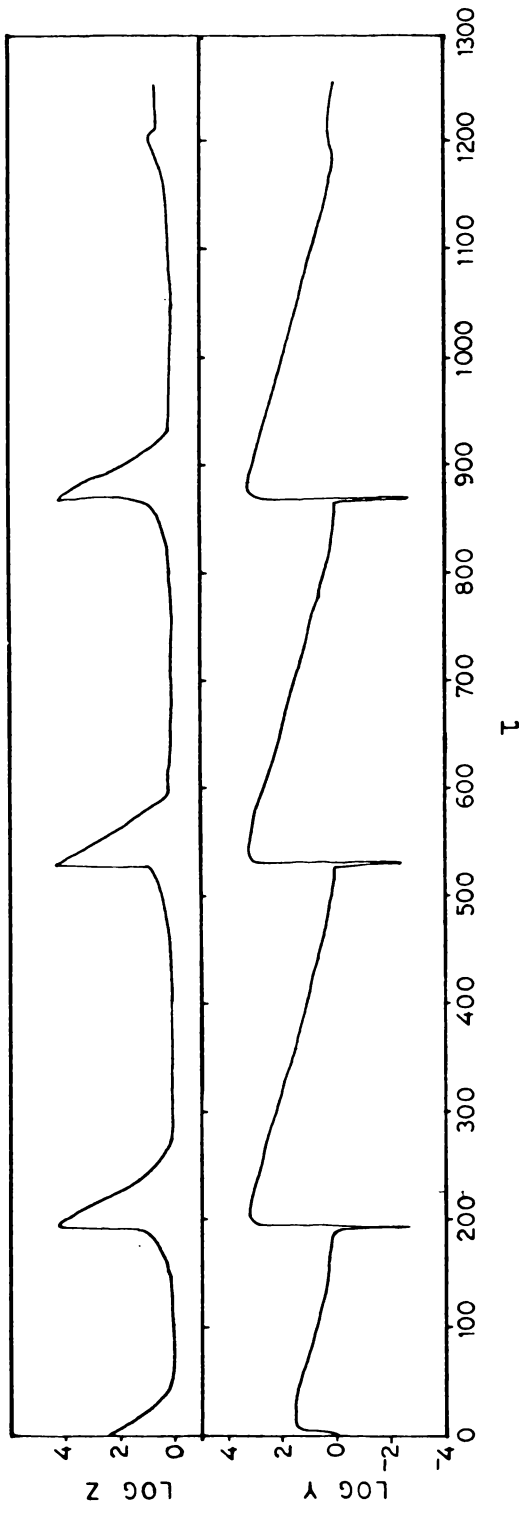


Fig.12

Fig.12. The three spikes corresponding to  $\log_{10} z$  and  $\log_{10} y$  obtained by tracing them against time ( $\tau$ ), on ontegration of (3.18) at  $f=1.595288$ . The spikes form respectively at  $\tau=193.0$ ,  $530.0$  and  $865.0$ .

From all these we can conclude that the critical bromide-ion concentration ( $[Br]_c$ ) varies as  $f$  varies.

A special type of behaviour for the trajectory of the system (3.18) at the parametric value 1.6 is to be mentioned. The trajectory starting from the initial value  $(y_0, z_0) = (1.0, 488.8)$  observed to be attracted by another steady state (1.297, 4.355). Fig.7(b) depicts the phase plane plot of  $\log_{10}z$  vs.  $\log_{10}y$  for the parametric value 1.6. The same type of behaviour is exhibited by the system (3.18) for some other parametric values, viz. 1.7, 1.8, 1.9, 2.0, 2.1., etc.

### 3.5. THREE-VARIABLE MODEL

The three-variable model (3.14) of the B-Z chemical reaction is a system of 'Stiff' differential equations, as stated earlier. It is convenient to express (3.14) in the vector form,

$$\dot{\mathbf{r}} = \mathbf{F}(\mathbf{r}; s, w, f, q); \quad \mathbf{r} = (x, y, z)$$

where

$$\mathbf{F} = \begin{bmatrix} s(y-xy+x-qx^2) \\ \frac{1}{s}(-y-xy+fz) \\ w(x-z) \end{bmatrix} \quad (3.41)$$

The possibility of oscillatory solutions, almost always depends on the existence of at least one unstable non-zero steady state of the system of governing equations. This point in  $r$ -space is enclosed by the trajectory of the periodic solution of (3.41) given by setting  $\dot{r} = 0$ , are

$$r = (0,0,0), \quad r = r_0 = (x_0, y_0, z_0)$$

$$z_0 = x_0, \quad y_0 = \frac{fx_0}{1+x_0} = \frac{1}{2}(1+f-qx_0) \quad (3.42)$$

where

$$qx_0^2 + [q-(1-f)]x_0 - (1+f) = 0 \quad (3.43)$$

(There is another steady state for which  $x_0 < 0$ , but this is unrealistic). In (3.42) and (3.43), if  $q \geq 0$ ,  $f \geq 0$ , then  $x_0 \geq 0$ ,  $y_0 \geq 0$ ,  $z_0 \geq 0$ .

The stability of the steady state is given by linearizing (3.41) about  $r = 0$  and  $r = r_0$ . First, let us consider the trivial equilibrium state  $r = 0$ . The linearized form of (3.14) is given by simply neglecting the quadratic terms and the corresponding linearized matrix  $A$  is as follows.

$$A = \begin{bmatrix} s & s & 0 \\ 0 & \frac{1}{s} & \frac{f}{s} \\ w & 0 & -w \end{bmatrix} \quad (3.44)$$



The eigen values  $\lambda$  of A satisfy

$$\lambda^3 - \lambda^2 \left[ s - \frac{1}{s} - w \right] + \lambda \left[ \frac{w}{s} - ws - 1 \right] - w(f+1) = 0 \quad (3.45)$$

The three solutions  $\lambda_1, \lambda_2$  and  $\lambda_3$  of (3.45) satisfy  $\lambda_1 \cdot \lambda_2 \cdot \lambda_3 = w(1+f) > 0$  and therefore, there is at least one root with a positive real part and so the equilibrium state  $r = 0$  is unstable. An oscillatory solution enclosing  $r = 0$  is physically uninteresting, since it would necessarily require negative values for  $x, y$  and  $z$ , that is, negative concentrations.

For the nontrivial steady state  $r=r_0$ , we take the linear transformation  $X = x-x_0, Y = y-y_0, Z = z-z_0$  and accordingly, we can have the linear matrix,

$$U = \begin{bmatrix} s-sy_0-2qsx_0 & s-sx_0 & 0 \\ -y_0/s & -1/s - x_0/s & f/s \\ w & 0 & -w \end{bmatrix} \quad (3.46)$$

From the  $\det |U - \lambda I|$ , we get the characteristic equation as,

$$\lambda^3 - \tau \lambda^2 + \delta \lambda - \Delta = 0$$

Where,

$$\begin{aligned}
T &= -(E+w), \quad \delta = wE+R, \quad \Delta = w[-R+f(1-x_0)] \\
E &= sy_0 + \left(\frac{1}{s} + 2qs\right)x_0 + \frac{1}{s} - s \\
R &= 2qx_0^2 - x_0(1-q) + f
\end{aligned} \tag{3.47}$$

The possibility of having limit cycle type oscillations is when  $(x_0, y_0, z_0)$  is an unstable critical point. Then at least one of the eigen values of U must have positive real part. The necessary and sufficient conditions for the roots of the cubic polynomial to have negative real parts are (2.15),

$$T < 0, \quad \Delta < 0, \quad \Delta - T\delta > 0.$$

The first two conditions are satisfied for all realistic values of the parameters  $s, w, f$  and  $q$ . Now let us consider the third inequality

$$\Delta - T\delta = Ew^2 + w(f(1-x_0) + E^2) + ER \tag{3.48}$$

Clearly, (3.48) is a quadratic in  $w$  and therefore

$$w = -\frac{1}{2E}(E^2 + f(1-x_0)) \pm \frac{1}{2E}[(E^2 + f(1-x_0))^2 - 4E^2R]^{\frac{1}{2}} \tag{3.49}$$

Then the instability condition which is the reverse of the third inequality can be cast in the form,

$$0 < w < w_c(f) \tag{3.50}$$

Where the stability curve  $w_c(f)$  is given by (3.49) and (3.50) is meaningful only if the right hand side is positive and this requires,

$$2qx_0^2 + x_0(q-1) + f < 0 \quad (3.51)$$

Applying the necessary and sufficient conditions (2.24) for the boundedness of solutions of (3.41), Murray [54] obtained the bounds of the solutions as

$$\begin{aligned} 1 \leq x \leq \frac{1}{q}, \quad y_1 \leq y \leq y_2, \quad 1 \leq z \leq \frac{1}{q} \\ y_1 = \frac{fq}{1+q}, \quad y_2 = \frac{f}{2q} \end{aligned} \quad (3.52)$$

Hastings and Murray [36] proved, using topological methods, that the model equations (3.14) possess at least one finite amplitude periodic trajectory. The same result is proved using bifurcation theory. The existence of a periodic solution for the complete model (3.14) is proved asymptotically by Stanshine (1975) [58].

The classical Hopf bifurcation theorem [35] is applied to estimate the Hopf bifurcation point (say)  $f_c$  of the system (3.14). If the characteristic equation (cubic) has purely imaginary roots,  $\lambda_{1,2} = \pm i\omega_0$  and one real root (say)  $\lambda_3$ , then the characteristic equation can

be expressed in the form,

$$\lambda^3 - \lambda_3 \lambda^2 + \omega_0^2 \lambda - \lambda_3 \omega_0^2 = 0$$

Comparing the coefficients of the above with the general cubic characteristic equation, we have,

$$\lambda_3 = \tau, \quad \delta = \omega_0^2, \quad \Delta = \lambda_3 \omega_0^2 \quad (3.53)$$

Hence,

$$\text{the real root} = - (E + w) \quad (3.54)$$

which is always negative.

and

$$\omega_0 = \pm i [ wE + R ]^{\frac{1}{2}} \quad (3.55)$$

Also,

$$- [ wE^2 + ER + w^2E + wR ] = wf(1-x_0) - wR$$

Putting  $R = R_1 + f$ , we have

$$- [ wE^2 + E(R_1 + f) + w^2E ] = wf(1-x_0)$$

$$\therefore f_c = \frac{-E [ w^2 + wE + R_1 ]}{E + w(1-x_0)} \quad (3.56)$$

Differentiating the general cubic characteristic equation, with respect to the parameter  $f$  and simplifying, we get,

$$\begin{aligned}
 \lambda'(f) &= \frac{wx_0 - \lambda}{3\lambda^2 - 2\lambda\Gamma + \delta} \\
 &= - \frac{[w(1+x_0) + E]}{\omega_0^2 + \Gamma^2} < 0 \quad (3.57)
 \end{aligned}$$

Thus the loss of stability at  $f = f_c$  given by (3.56) is a classical Hopf bifurcation.

Results are obtained numerically to support the above fact, viz. for certain values of  $f$ , stable limit cycles exist for the system. This indicates that the system (3.14) exhibits Hopf bifurcation. Field and Noyes[19] have considered the case for only one parametric value,  $f = 1.0$ .

Since the complete model (3.14) is stiffly coupled, it cannot be integrated directly. The true solutions of differential equations, as  $y$  tends to large values,  $x$  tends to 1.0 and  $\frac{dx}{d\tau}$  tends to zero. That is, for higher values of  $y$ , slight errors in  $x$  caused by round off, propagate to produce very large computed values of  $\frac{dx}{d\tau}$ , when its value is actually approaching to zero. This problem can be eliminated by putting  $\frac{dx}{d\tau} = 0$ , where  $x$  and  $\frac{dx}{d\tau}$  began to oscillate during the integration. A complete limit cycle in the  $y$ - $z$  phase plane is obtained [19] for  $f = 1.0$ , with a period  $\tau = 309.2$ . A limit cycle in the  $y$ - $x$  phase plane is also obtained for the same parametric value.

If a reasonable accuracy is to be maintained, the integration must be carried out over exceedingly small increments. We used the Runge-Kutta method, with the step doubling technique (Section 2.6) to integrate the complete Oregonator Model (3.14). We obtained closed isolated trajectories in the  $y-x$  phase plane only. Fig.13 gives the isolated limit cycle of the system (3.14) in the  $y-x$  phase plane for the parametric value  $f = 1.0$  and it closes at  $\tau = 143.5$ . A limit cycle in the  $y-x$  phase plane, for one more parametric value viz.  $f = 1.1$  is obtained (Fig.14) with a period  $\tau = 148.9$ .

For the three-variable model (3.14), complete limit cycle in the  $y-z$  phase plane is not observed using the Runge-Kutta step doubling method. The solution trajectory in this phase plane blows out (Fig.15) at  $\tau = 143.5$ , for the parametric value  $f = 1.0$ . The same behaviour for the solution trajectory is obtained in the  $y-z$  phase plane for  $f = 1.1$  also. The numerical integration of the complete model is very much time consuming.

### 3.6. DISCUSSION

To study the temporal oscillations in the B-Z reaction quantitatively, the model proposed by Field and Noyes [19] is used here. The overall net reaction of the

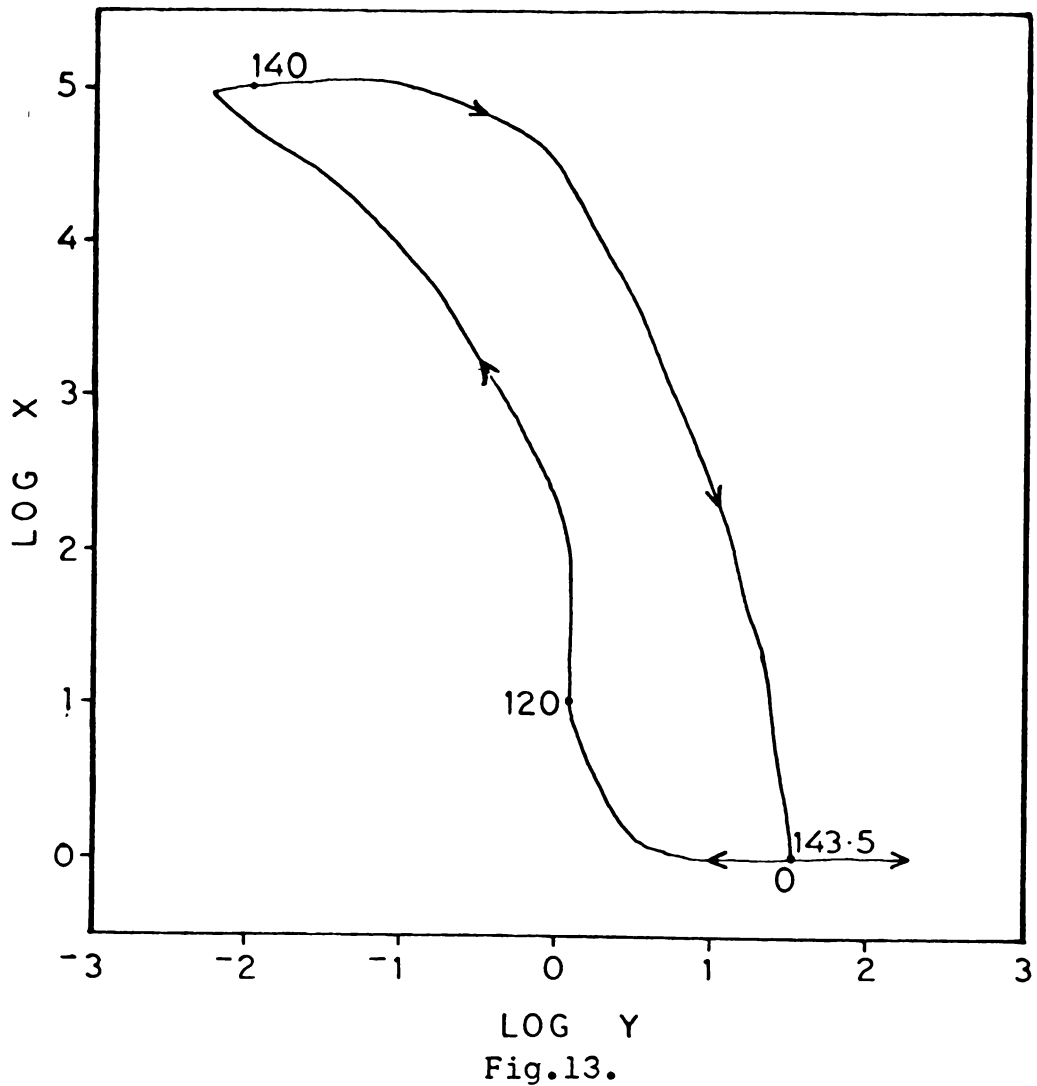
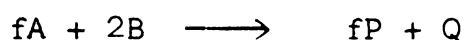


Fig.13. Projection of limit cycle solution for the complete Oregonator model (3.14) in the space of logarithmic variables  $y$  and  $x$  for the parametric value  $f=1.0$ . Note  $\log_{10}$  scale. The initial value taken for the integration of the X-Y-Z system is  $(x_0, y_0, z_0) = (488.8, 1.0, 488.8)$ . The values taken for the parameters  $s, w$  and  $q$  are respectively 77.27, 0.161 and  $8.375 \times 10^{-6}$ . The arrow heads indicate the direction of time evolution and the numbers indicates times in the cycle.  $\tau=143.5$  for the entire cycle.

T  
 1.17.73  
 MEK

five step reaction model (3.11) according to Field and Noyes [19] is as follows:



Here,  $f$  is the stoichiometric factor and which indicates the quantity of production of the control intermediate ( $\text{Br}^-$ ) in the second half of the oscillatory process. As the concentration of the bromide ion crosses the critical concentration value, the first half of the reaction (3.2) proceeds. Thus actually, the oscillatory mode depends on the controlling parameter  $f$ . Hence it is necessary for us to investigate the behaviour of the model for several values of  $f$ .

The oscillatory behaviour of the complete model (3.14) as well as the two-variable model (3.18) is studied in detail only for  $f = 1.0$  so far. A topological proof for the existence of at least one periodic solution for the complete model (3.14) is given by Hastings and Murray [36]. The bounds for the solutions of the complete model was given in 1974 [54]. The reversibility of each reaction step was also taken into consideration by Field [15]. In the CSTR Model [41] the species A (or  $[\text{BrO}_3^-]$ ) and P (or  $[\text{HOBr}]$ ) are treated as dynamic variables and so it is a five-dimensional model. They predict that at  $A = 0.06\text{M}$  and  $k_6 = 1$ , the steady state of the model is unstable and oscillation occurs for the parametric range,  $0.5010693 < f < 1.526776$ .

-G4051-



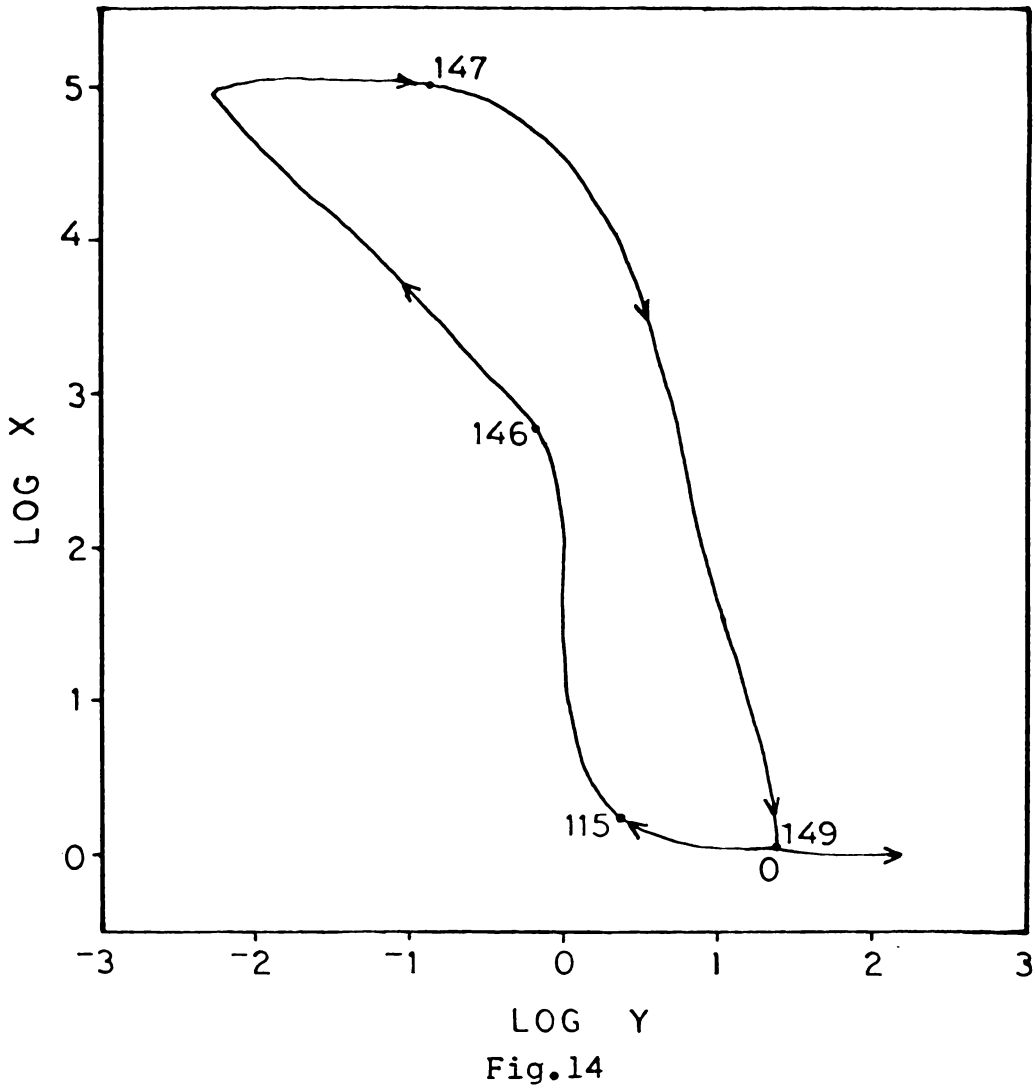


Fig.14. Stable limit cycle of the complete model (3.14) in the  $\log_{10}Y - \log_{10}X$  plane at the parametric value  $f=1.1$ . The initial values of the variables and the other parametric values are taken as mentioned in Fig.13.  $\tau = 148.9$  for the entire cycle.

Tyson [75] investigated the behaviour of solutions of the Oregonator model and predicted that, for  $\frac{1}{2} < f < 1 + \sqrt{2}$ , there exists a stable limit cycle for the model. Hard self excitation (subcritical bifurcation) is believed to occur in the B-Z reaction.

In the investigation of the oscillatory behaviour of the y-z system, limit cycles are obtained numerically for several values of f in the range  $\frac{1}{2} < f < 1 + \sqrt{2}$ . Isolated limit cycles are observed for the parametric values, 0.5001, 0.74, 0.9, 1.0, 1.3, 1.4 and 1.5 in the y-z phase plane, for the simplified model (3.18). It is interesting to note that, at  $f = 1.1$ , two limit cycles are observed. Again at  $f = 1.2$  and  $f = 1.595288$ , three limit cycles are seen. At these points, some behaviour other than oscillatory is observed. The excitability property of the system is expected at these values of f. When the system jumps from the oscillatory mode to the excitable mode or vice-versa, SNIPER (Stable Node Infinite Period) bifurcation may occur, for certain parametric values. Then we could expect some special properties like SNIPER in some particular range of f as suggested by Bar Eli and Noyes [3]. The chaotic behaviour of the B-Z reaction is discussed by Hudson and Mankin [38].

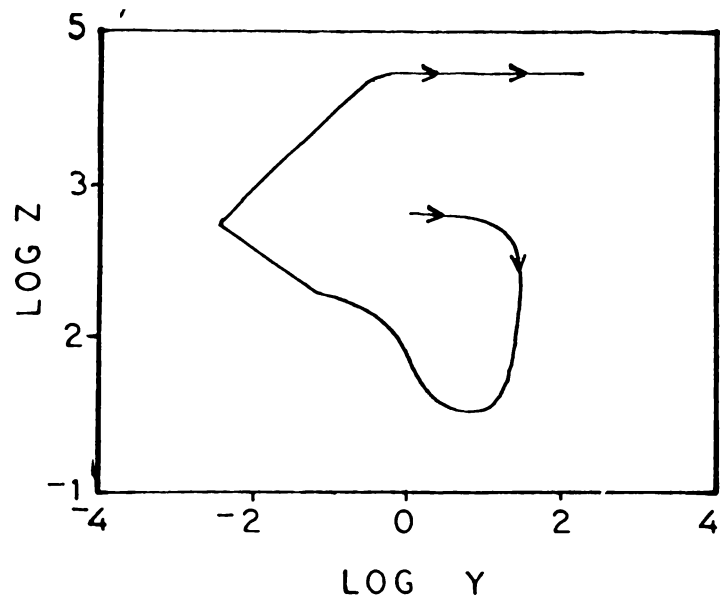


Fig.15.

Fig.15. The trajectory obtained by the numerical integration of the complete model (3.14) in the  $\log_{10}y$ - $\log_{10}z$  plane for  $f=1.0$ . The solution blows out at  $\tau=143.5$ . Same type of trajectory is obtained for the system(3.14) at  $f=1.1$  also.

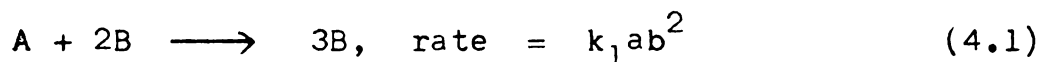
## Chapter 4

### MODEL STUDIES ON A CUBIC AUTOCATALYTIC SYSTEM

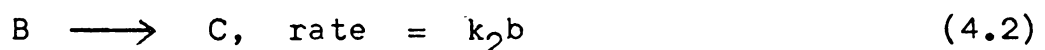
#### 4.1. INTRODUCTION

The interest in the theoretical and experimental studies of oscillating reactions is increasing very rapidly. The pioneering work of Lotka (1920) [34] and Volterra (1931) on the oscillatory behaviour of the competing biological species lead to the discovery of many mathematical models to explain the observed periodicities. An important feature common to many of the observed oscillatory reactions, isothermal in nature, is that of autocatalysis.

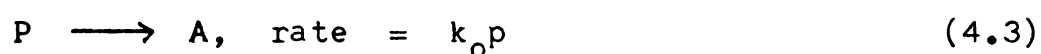
Gray and Scott [27,28,29] and Scott [52] introduced a two reaction scheme which constitutes one of the simplest known oscillators that operated in an isothermal well-stirred open system. This is also a good example of the Continuously Stirred Tank Reactor (CSTR). This model involves a cubic autocatalysis.



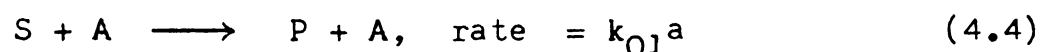
and a first order decay reaction



with only these two components, the analysis provide a complete, algebraically tractable system which exhibit many complex patterns of behaviour. Merkin et al. [52] investigated an adaptation of the Gray-Scott cubic autocatalator, as a model for long-lived oscillatory behaviour in a closed vessel. Instead of having a constant inflow, the reactant A is envisaged as being formed by the decay of a precursor species P,



In this study we adapt the following reaction step

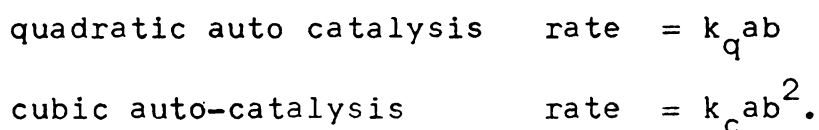


where S is the substrate and which is in abundance. The species P undergoes chemical transformation through two intermediate species A and B to the final product C, which is thermodynamically more stable. This transition is interrupted by a train of oscillatory excursions in the concentrations of the intermediates. In a system, where the species P decreases steadily initially, A,B (autocatalyst) and C increases in the beginning, then the oscillations sets in the concentrations of A and B. Eventually the oscillations die out. In our model, the oscillations in the species P also sets in. This oscillatory behaviour remains for a very long time.

We have presented briefly in Section (4.2) the MNS model analysed by Merkin et al. [52]. In Section (4.3) the more detailed model of the oscillator involving autocatalysis is presented. The stationary states and the oscillatory behaviour of the present model is discussed in Section (4.4). The limit cycles obtained in the X-Y, Y-Z and Z-X phase planes for the system numerically are presented in Section (4.5).

#### 4.2. MNS MODEL

Autocatalysis is shared not only by the Belousov-Zhabotinskii reaction, a wide range of halide-based oscillators but by numerous enzyme systems. All mechanistic schemes include autocatalytic steps. However, even the simplified forms of these schemes (for eg. Brusselator [58] and Oregonator [19] ) are still complicated and necessitates studies of even simpler prototypes in a logically ordered way. Gray and Scott [27,28,29] considered the overall stoichiometry,  $A \longrightarrow B$ , satisfying the rate law  $= k_a$ . When the same change is catalyzed by a species Y and has a rate  $= k_{ay}$ , this is considered as  $A+Y \longrightarrow B+Y$ . Autocatalysis corresponds to catalysis by the product itself. Two exemplary cases [27,29] span the whole range of behaviour likely to be encountered,



These may be represented by the chemical equations,



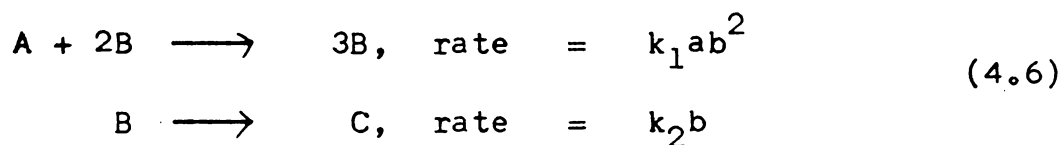
and



The simplest decay of B is via a first order process,



This adds another dimension to the system, as there are three species concentrations and still only one relationship exists between them. Most importantly, the concentrations of A and B may now vary independently of each other— a requirement for oscillatory behaviour. Almost all of the special features of these autocatalytic systems can be highlighted by studying the system,



This initial concentrations of A and B are taken as  $a_0$  and  $b_0$ . It is to be noted that,  $k_1 a_0^2$  has units of  $S^{-1}$ . It is the inverse of a characteristic [27,28] chemical time scale,

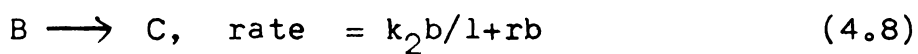
$$t_{ch} = 1/k_1 a_0^2 \quad (4.7)$$

where  $a_0$  is the initial concentration of A in the reactor flow.

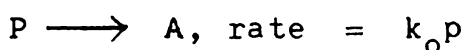
Note that, we need not consider a third differential equation for the concentration of the product C, as this is uniquely determined at all times by the concentrations of A and B in the reactor and the inlet conditions,

$$c = (a_0 + b_0) - (a+b)$$

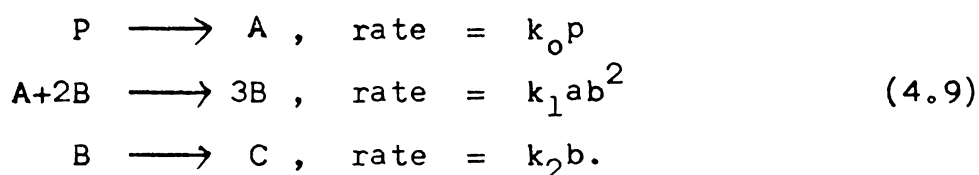
Merkin et al. [50,51] studied the quadratic autocatalytic system, with a modification viz. the quadratic step is coupled with a more complex removal of the autocatalyst,



In 1986, Merkin et al. [52] (MNS Model) modified the cubic autocatalytic reaction scheme of Gray and Scott [27,28,29], by considering a new reaction step. In this scheme, the first intermediate A is formed via, the slow decay of a reactant or precursor species P as,



Thus the MNS scheme is





Now, the governing differential rate equations are,

$$\begin{aligned}\frac{dp}{dt} &= -k_0 p \\ \frac{da}{dt} &= k_0 p - k_1 a b^2 \\ \frac{db}{dt} &= k_1 a b^2 - k_2 b\end{aligned}\tag{4.10}$$

On introducing the dimensionless concentrations and time

$$\begin{aligned}\alpha &= a/a_0, \quad \beta = b/a_0 \\ \pi &= p/a_0 \text{ and } \tau = k_1 a_0^2 t\end{aligned}$$

(4.10) becomes

$$\begin{aligned}\frac{d\pi}{d\tau} &= -\eta' \pi \\ \frac{d\alpha}{d\tau} &= \eta' \pi - \alpha \beta^2 \\ \frac{d\beta}{d\tau} &= \alpha \beta^2 - \beta/\tau_2\end{aligned}\tag{4.11}$$

where  $\tau_2 = k_1 a_0^2 / k_2$  is the dimensionless catalyst time, and

$$\eta' = k_0 / k_1 a_0^2.$$

The system (4.11) is nonlinear, coupled and it cannot be solved easily. The 'pool chemical approximation' was used to reduce the system (4.11) into a simpler two dimensional

model. Under this approximation, the early period of the reaction is modelled with the precursor concentration assumed constant and set equals to its initial value  $p_0$ . The first of the above equations (4.11) involves only the concentration of the precursor and can be integrated to give,

$$\pi = \pi_0 e^{-\eta'\tau}$$

where  $\pi_0 = p_0/a_0$  in the dimensionless form for the initial concentration of P. Introducing this result into the three dimensional model (3.11) gives rise the following two dimensional model

$$\begin{aligned} \frac{d\alpha}{d\tau} &= e^{-\eta'\tau} - \alpha\beta^2 \\ \frac{d\beta}{d\tau} &= \alpha\beta^2 - \beta/\tau_2 \end{aligned} \tag{4.12}$$

where  $\mathcal{K} = \eta' \pi_0$ .

The initial conditions are taken as  $\alpha(\tau = 0) = 1$ ,  $\beta(\tau = 0) = \beta_0 = b_0/a_0$  is some constant. Because A is being formed from the precursor p, which is in great excess, so that  $\alpha$  and eventually  $\beta$  may come to exceed unity. Taking,

$$x = \alpha^{1/2} \tau_2, \quad y = \beta^{1/2} \tau_2 \quad \text{and} \quad t = \tau/\tau_2 \tag{4.13}$$

where  $x$  and  $y$  are new dimensionless measures of the concentrations of A and B respectively and  $t$  is a new dimensionless

time  $\bar{t} = k_2 t$ , (4.12) becomes,

$$\frac{dx}{d\bar{t}} = \mu e^{-\eta\bar{t}} - xy^2 \quad (4.14)$$

$$\frac{dy}{d\bar{t}} = xy^2 - y$$

Here,  $\mu = \mathcal{K}\tau_2^{3/2}$  is of order unity and  $\eta = \tau_2\eta' = k_0/k_2$  is a small quantity,  $\eta \leq 1$ . This has only one parameter  $\mu$ , while the system (4.12) contains two parameters, viz.  $\mathcal{K}$  and  $\tau_2$ . The pool chemical approximation forms are obtained from (4.12) or (4.14) by considering the limit in which (4.12) or (4.14) by considering the limit in which  $\eta'$  or  $\eta$  become zero. Thus the pool chemical approximation equations are

$$\frac{d\alpha}{d\bar{t}} = \mathcal{K}_p - \alpha\beta^2 \quad (4.15)$$

$$\frac{d\beta}{d\bar{t}} = \alpha\beta^2 - \beta/\tau_2$$

and from (4.14)

$$\frac{dx}{d\bar{t}} = \mu_p - xy^2 \quad (4.16)$$

$$\frac{dy}{d\bar{t}} = xy^2 - y$$

The constants  $\mathcal{K}_p$  and  $\mu_p$  represent the constant rate of formation of A from the inexhaustible supply of precursor P.

The system (4.15) has a unique non zero stationary-state solution  $(\alpha_0, \beta_0)$ , at which the derivatives vanish simultaneously.

$$\alpha_0 = \frac{1}{\tau_2^2 \kappa_p} \quad , \quad \beta_0 = \tau_2 \kappa_p \quad (4.17)$$

The stationary-state concentrations of intermediates A and B vary inversely and linearly with the group  $\kappa_p$  respectively. The local stability of this stationary state is determined by considering how small perturbations decay or grow. The linearized matrix at  $(\alpha_0, \beta_0)$  is evaluated and the characteristic roots are obtained from

$$\lambda^2 - \lambda \left( \frac{1}{\tau_2} - \tau_2 \kappa_p^2 \right) + \tau_2 \kappa_p^2 = 0 \quad (4.18)$$

$$\therefore \quad \text{Trace} = \tau_2^{-1} (1 - \tau_2^3 \kappa_p^2), \quad \det = \tau_2 \kappa_p^2 .$$

The determinant is always positive and which implies the product of roots  $\lambda_1, \lambda_2$  is positive. Thus the critical point is either a stable node or an unstable one. Systems for which the groups  $\tau_2$  and  $\kappa_p$  have values such that

$$\kappa_p^2 \tau_2^3 > 1 \text{ are stable,}$$

$$\begin{aligned} \kappa_p^2 \tau_2^3 &\geq 3 + \sqrt{8} && \text{stable node} \\ 1 < \kappa_p^2 \tau_2^3 < 3 + \sqrt{8} && \text{stable focus} \end{aligned} \quad (4.19)$$

For  $\mathcal{K}_p$  and  $\mathcal{C}_2$  such that,  $\mathcal{K}_p^2 \mathcal{C}_2^3 < 1$ , the stationary state is locally unstable with,

$$\begin{aligned} 3 - \sqrt{8} < \mathcal{K}_p^2 \mathcal{C}_2^3 < 1 & \text{ unstable focus} \\ 0 < \mathcal{K}_p^2 \mathcal{C}_2^3 < 3 - \sqrt{8} & \text{ unstable node} \end{aligned} \quad (4.20)$$

As the group  $\mathcal{K}_p^2 \mathcal{C}_2^3$  ( or  $k_0^2 k_1 p_0^2 / k_2^3$  ) is reduced through unity, eg. by decreasing the initial precursor concentration, there is a Hopf bifurcation. Here a stable limit cycle emerges. This point heralds the onset of sustained oscillations. Also, it is to be noted that, this Hopf bifurcation occurs when the stationary state concentration of the two intermediate species A and B are equal (ie.  $\alpha_0 = \beta_0 = \mathcal{C}_2^{-1/2}$ ).

The unique steady state corresponding to (4.16) is

$$x_0 = \mu_p^{-1}, \quad y_0 = \mu_p \quad (4.21)$$

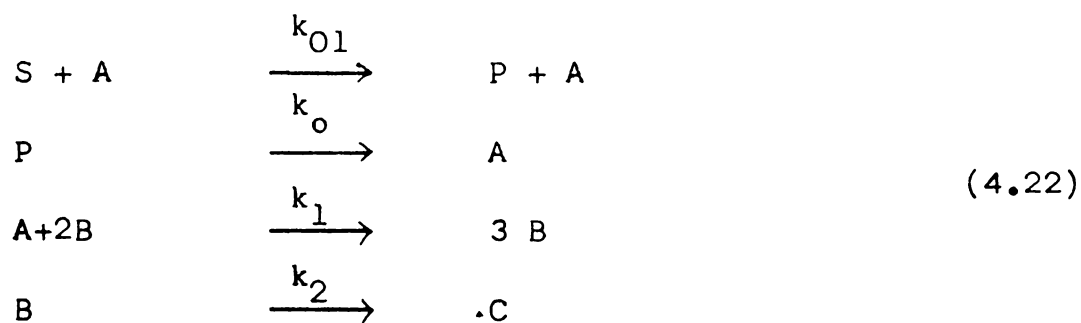
It is seen that  $(x_0, y_0)$  is stable for  $\mu_p > 1$  and unstable for  $\mu_p < 1$  with changes between nodal and focal character at  $\mu_p = \sqrt{2} \pm 1$ . The Hopf bifurcation at  $\mu_p = \mu_p^* = 1$  (when  $x_0 = y_0 = 1$ ) produces a stable limit cycle, as above with vanishingly small amplitude. As  $\mu$  is decreased below unity, the limit cycle grows in size and the corresponding oscillatory amplitude and period increase.

The MNS model discussed above is two dimensional and simple compared to the following modification, which is three dimensional, nonlinear and coupled. A comparison study is given in the discussion section.

#### 4.3. A MODIFIED MODEL

We consider a chemical reaction scheme containing a cubic autocatalator, with the intermediate species A produced via, a simple first order decay process from a precursor or reactant P, in which the decay process is controlled by the production of A.

Thus the scheme is



where  $k_{01}$ ,  $k_0$ ,  $k_1$  and  $k_2$  are the rate constants.

The kinetic behaviour of the model can be described by the equations (4.23) involving concentrations of P and the intermediates A and B. By the law of mass action, the

governing differential equations are,

$$\begin{aligned}\frac{dp}{dt} &= -k_0 p + k_{01} a \\ \frac{da}{dt} &= k_0 p - k_1 a b^2 \\ \frac{db}{dt} &= k_1 a b^2 - k_2 b\end{aligned}\tag{4.23}$$

where  $p = [P]$ ,  $a = [A]$ ,  $b = [B]$

ie. the concentrations of the reactants.

Equations (4.23) could be handled more easily and the general nature of the solution could be emphasized by casting the concentrations and time in the dimensionless variables  $x, y, z$  and  $\tau$ , and the dimensionless parameters  $\eta, \mathcal{K}$  and  $\tau_2$  defined in (4.25). We nondimensionalise the characteristic system (4.23) with the characteristic time scale  $t_{ch}$  given by (4.7).

$$\begin{aligned}\frac{dx}{d\tau} &= -\eta' x + \mathcal{K} y \\ \frac{dy}{d\tau} &= \eta' x - y z^2 \\ \frac{dz}{d\tau} &= y z^2 - z/\tau_2\end{aligned}\tag{4.24}$$

where

$$x = p/a_0, \quad y = a/a_0, \quad z = b/a_0, \quad t = \tau/k_2 \hat{\tau}_2$$

$$\text{where } \hat{\tau}_2 = k_1 a_0^2 / k_2 \quad (4.25)$$

$$\eta' = k_0/k_1 a_0^2, \quad \mathcal{K} = k_{01}/k_1 a_0^2$$

The system (4.24) is a three dimensional nonlinear coupled system of differential equations and are not easily integrated. The previous studies [52] have been concerned with the neglect of reactant consumption, or the 'pool chemical approximation' under which the early period of the reaction is modelled with the precursor concentration assumed constant (ie.  $\mathcal{K} = 0$ ) and set equal to its value ( $p_0$ ). In such a case, the number of species with varying concentrations reduces from three to two. The oscillatory dynamics of such a two-dimensional system has been studied in detail. In the system (4.24) the oscillations occur in the three species P, A and B simultaneously for a long interval of time. Since the decay of P is controlled by the production of A, we can observe the oscillations from the beginning itself. But in the model presented in the last Section (4.2), the oscillations begin only after a long time and the oscillations decay soon after a certain time.



#### 4.4 STATIONARY STATES AND OSCILLATIONS

The effect of including the control mechanism in the simple first order decay of the precursor P is studied here, among the other species. We want to investigate the possibility of having chemical oscillations of the limit cycle type. An indication of the existence of such solutions if  $(x_0, y_0, z_0)$  is an unstable critical point. Critical points in r-space are given by the solutions of

$$\begin{aligned} (\dot{r} = 0 = F(r; \eta', \mathcal{K}, \tau_2) \\ r = (0, 0, 0), \quad r = r_0 = (x_0, y_0, z_0) \\ x_0 = \frac{\mathcal{K}^{\frac{1}{2}}}{\eta' \tau_2}, \quad y_0 = \frac{\mathcal{K}^{-\frac{1}{2}}}{\tau_2}, \quad z_0 = \mathcal{K}^{\frac{1}{2}} \end{aligned} \quad (4.26)$$

The stationary state concentrations of P and B varies with  $\mathcal{K}^{\frac{1}{2}}$ , while that of the intermediate A, varies with  $\mathcal{K}^{-\frac{1}{2}}$ . We are considering in (4.24) only those points, which are physically realistic, viz. those at which  $x_0 \geq 0$ ,  $y_0 \geq 0$ ,  $z_0 \geq 0$ . The critical points at the origin is always unstable, since the eigen values  $\lambda$  satisfy

$$\lambda^3 + \lambda^2 \left[ \eta' + \frac{1}{\tau_2} \right] + \lambda \left[ \frac{\eta'}{\tau_2} - \mathcal{K} \eta' \right] - \frac{\mathcal{K} \eta'}{\tau_2} = 0 \quad (4.27)$$

The three solutions  $\lambda_1, \lambda_2, \lambda_3$  satisfy the condition  $\lambda_1 \cdot \lambda_2 \cdot \lambda_3 = \frac{\mathcal{K} \eta'}{\tau_2} > 0$  and hence there is always at least one root with a positive real part.

By linearizing the system (4.24) around  $(x_0, y_0, z_0)$  we have

$$J = \begin{bmatrix} -\eta' & \mathcal{K} & 0 \\ \eta' & \mathcal{K} & -2/\tau_2 \\ 0 & \mathcal{K} & 1/\tau_2 \end{bmatrix} \quad (4.28)$$

The eigen values  $\lambda$ , for the critical point  $r_0$  satisfy

$$\lambda^3 - \tau \lambda^2 + \delta \lambda - \Delta = 0$$

where

$$\tau = \frac{1}{\tau_2} - \mathcal{K} - \eta', \quad \delta = \frac{\mathcal{K} - \eta'}{\tau_2}, \quad \Delta = \frac{-2\eta'\mathcal{K}}{\tau_2} \quad (4.29)$$

The necessary and sufficient conditions for all the solutions  $\lambda$  to have negative real parts are,

$$\tau < 0, \quad \Delta < 0, \quad \Delta - \tau\delta > 0$$

The first inequality is satisfied when  $\frac{1}{\tau_2} < (\mathcal{K} + \eta')$ . The second condition is already satisfied for all possible realistic values of the parameters  $\eta'$ ,  $\mathcal{K}$  and  $\tau_2$ . Using the third condition, we get the range of the control parameter  $\mathcal{K}$ , for which the solutions of (4.24) are in the stable region. Thus the stability curve can be cast

in the form,

$$\tau_2 \mathcal{K}^2 - \mathcal{K}(1 + 2\tau_2 \eta') + \eta' - \tau_2 \eta'^2 = 0 \quad (4.30)$$

The unstable solutions of (4.24) fall in the range,

$$\mathcal{K}_{1c} < \mathcal{K} < \mathcal{K}_{2c}$$

where

$$\begin{aligned} \mathcal{K}_{1c} &= [(1 + 2\tau_2 \eta') - (1 + 8\tau_2^2 \eta'^2)^{1/2}] / 2\tau_2 \\ \mathcal{K}_{2c} &= [(1 + 2\tau_2 \eta') + (1 + 8\tau_2^2 \eta'^2)^{1/2}] / 2\tau_2 \end{aligned} \quad (4.31)$$

When  $\mathcal{K}$  crosses the value  $\mathcal{K}_{1c}$ , the stable solutions become unstable. Again  $\mathcal{K}$  crosses the value  $\mathcal{K}_{2c}$ , the unstable branch becomes a stable one. Hence  $\mathcal{K}_{1c}$  and  $\mathcal{K}_{2c}$  are the two critical points at which the solutions of (4.24) has a qualitative change. The possibility of appearance of the periodic solutions out of the equilibrium state, when  $\mathcal{K}$  crosses the critical value is examined.

Using bifurcation analysis, one finds that in the vicinity of  $\mathcal{K}_{1c}$  and  $\mathcal{K}_{2c}$ , the singular point behaves like a focus, unstable (if  $\mathcal{K}_{1c} < \mathcal{K} < \mathcal{K}_{2c}$ ) or stable (if  $\mathcal{K} < \mathcal{K}_{1c}$  or  $\mathcal{K} > \mathcal{K}_{2c}$ ). Comparing the coefficients of the general cubic with real root  $\lambda_3$  and pure imaginary

roots  $\lambda_{1,2} = \pm i\omega_0$ , with the following cubic

$$\lambda^3 - \left(\frac{1}{\tau_2} - \mathcal{K} - \eta'\right) \lambda^2 + \left(\frac{\mathcal{K} - \eta'}{\tau_2}\right) \lambda + \frac{2\eta'\mathcal{K}}{\tau_2} = 0 \quad (4.32)$$

We have,

$$\begin{aligned} \lambda_3 &= \frac{1}{\tau_2} - \mathcal{K} - \eta' \\ \lambda_{1,2} &= \pm i \left[ \frac{\mathcal{K} - \eta'}{\tau_2} \right]^{1/2} \end{aligned} \quad (4.33)$$

and

$$\tau_2 \mathcal{K}^2 - \mathcal{K}(1 + 2\tau_2 \eta') + (\eta' - \tau_2 \eta'^2) = 0 \quad (4.34)$$

$$\mathcal{K}_{1c} = \left[ (1 + 2\tau_2 \eta') - (1 + 8\tau_2^2 \eta'^2)^{1/2} \right] / 2\tau_2 \quad (4.35)$$

$$\mathcal{K}_{2c} = \left[ (1 + 2\tau_2 \eta') + (1 + 8\tau_2^2 \eta'^2)^{1/2} \right] / 2\tau_2$$

Differentiating (4.32) with respect to  $\mathcal{K}$ , we have,

$$\lambda'(\mathcal{K}) = - \frac{\left( \lambda^2 + \frac{\lambda}{\tau_2} + \frac{2\eta'}{\tau_2} \right)}{3\lambda^2 - 2\lambda \left( \frac{1}{\tau_2} - \mathcal{K} - \eta' \right) + \left( \frac{\mathcal{K} - \eta'}{\tau_2} \right)} \quad (4.36)$$

$$\therefore \text{Re. } \lambda'_i(\mathcal{K}) = \frac{2\eta' + \Gamma - \omega_0^2 \tau_2}{2\tau_2 [\omega_0^2 + \Gamma^2]} \neq 0$$

$$\lambda'_i(\mathcal{K}_{1c}) > 0 \quad \text{and} \quad \lambda'_i(\mathcal{K}_{2c}) < 0 \quad (4.37)$$

Note that (4.31) and (4.35) are the same. From (4.37) it is evident that  $\mathcal{K}_{1c}$  and  $\mathcal{K}_{2c}$  are the critical Hopf bifurcation points for the system (4.24). For  $\mathcal{K} > \mathcal{K}_{1c}$  (ie.  $\text{Re. } \lambda_1'(\mathcal{K}) > 0$ ) the existing periodic solutions are supercritical and for  $\mathcal{K} < \mathcal{K}_{1c}$ , the existing periodic solutions are 'subcritical'. For any value of  $\hat{\eta}^2$ ,  $\mathcal{K}_{1c}$  and  $\mathcal{K}_{2c}$  cannot be merged (a non-degenerate Hopf bifurcation). At the upper Hopf bifurcation point,  $\mathcal{K}_{2c}$ , a stable limit cycle emerges (numerically found) with an infinitely small amplitude. Sustained oscillatory responses in the concentrations P, A and B are found for certain other values of the controlling parameter. For a parametric value  $\mathcal{K}$  lying between  $\mathcal{K}_{1c}$  and  $\mathcal{K}_{2c}$ , the critical point is an unstable focus. Large amplitude oscillatory responses can be seen at this region.

#### 4.5 NUMERICAL RESULTS

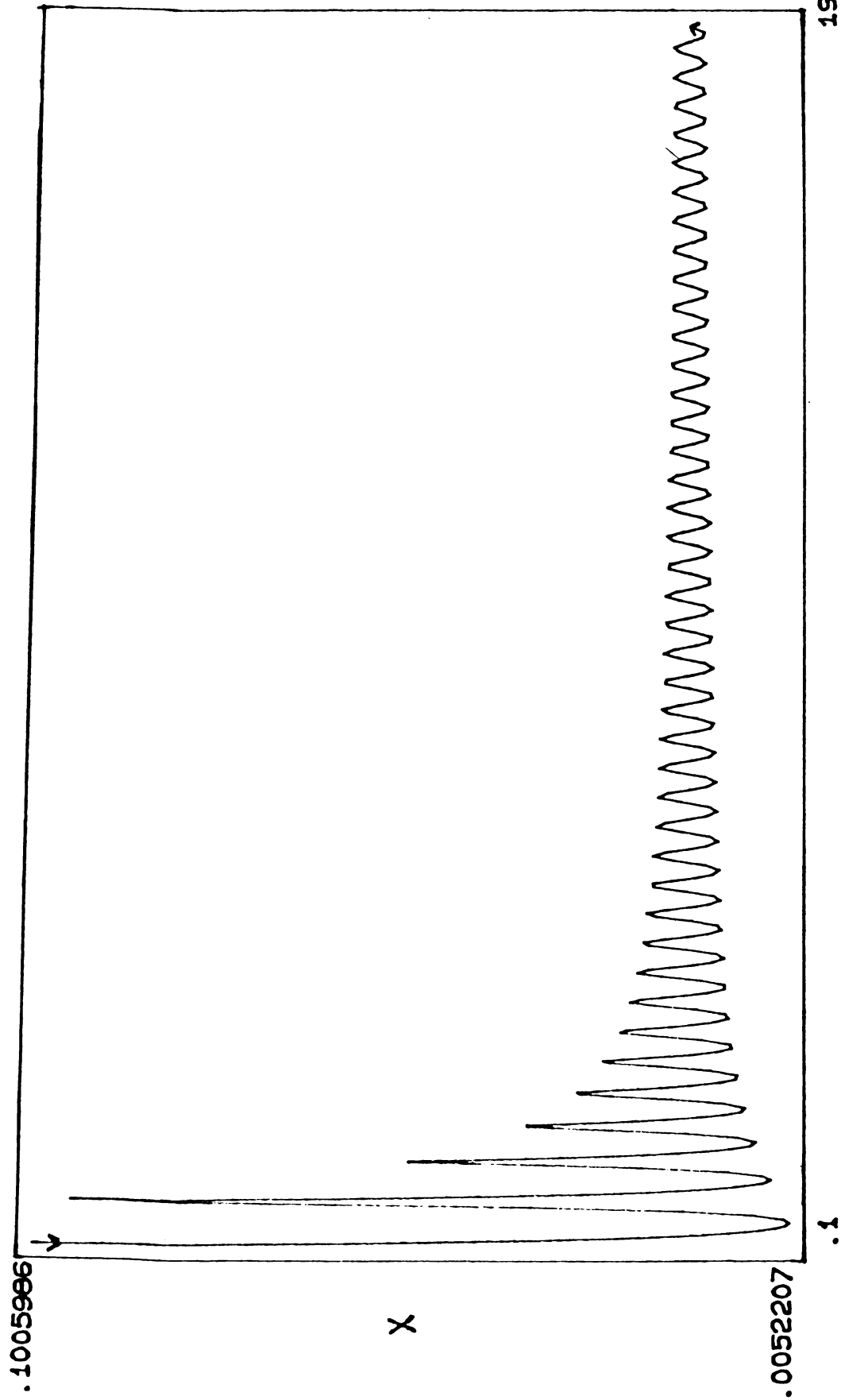
The chemical reaction model under consideration (4.24) is a system of nonlinear coupled differential equations. We used the fourth order Runge-Kutta Method with the step doubling (Section 2.6) to integrate the system numerically. The results of the previous sections have established that, the system exhibits Hopf bifurcation resulting in sustained oscillations in this model.

The oscillations in the concentrations of the reactants P, A and B start immediately, when the reaction is switched on. When the parametric values  $\tau_2 = 10^4$  and  $\eta' = 10^{-4}$  are used, the numerical values for  $\mathcal{K}_{1c}$  and  $\mathcal{K}_{2c}$  are obtained as

$$\mathcal{K}_{1c} = 0.0 \quad \text{and} \quad \mathcal{K}_{2c} = 0.0003 \quad (4.38)$$

In the figures we have used X,Y,Z for the concentration of the reactants P, A and B respectively. At the supercritical Hopf bifurcation point  $\mathcal{K}_{2c} = 0.0003$ , the oscillations in the corresponding constituents P, A and B are shown schematically (Fig. 16 (a), (b), (c) ). The amplitude of these oscillations decreases as time progresses. After a certain time  $\tau = 3 \times 10^5$ ,  $t \cong 30$ , the oscillations become uniform neither the amplitude nor the distance between each spike increases. Before this time, the period between peaks lengthens and the oscillations become less spiky than earlier in character.

The reactant P oscillates [ Fig.16(a) ] with a higher amplitude than that of A and B [ Fig. 16(b), (c) ]. The dimensionless time  $\tau$  is plotted in the x-axis, while the concentrations of P, A and B are plotted in the y-axis, [Fig.16(a), (b) and (c)] respectively. Initially P is in abundance and gradually it is converted to A. Then by the autocatalytic step, B is produced rapidly and finally is



1900143

Fig.16(a)  $\tau$

Fig.16(a). Trace of the concentration  $x(P)$  vs. time ( $\tau$ ) obtained by the numerical integration of the system (4.24), for  $\mathcal{K} = 3 \times 10^{-4}$ . The integration used the parametric values,  $\eta' = 10^{-4}$ ,  $\tau_2 = 10^4$  and the initial steady state is  $x_0, y_0, z_0 = 0.1$  throughout this chapter. The oscillation of  $P$  continues steadily (neither increasing or decreasing) after a time  $\tau = 3 \times 10^5$ . The arrows indicate the direction of time evolution.

converted to C, after a very long time. The first of the three reactants P, A and B forms at  $\tau = 7 \times 10^4$ .

The wave corresponds to P is more straight and spiky, while that of A is sliding rightwards (or forward) and that of B is sliding leftwards (or backward). P is decaying and the speed of decay is controlled by the production of A. Oscillations in the various species continue for a long time, since the decay of P is controlled by the production of A, unlike in the 'pool chemical approximation model'.

The stationary-state solution of the full equations for the system (4.24) shows two changes between stable and unstable focus as the time is increased. Both these changes give rise to Hopf bifurcations. The nature of the limit cycles produced at each bifurcation point has to be examined, numerically and this has been done for two periodic values,  $\mathcal{K} = 0.0002$  and  $\mathcal{K} = 0.0003$  [ $\mathcal{K}_{2c}$ ], while the other parameter values  $\tau_2 = 10^4$ ,  $\eta' = 10^{-4}$  are fixed. For  $\mathcal{K} = 0.0003$ , stable limit cycles are obtained in the x-y (Fig.21), y-z (Fig.22) and x-z (Fig.23) planes. When  $\mathcal{K} = 0.0002$ , it is found that the trajectories are unwinding from a singular point and some compartments (or boxes) are appeared [ Fig. 27, 28, 29 ]. We shall discuss the behaviour of the solutions at each of these points separately.



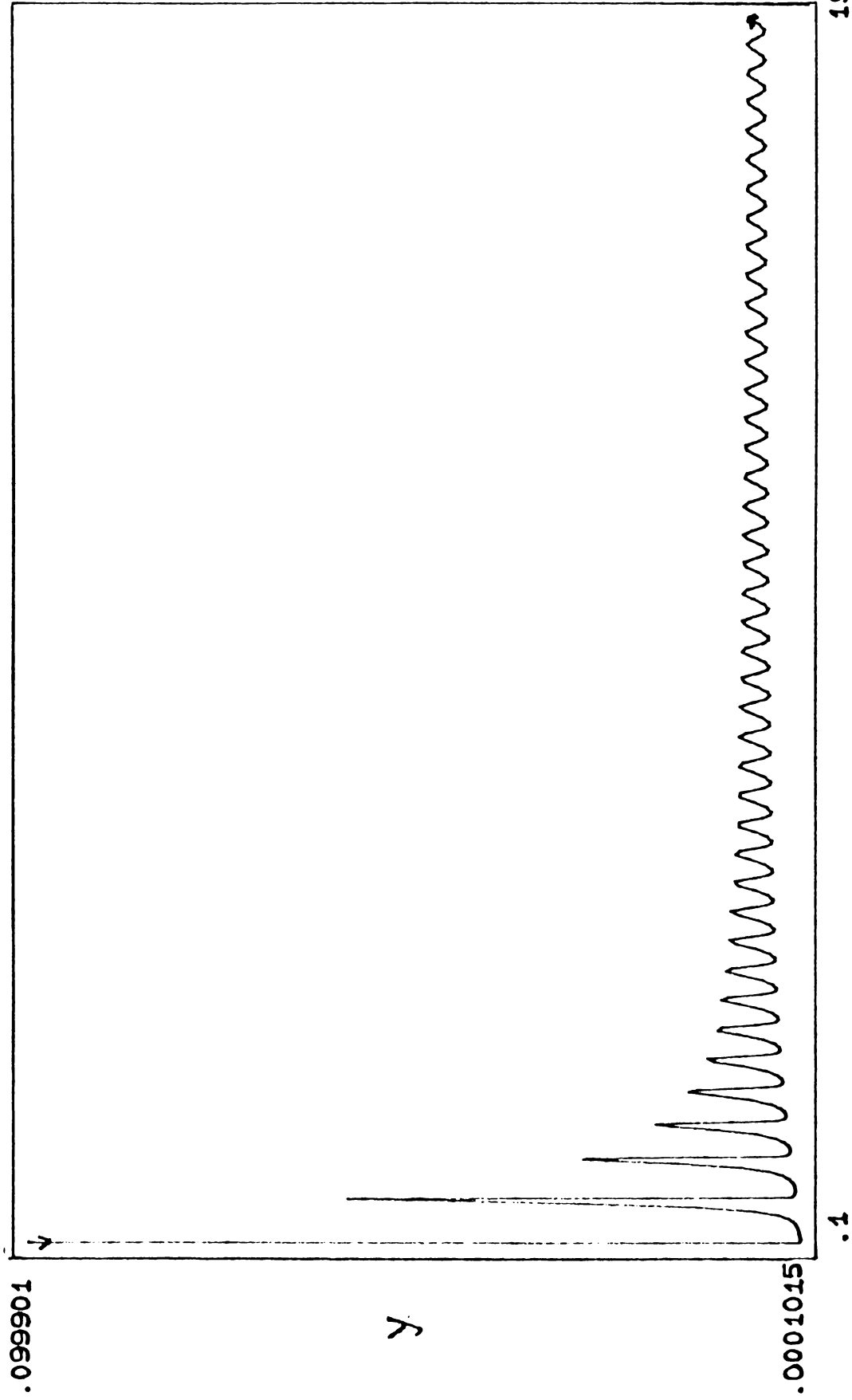


Fig.16(b)

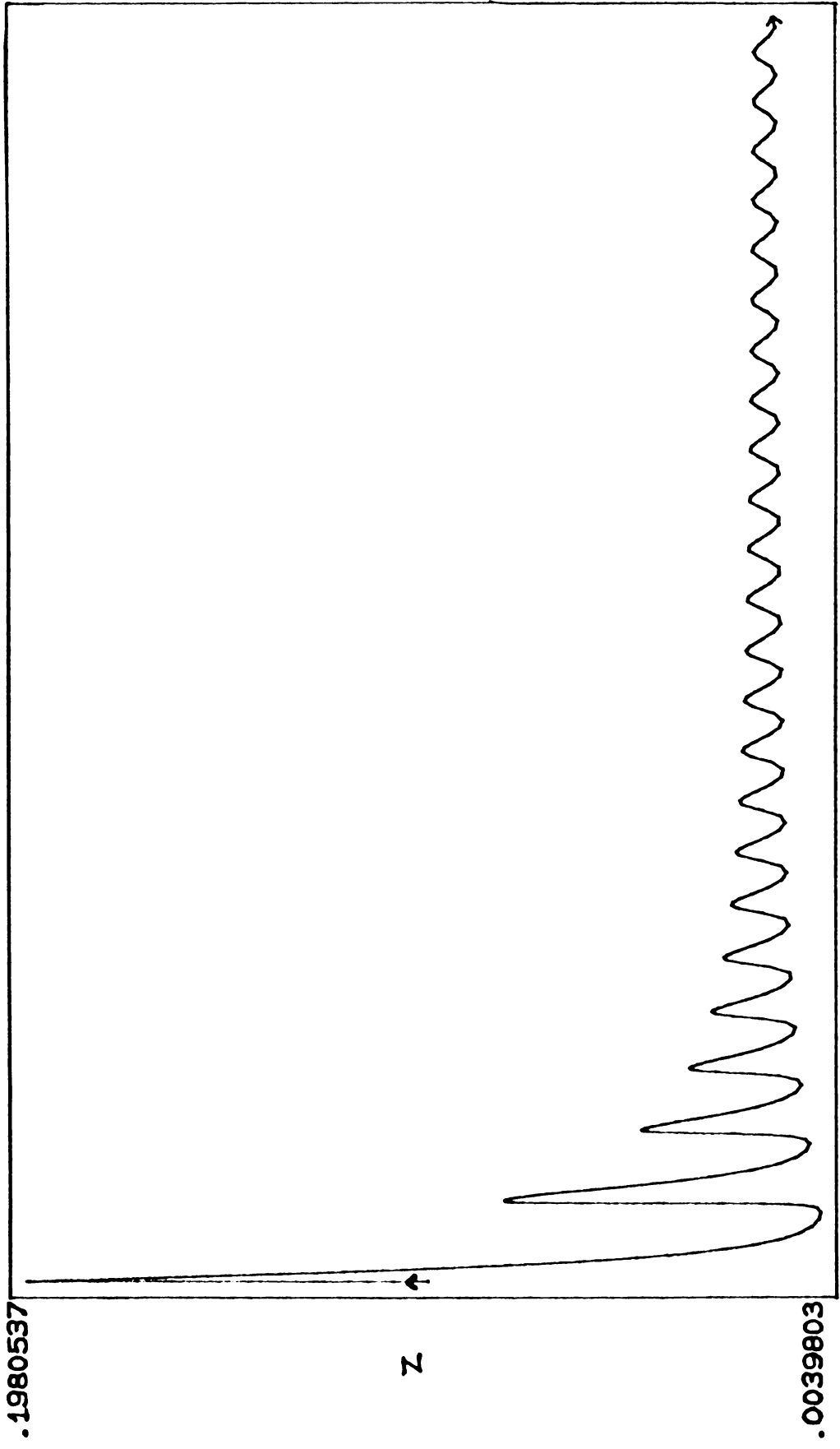
Fig.16(b). Concentration profile of  $y(A)$  vs. time ( $\tau$ ) obtained by the numerical integration of equations (4.24) at  $\mathcal{X} = 3 \times 10^{-4}$  from  $\tau = 0$  to  $\tau = 1900143$ . The A-wave propagates steadily after  $\tau = 3 \times 10^5$ .

Let us first consider the behaviour of the solutions of (4.24) at the bifurcation point  $\mathcal{K} = 0.0003$ . The concentration profiles of P and A are plotted against the time  $\tau_1$  [Fig.17(a)], (scaled as  $\hat{\tau}_1 = \tau_1 \times 10^{-3}$ ) upto  $\tau_1 = 300$ . The limit cycle formed by the combination P and A is shown in Fig.17(b). The limit cycle corresponds to P and A seems to be formed at  $\hat{\tau} = 494351$ . Similarly Fig.19(a) represents the oscillations of the combination P and B upto the time  $\tau_1 = 300$ . The limit cycle formed when B vs. P plotted in the z-x phase plane at  $\tau = 456770$ . This is shown in Fig.19(b). The oscillations of A and B plotted against  $\tau$  is shown in Fig.18(a). The corresponding limit cycle is shown in Fig.18(b), which forms at  $\tau = 375803$ .

Fig.21 describes the portrait associated with the solutions P and A, where P is plotted in the x-axis and A is plotted in the y-axis. The solution curve of (4.24) is spiralling towards the critical point, as the time increases and hence we get the asymptotically stable solution. The small amplitude decaying oscillations in Fig.18(a) corresponds to the dense spiral in Fig.21.

The phase plane portrait associated with P and B is shown in Fig.23, where P is plotted in the x-axis and B is plotted in the y-axis. The decaying (or steady)

.1980537



.1

1143727

Fig.16(c)

Fig.16(c). Concentration profile of  $z(B)$  vs. time ( $\tau$ ) of the system (4.24) at  $\mathcal{X} = 3 \times 10^{-4}$  from  $\tau = 0.1$  to  $\tau = 1143727.0$ . The B-wave proceeds steadily after  $\tau = 3 \times 10^5$ .

oscillations correspond to the dense spiral is shown in this figure. Again Fig.22 represents the portrait of A and B where A is plotted in the x-axis and B is plotted in the y-axis.

The interaction among the chemical constituents for  $\mathcal{K} = 0.0003$  is also studied numerically. The concentration profile of P (or P-wave) intersects with the concentration profile of A (or A-wave) only once and which is in the initial stage of the reaction, at  $\tau_1 = 60$  (Fig. 17(a)). It is very interesting to note that the interaction between P and B continues indefinitely (Fig.19(a)). From Fig.18(a), we note that the interaction between A and B stops at  $\tau_1 = 280$ . The interaction of the three reactants P, A and B is shown in Fig.20.

The same type of oscillatory behaviour of the system (4.24) is obtained for other values of the catalyst decay constant  $\tau_2$  viz. 9999.0, 10001.0, 10002.0, 10004.0, 10005.0, 10007.0, 10008.0 and 10009.0 with  $\eta' = 10^{-4}$  and  $\mathcal{K} = 3 \times 10^{-4}$ .

Now let us discuss the behaviour of the solutions of (4.24) at the parameter value  $\mathcal{K} = 0.0002$ . We have seen analytically that, the equilibrium solution  $(x_0, y_0, z_0)$  of (4.24) is unstable for the range of parameter,  $\mathcal{K}_{1c} < \mathcal{K} < \mathcal{K}_{2c}$ . The result is confirmed, numerically for the parametric value  $\mathcal{K}$  lies in this particular range. The equilibrium

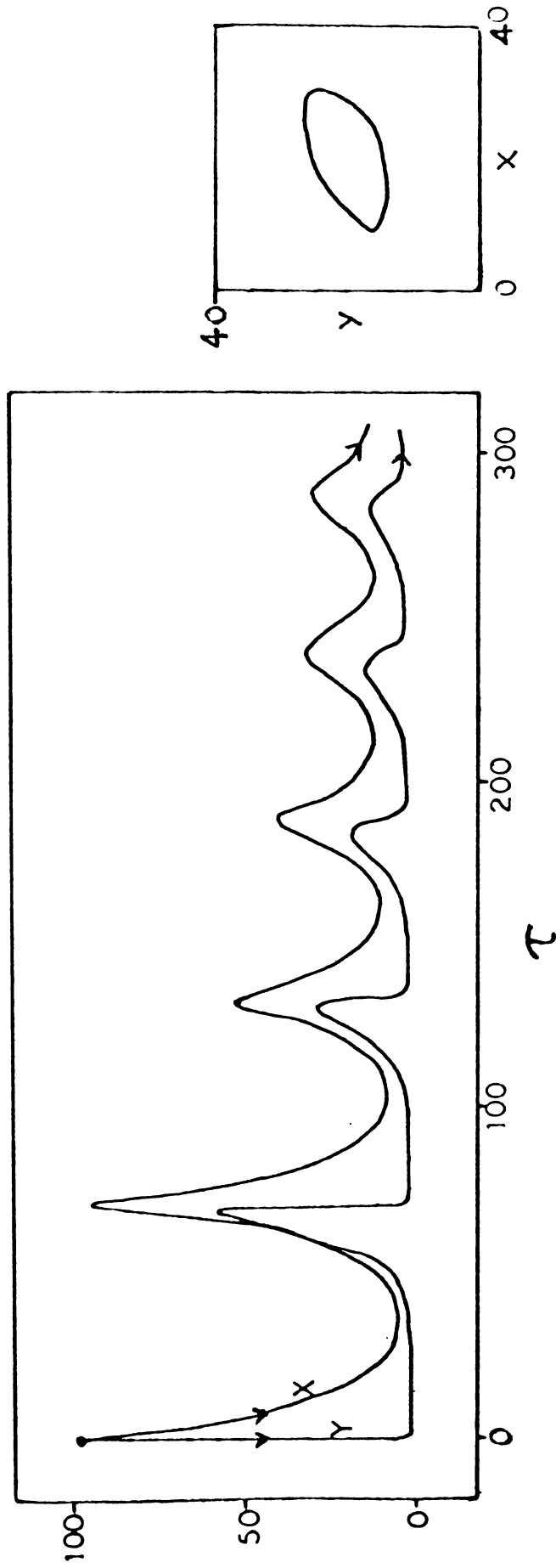


Fig.17(a)

Fig.17(b)

Fig.17(a). Traces of  $x(P)$  and  $y(A)$  for the system (4.24) at  $\mathcal{K} = 3 \times 10^{-4}$ , simultaneously plotted against the time  $\tau$ , [ $\tau_1 = \tau \times 10^{-3}$ ] from  $\tau_1=0$  to  $\tau_1 = 300$ . The competition between the P-wave and the A-wave stops at  $\tau_1 = 60$ .

Fig.17(b). The limit cycle corresponds to the system (4.24) at  $\mathcal{K} = 3 \times 10^{-4}$  in the  $x-y$  phase plane. This closes at  $\tau = 494351.0$ .

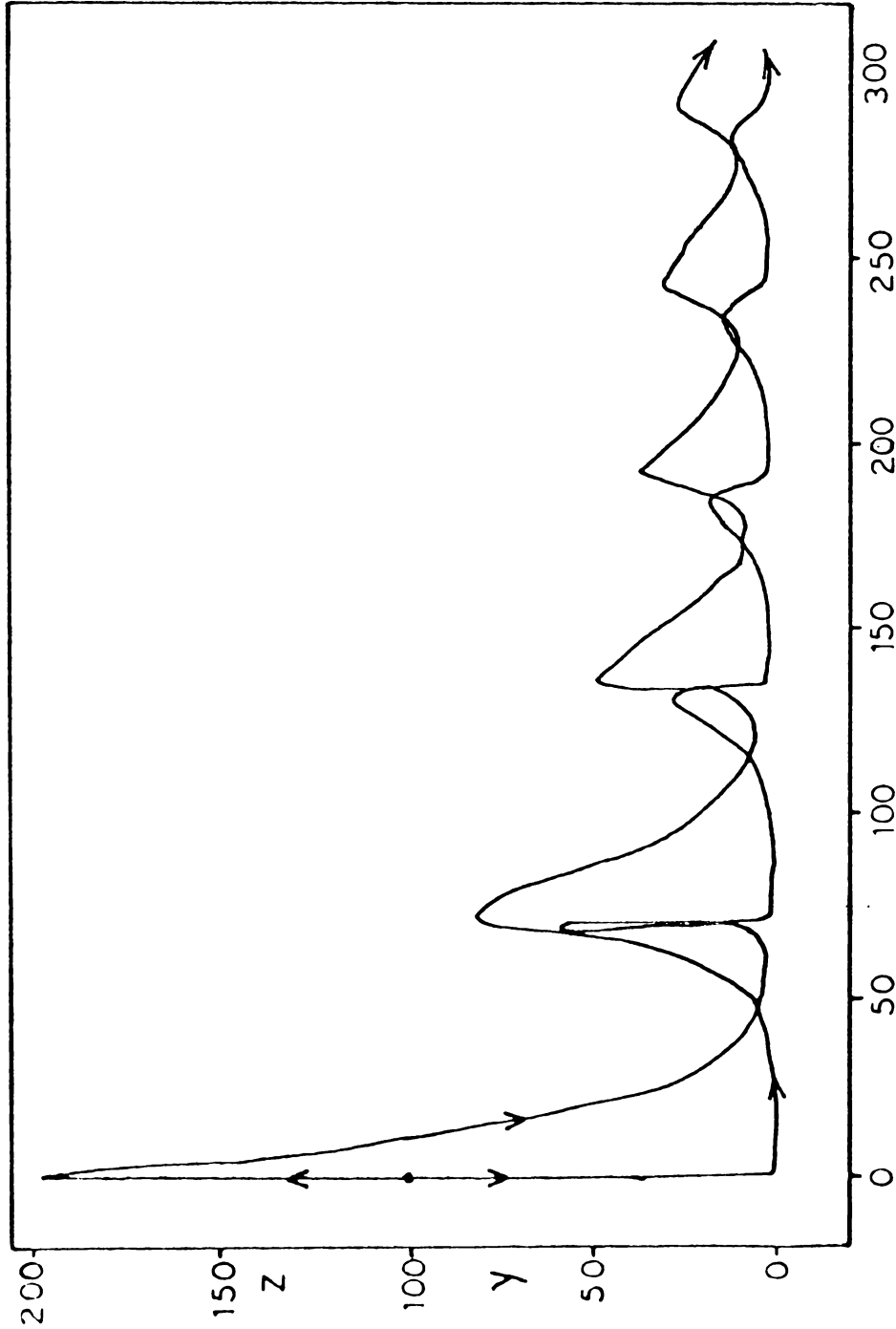


Fig.18(a)  $\tau$

Fig.18(a). Concentration profiles of A and B(y and z) traced simultaneously against the time  $\tau_1$ , from  $\tau_1=0$  to  $\tau_1=300$  of the system (4.24), at the parametric value  $\mathcal{K} = 3 \times 10^{-7}$ . Note the interaction islands of A-wave and B-wave. The competition stops at  $\tau_1 = 280$ .

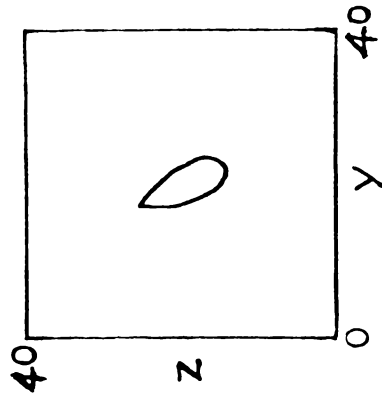


Fig.18(b).

Fig.18(b). The limit cycle of the System (4.24) in the y-z phase plane, at the parametric

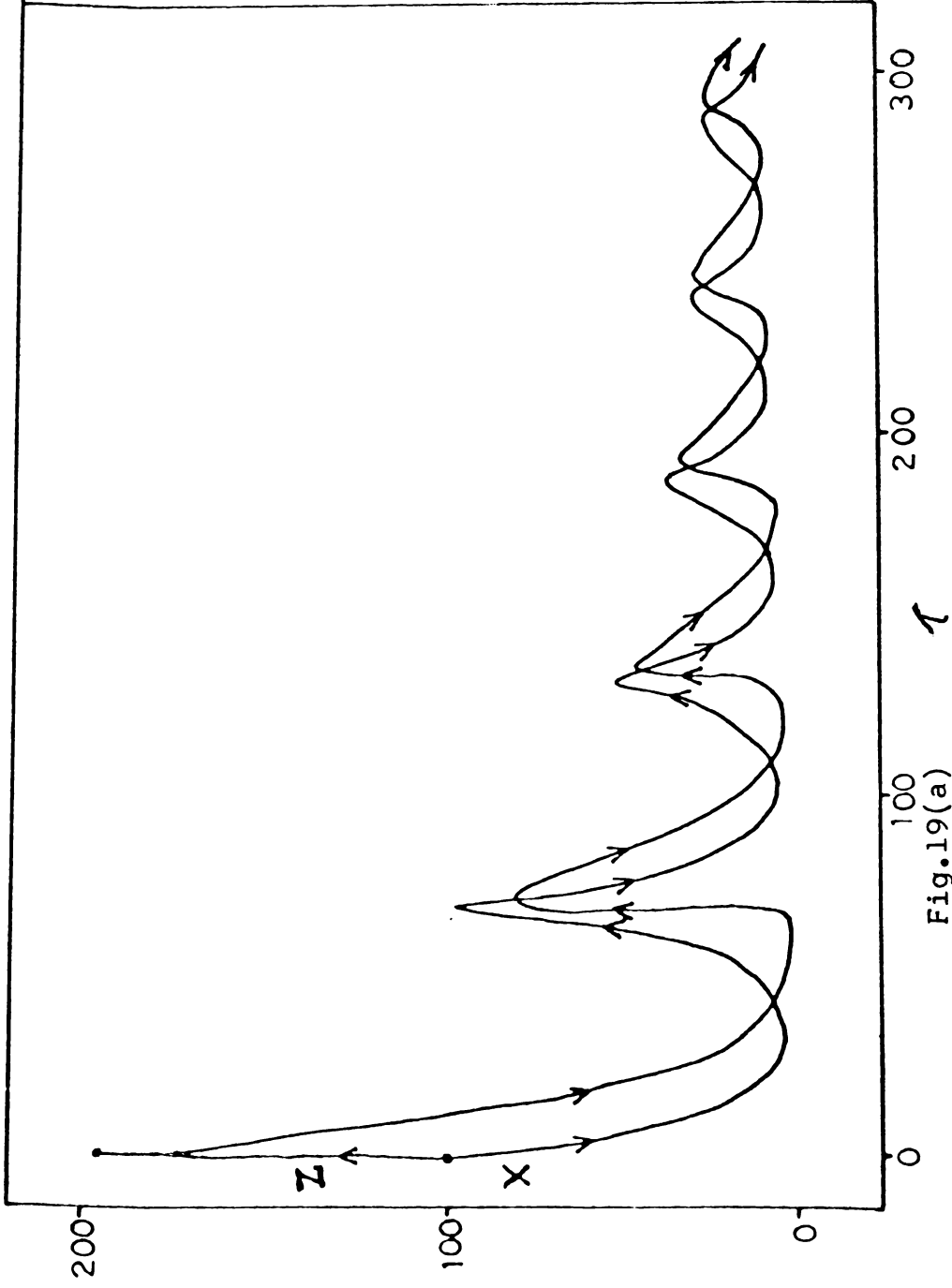


Fig.19(a)

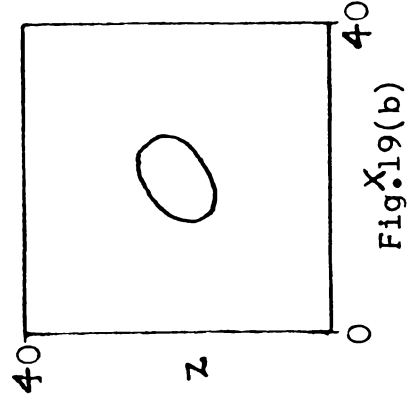


Fig.19(b)

Fig.19(a). P-wave and B-wave are plotted simultaneously against the time  $\tau$  of the system (4.24) at the parametric value  $\mathcal{K} = 3 \times 10^{-4}$ , from  $\tau_1=0$  to  $\tau_1=300$ . Note the competition between P and B continues indefinitely.

Fig.19(b). The limit cycle obtained when the system (4.24) is integrated in the x-z phase plane, closes at  $\tau = 456770.0$ .

solution of (4.24) is an unstable focus at the critical parameter value  $\mathcal{K} = 0.0002$ . Evidently,  $\mathcal{K}_{2c} = 0.0003$  is a Hopf bifurcation point, since at this critical point the qualitative behaviour of the solution of the system changes. When  $P$  is plotted against the dimensionless time  $\hat{\tau}$  [Fig.24] we note that as time increases, the amplitude of the  $P$ -wave [Fig.9] increases. Fig. 25 describes the concentration profile of  $A$  which is plotted against the dimensionless time  $\hat{\tau}$  for the parametric value  $\mathcal{K} = 0.0002$ ,  $\hat{\tau}_2 = 10^4$  and  $\eta' = 10^{-4}$ . The amplitude of the  $A$ -wave increases indefinitely as the time increases. Similarly, Fig.26 shows the concentration profile of the catalyst  $B$ , when plotted against the nondimensionalised time  $\hat{\tau}$ . The amplitude of the  $B$ -wave increases rapidly as the time increases. It is very interesting to note that, as soon as the reaction is switched on, within no time, the oscillations in the reactants  $P$ ,  $A$  and  $B$  shoots up. The three waves,  $P$ -wave,  $A$ -wave and  $B$ -wave are plotted against the time  $\hat{\tau} = 69.90175$  to  $\hat{\tau} = 454116.5$ , for our convenience. The concentration corresponds to the time  $\hat{\tau} = 69.90175$  of  $P$ ,  $A$  and  $B$  respectively are  $0.0032832$ ,  $0.0000849$  and  $0.0003354$ . The amplitudes of the three waves in the time range  $69.90175$ - $454116.5$  increases somewhat uniformly. The maximum amplitude attained in this time range by the  $P$ ,  $A$  and  $B$  waves respectively are  $0.8627064$ ,  $0.8428407$  and  $0.863683$ .



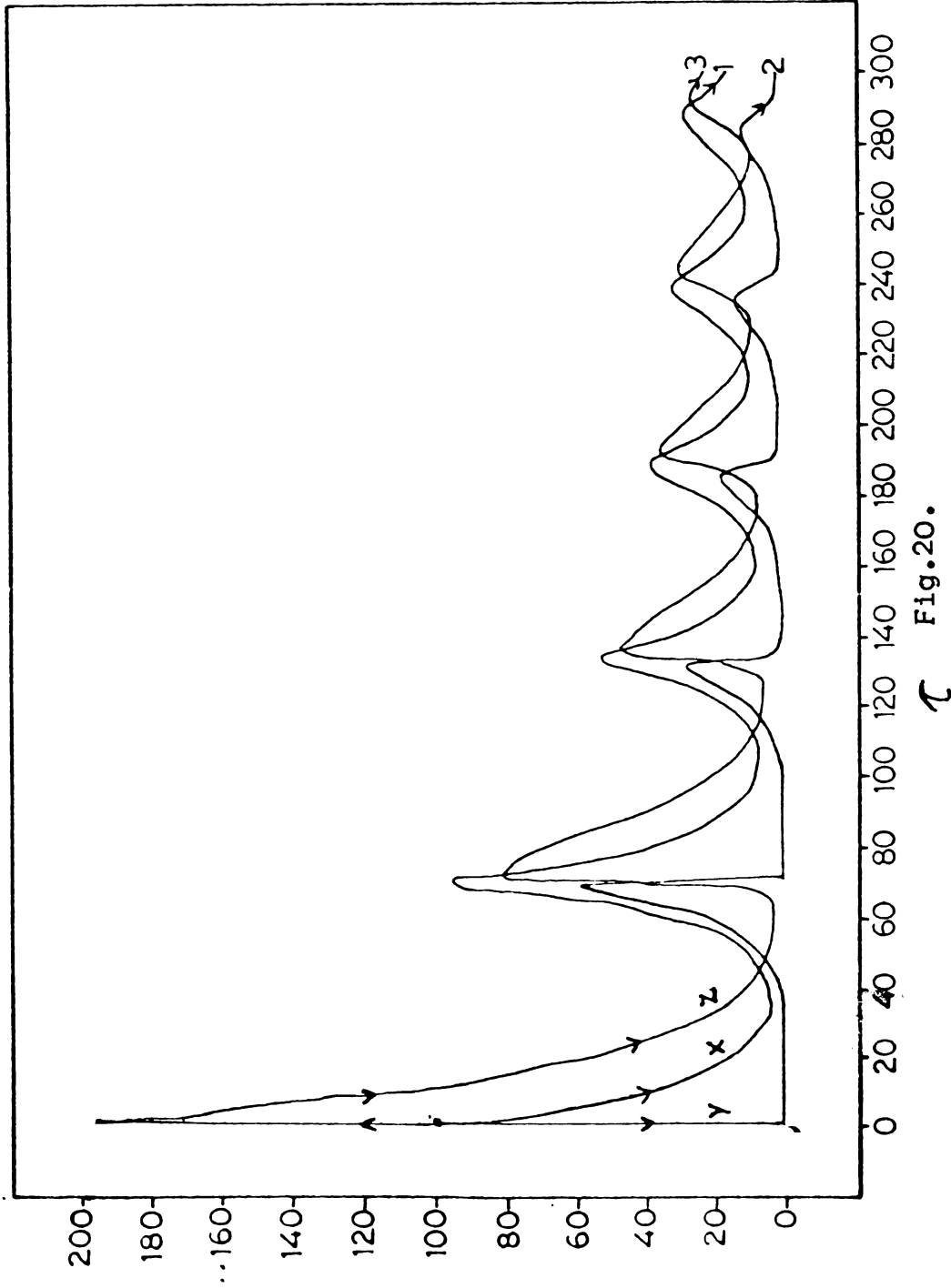


Fig.20.

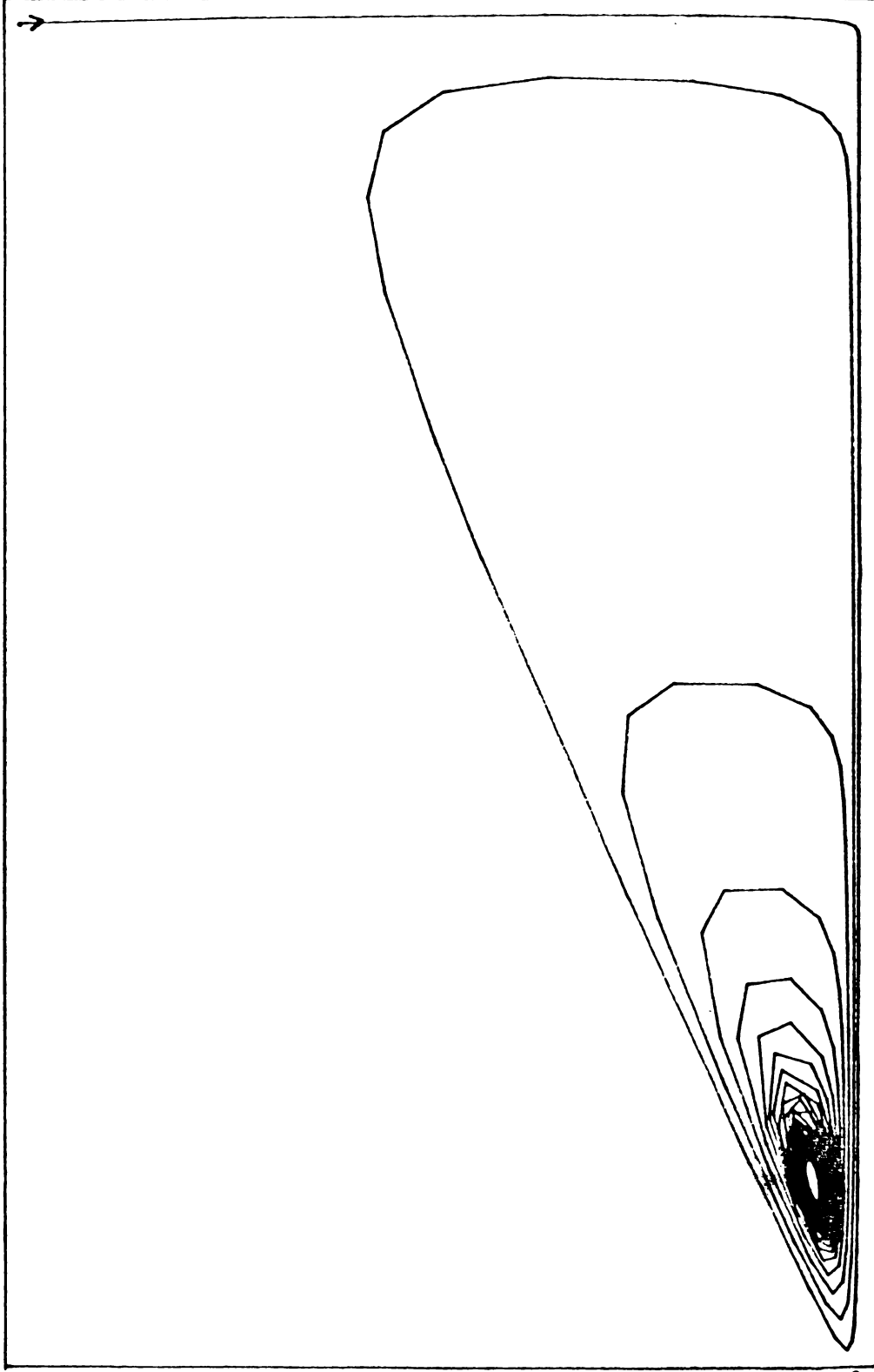
Fig.20. The concentration profiles of P,A and B (x,y and z) plotted simultaneously against the time  $\tau_1$  of the system (4.24) at the parametric value  $\mathcal{K} = 3 \times 10^{-4}$ . The numbers 1,2 and 3 indicate the P-wave, A-wave and B-wave respectively.

From the figures, it should be noted that the A-wave spikes are tilted towards the right and the B-wave spikes are tilted towards the left in comparison with the spikes of the P-wave. This may be due to the relative strength of interacting constituents in the chemical reaction.

The phase plane plots corresponding to each pair viz. A vs. P, B vs. A and B vs. P are much more interesting. Corresponding to the parametric value  $\mu = 0.0002$ , the solution trajectory of the oscillator (4.24) unwinds from a fixed point and making boxes from smaller to bigger ones. Fig.27 represents the phase plane plot of A and P, which is obtained by plotting A against P. Triangular shaped boxes, four in number, are formed during an interval of time,  $\tau = 454116.5$ . The unstable focus has less the coordinates  $(3.2 \times 10^{-3}, 8.4 \times 10^{-5})$ . As time increases, an infinite number of boxes are observed at the parametric value  $\mu = 0.0002$ .

The phase plane plot of the intermediates A and B is shown in Fig.28. The concentration of B is plotted against the concentration of A. The minimum value of  $(A,B) = (0.0000849, 0.0003354)$  and the maximum value of  $(A,B) = (0.8428407, 0.863683)$  in the short interval of time considered. The initial box is inserted in the second, and the second is inserted in the third and so on. As time

.099901



.0052207

Fig.21. X

.1005986

Fig.21. The phase plane plot of Y and X for the system (4.24) at  $X = 3 \times 10^{-4}$ . The concentration of A(Y) is plotted against P(X). The minimum concentration of (P,A) = (0.0052, 0.0001) while the maximum value of (P,A) = (0.1, 0.09). The dense spiral corresponds to the limit cycle.

increases a 'nest of similar boxes' are formed.

The concentration of the catalyst B is plotted against the concentration of P in Fig.29. The phase plane plot of the system (4.24) in the X-Z plane looks like a feather of a bird. The smallest one forms first and the rest forms one after the other as the time increases. The minimum value of  $(P,B) = (0.003282, 0.0003354)$  and the maximum value of  $(P,B) = (0.8627064, 0.863683)$  in the time interval considered here.

#### 4.6 DISCUSSION

The chemical reaction model studied here is based on a cubic autocatalator. We have considered here, the precursor P to be produced from the substrate S and the decay of P is controlled by the production of A. The cubic autocatalytic step is coupled with a simple decay of the autocatalyst B to the final product C.

The common feature of oscillators is the autocatalysis. The Lotka (1920) mechanism includes two autocatalytic reactions, but autocatalysis is not essential for sustained oscillations. The Brusselator, a model chemical reaction suggested by Prigogine and Lefever [63] is perhaps the simplest oscillator obtainable from a chemical

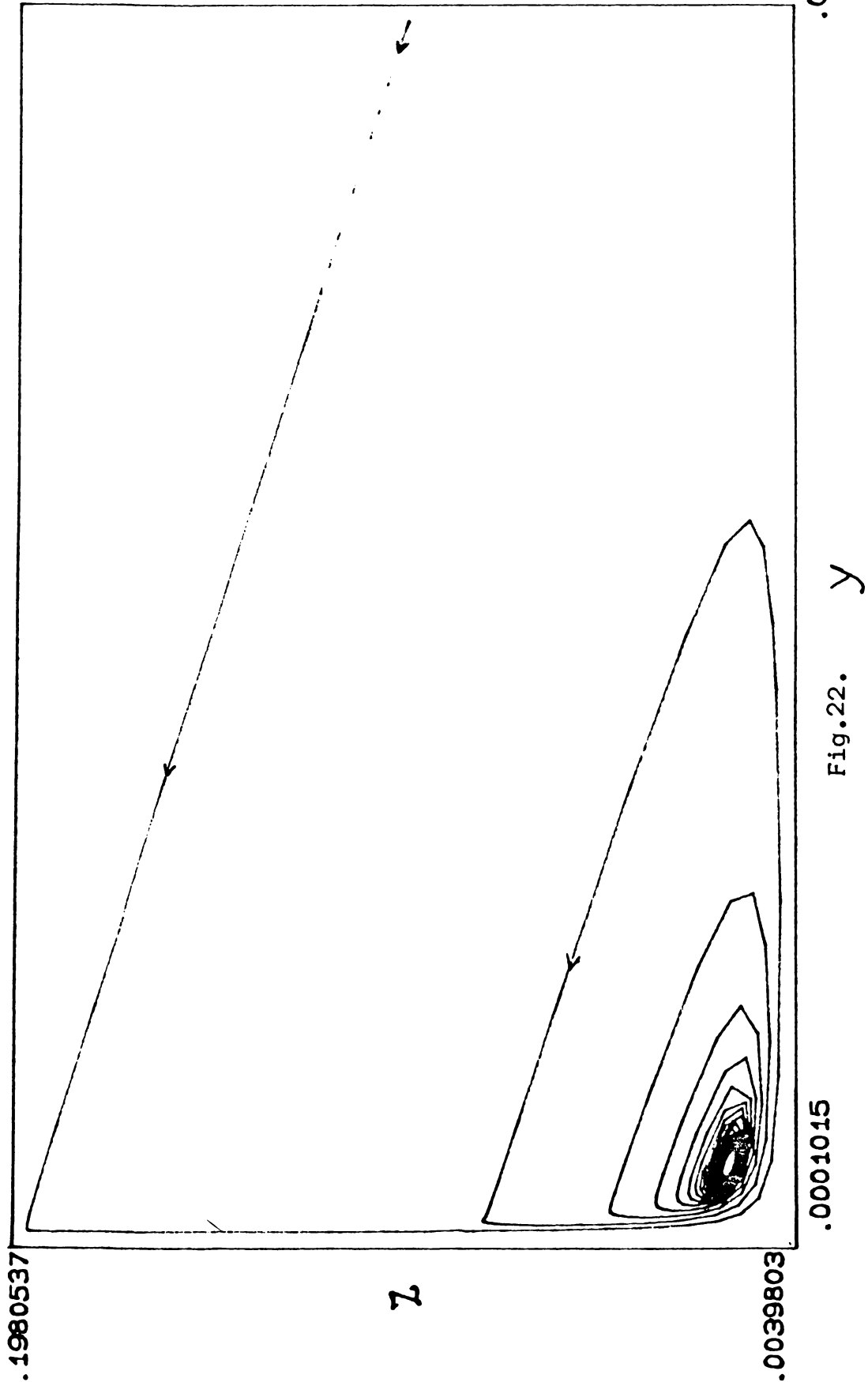


Fig.22.

Fig.22. The phase plane plot of Z and Y for the system (4.24) at  $K = 3 \times 10^{-4}$ . The concentration of B is plotted against A. The minimum concentration of (A,B) = (0.0001, 0.0039), while the maximum value of (A,B) = (0.099, 0.198). The dense spiral corresponds to the limit cycle in the Y-Z plane.

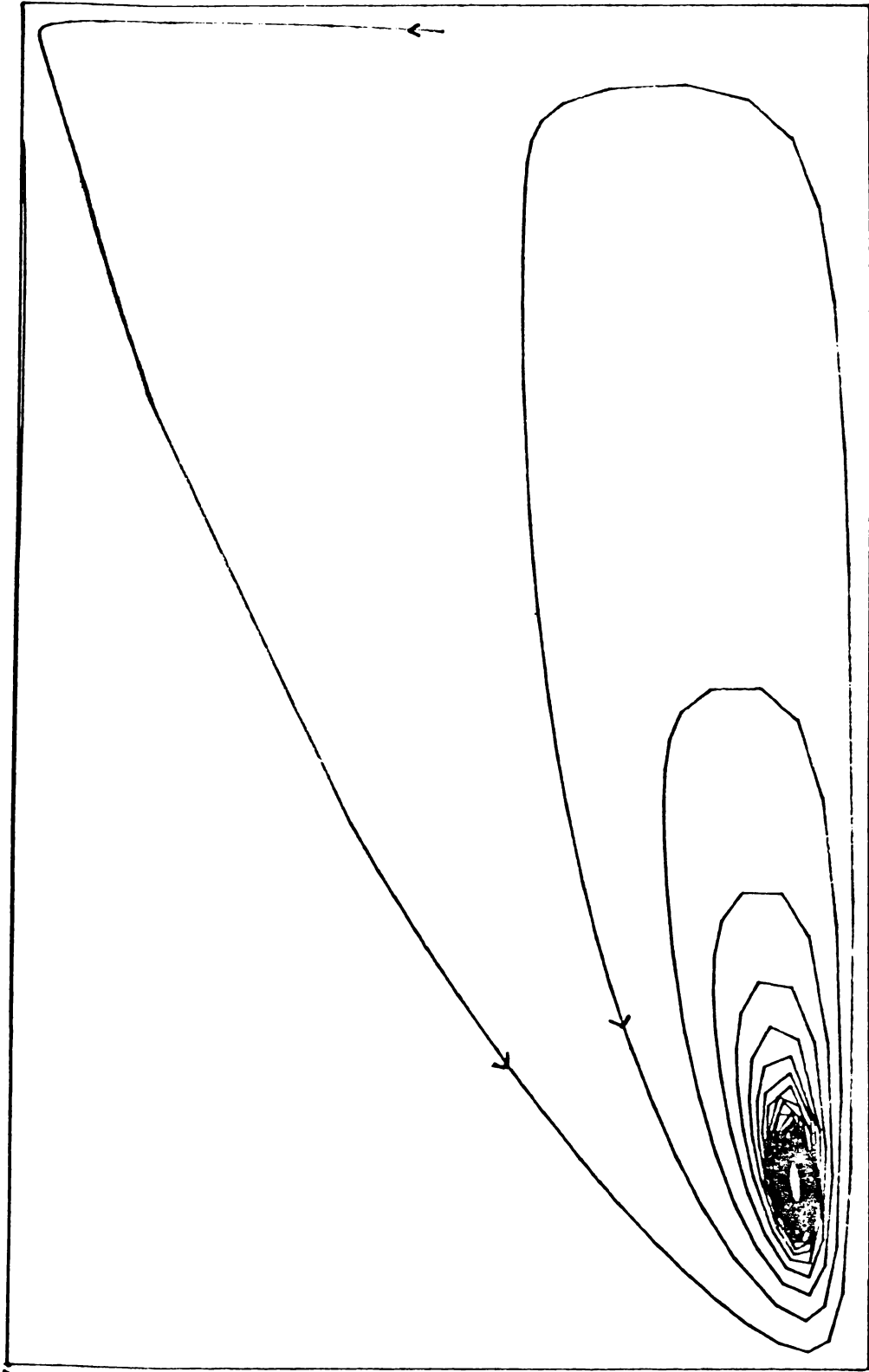
reaction model based on a cubic autocatalytic step. The well known Oregonator discussed in the previous chapter consists of single quadratic autocatalytic step.

Gray and Scott [27,28,29] discussed the simple schemes, consisting only either a quadratic autocatalytic reaction step (4.1), coupled with the catalyst decay or a cubic autocatalytic reaction step (4.2), coupled with the catalyst decay. These models contain only two dynamic variables viz. A and B. Merkin et al. [50,51] studied the quadratic autocatalytic system, coupled with a more complex removal of the catalyst.

The system containing the quadratic autocatalytic reaction step coupled with the catalyst decay (4.8) has a unique, physically acceptable stationary state [50] at any given residence time. The system exhibits Hopf bifurcations and at the critical point sustained oscillations in the concentrations A and B appear. The oscillatory patterns of behaviour exhibited by this system were examined in detail [51].

The reaction model (4.9) exhibiting oscillatory behaviour was discussed by Merkin et al. [52]. Besides the cubic autocatalytic reaction step (4.1) and the catalyst decay (4.2), the scheme (4.9) has a precursor chemical decaying (4.3) continuously. In this model (MNS), the first

.1980537



.0039803

.0052207

Fig.23. X

.1005986

Fig.23. The phase plane plot of Z and X for the system (4.24) at  $k = 3 \times 10^{-4}$ . The concentration of B is plotted against P. The minimum of (P,B) = (0.0052, 0.0039) while the maximum of (P,B) = (0.1, 0.198). The dense spiral corresponds to the limit cycle in the X-Z plane.

intermediate A is formed, via. the slow decay of the precursor species P, which is present in the reaction mixture in excess. The concentrations of various species at first change steadily with that of P decreasing while A, B and C increase. This period is followed by the onset and growth of oscillations in the concentrations of the intermediates A and B. The oscillations in this model starts only after a long time, at  $t = 7700$ , for  $t > 1790$ , there is a damped oscillatory return to the stable stationary state solution. By the 'pool chemical approximation', the three dimensional model (4.11) is converted to the more convenient two-dimensional model (4.12).

In the model (4.22), we consider P as produced from a substrate S and the decay of P is controlled by the production of A. This adds another dimension to the system. The system (4.24) is richly rewarded than the 'pool chemical approximation model' (4.16) [52], where the reaction system is a three-dimensional one, which has a more complicated structure. In this model, the dynamics of the three reactants P, A and B is to be taken into account, unlike in the two dimensional model (4.16). Hence the complete structure of our system (4.24) is different and complicated than the system with the 'pool chemical approximation'.



In the 'pool chemical approximation' model, where the concentration of P is maintained indefinitely, the concentration of A grows without limit in this region, while that of B falls quickly to zero. The oscillations in the concentrations of A and B start only after a certain interval of time.

Below a certain critical value of the parameter, the intermediate B decays more quickly than it is formed. Once the concentration of B is zero, the autocatalytic step, which is the sole route from A to B stops completely. Thus we arrive at a situation where A is continually being produced from P and not being removed. This behaviour can be removed quite simply by introducing the controlling of the precursor decay, by the production of A.

The oscillations in the intermediates of the system (4.24) start immediately, when the reaction is switched on. At the subcritical Hopf bifurcation point  $\kappa_{2c} = 3 \times 10^{-4}$  (where  $\tau_2 = 10^4$ ,  $\eta' = 10^{-4}$ ) the system (4.24) exhibit oscillations in the concentrations of P, A and B simultaneously. The amplitude of these oscillations decreases as the residence time is increased. At the same time the period between peaks lengthens and the oscillations becomes less spiky than earlier in character.

The numerical results obtained for the system (4.24) supports strongly the analytic results. Analytically, we found the range of the controlling parameter  $\mathcal{K}$ , where the system (4.24) to have unstable equilibrium solutions. By applying the classical Hopf bifurcation theorem, we found that the system has complex eigen values in this parametric range. The equilibrium solutions of (4.24) coming in the range ( $\mathcal{K}_{1c} < \mathcal{K} < \mathcal{K}_{2c}$ ) will be unstable and will be of the focal nature. When  $\mathcal{K}$  crosses the critical value  $\mathcal{K}_{2c}$ , the unstable focus becomes a stable focus. The figures given in the previous section supports the argument stated here.

The behaviour of the solutions of the system (4.24) one more parameter value, viz.  $\mathcal{K} = 0.0002$  is examined in detail. Numerically, this  $\mathcal{K} < \mathcal{K}_{2c} = 0.0003$ . The system (4.24) is integrated numerically for the parameter value  $\mathcal{K} = 0.0002$ ,  $\tau_2 = 10^4$  and  $\eta' = 10^{-4}$ . The oscillations in the intermediates P, A and B start immediately. The amplitude of these oscillations increases as the residence time is increased. Evidently the steady state of the system is an unstable focus, when the parameter value lies in the range  $\mathcal{K}_{1c} < \mathcal{K} < \mathcal{K}_{2c}$ . At the critical Hopf bifurcation point  $\mathcal{K}_{2c} = 0.0003$ , we observe the qualitative change of the steady state solution from unstable focus to the stable one. The phase plane plots of the system (4.24) on numerical integration for the parametric value  $\mathcal{K} = 0.0002$

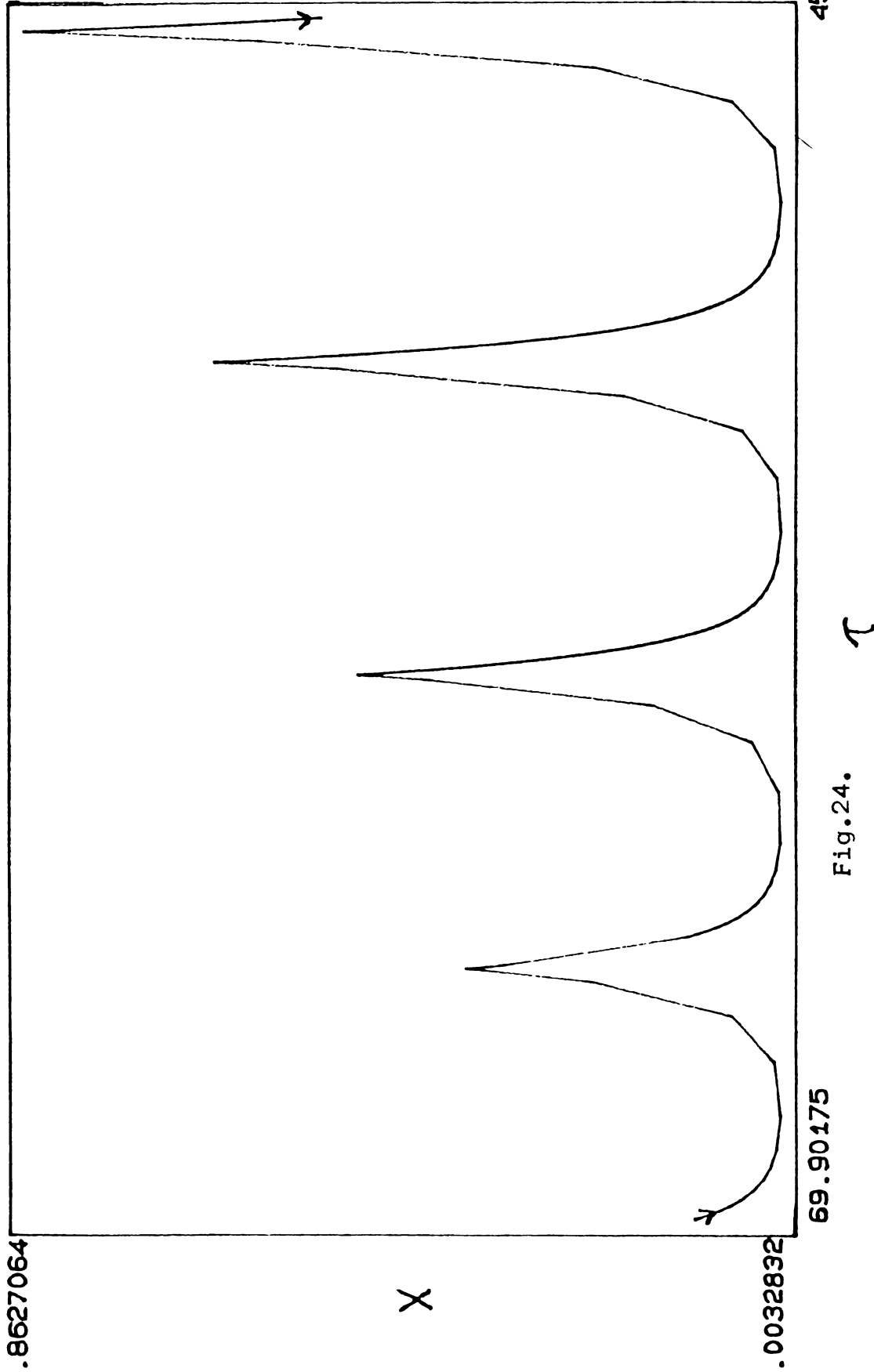
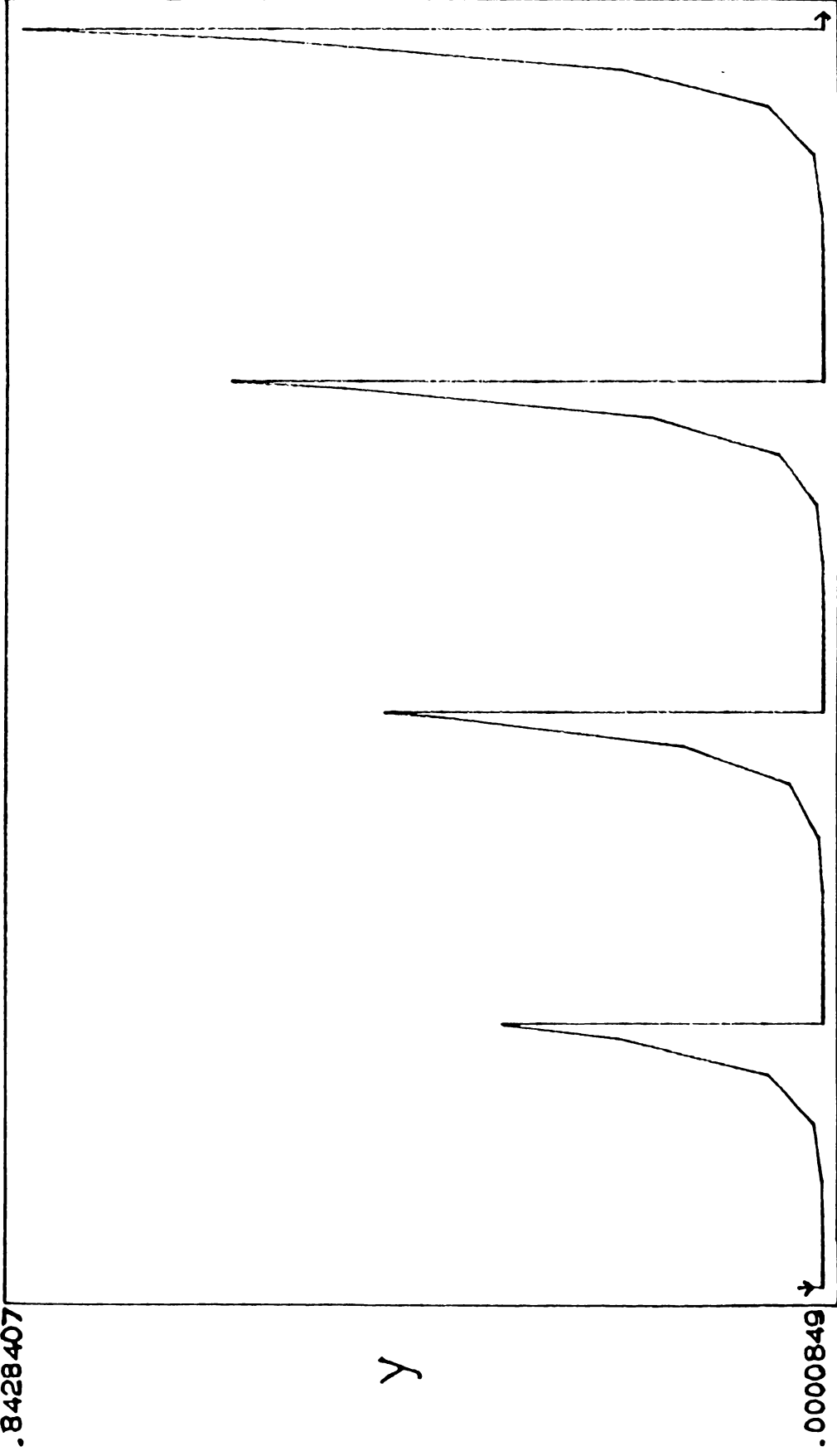


Fig.24.

Fig.24. Concentration profile of X(or P) plotted against the time ( $\tau$ ) of the system (4.24) for the parametric value  $\mathcal{K} = 2 \times 10^{-4}$ . The amplitude of the P-wave increases as time progresses. The concentration of P increases from 0.0032 to 0.8627.

.8428407



.0000849

69.90175

454116.5

$\tau$

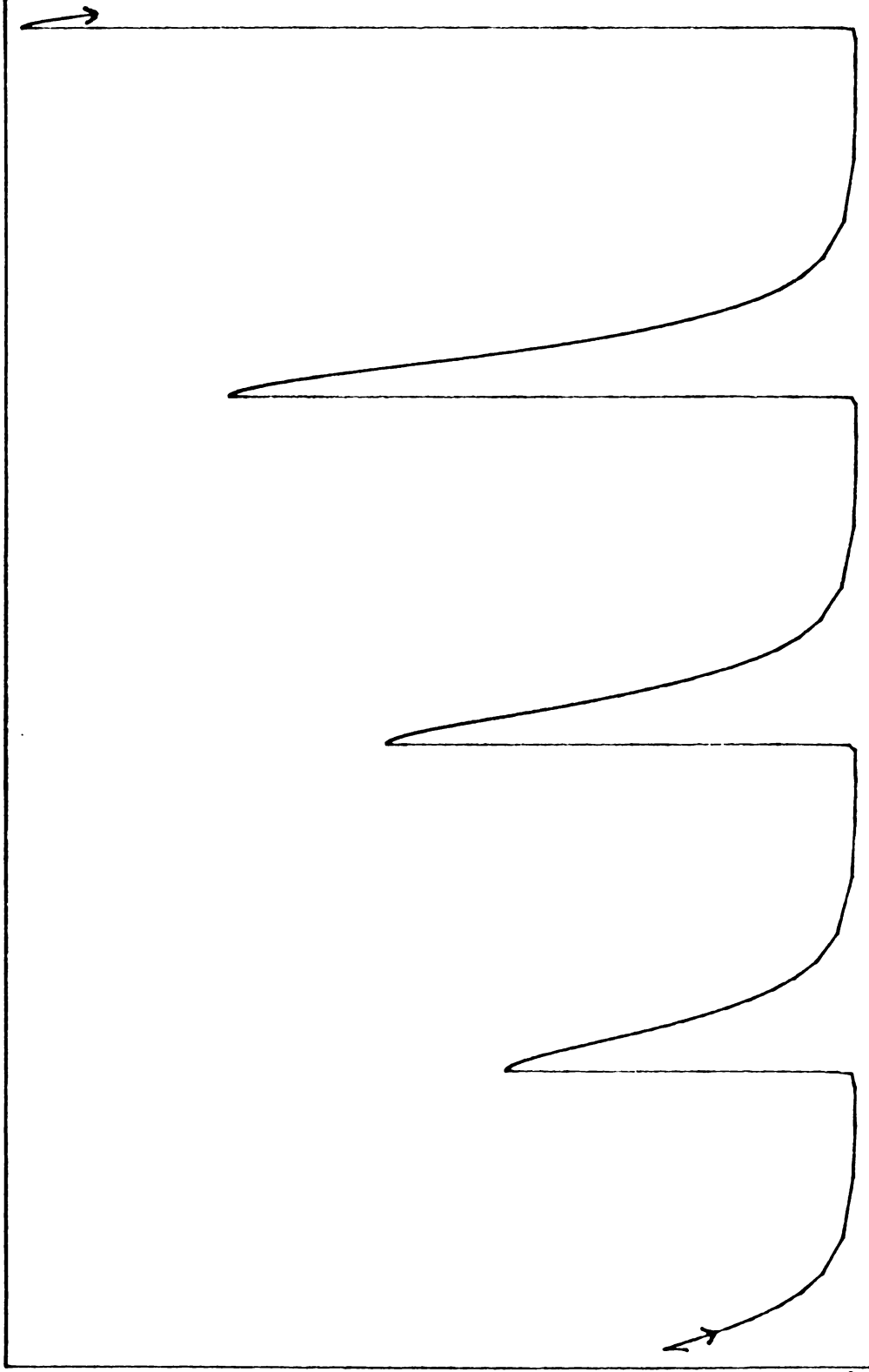
Fig.25.

Fig.25. Concentration profile of Y(or A) plotted against the time ( $\tau$ ) from  $\tau=69.9$  to  $\tau = 454116.5$  of the system (4.24) for the parametric value  $\lambda = 2 \times 10^{-4}$ . The concentration of A increases from  $8 \times 10^{-5}$  to  $8 \times 10^{-1}$ .

.863683

Z

.0003354



69.90175

454116.5

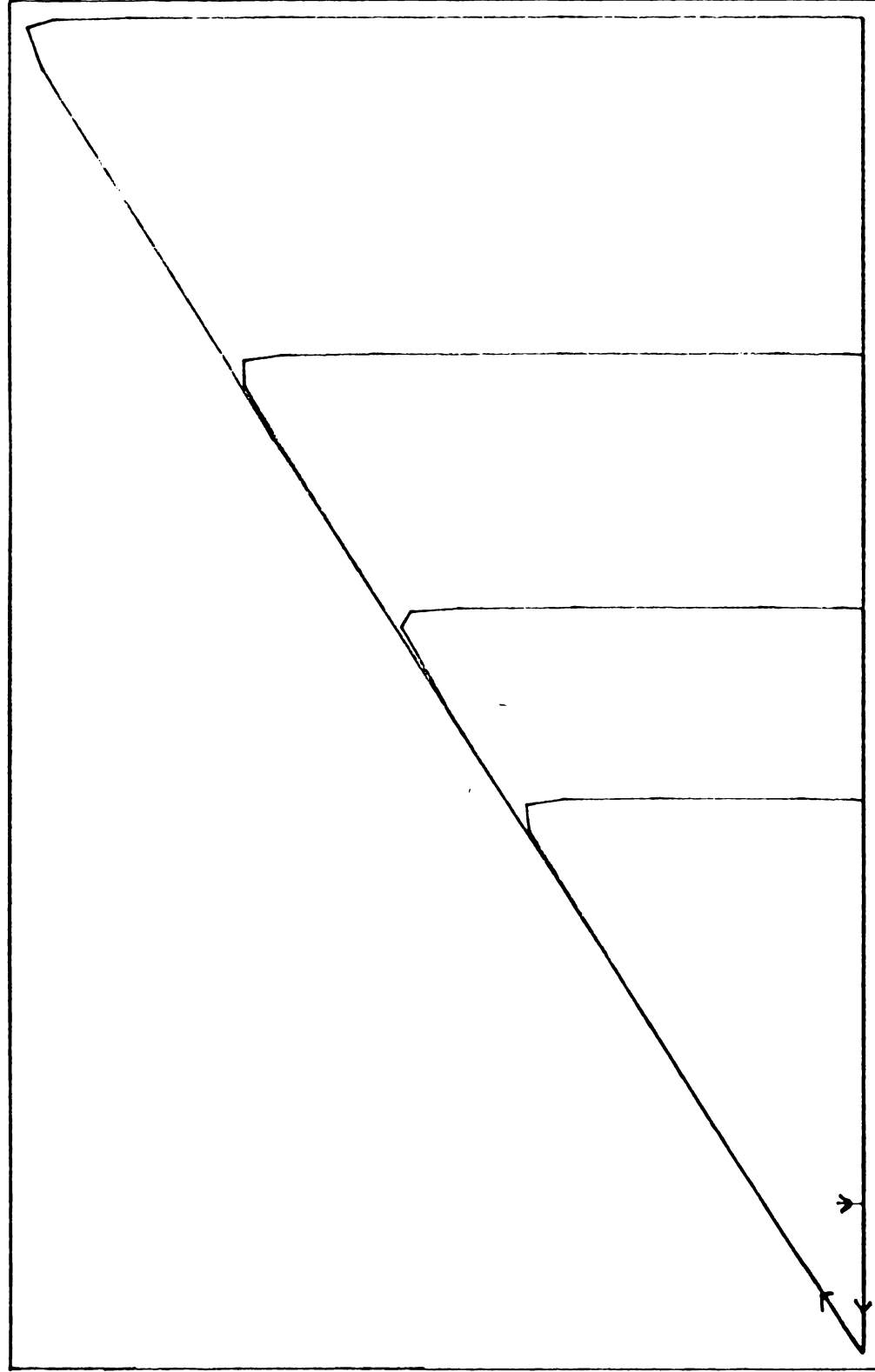
Fig.26.  $\tau$

Fig.26. Concentration profile of Z(or B) plotted against the time ( $\tau$ ), from  $\hat{\tau} = 69.9$  to  $\hat{\tau} = 454116.5$  of the system (4.24) for the parametric value  $\mathcal{A} = 2 \times 10^{-4}$ . The concentration of B increases from  $3.3 \times 10^{-4}$  to  $8.6 \times 10^{-1}$ .

in the X-Y, Y-Z and Z-X planes are very interesting to study. Thus we get large amplitude oscillations for the system at  $\mathcal{X} = 0.0002$ .

In the earlier studies [52] the precursor P has been treated as a reactant whose concentration falls in time. Such a scheme has distinct similarities to the isothermal schemes. When the pool chemical approximation is contemplated, there is a unique stationary state  $(x_0, y_0, z_0)$ . The system (4.24) contains three variables  $x, y, z$  and three parameters,  $\mathcal{X}$ ,  $\mathcal{C}_2$  and  $\eta'$  while the system (4.16) contains only two variables  $x, y$  and one parameter  $\mu_p$ . The subcritical and supercritical Hopf bifurcation points of the system (4.24) found numerically as (4.38). The configuration sketched in Fig.21 shows that, the system jumps abruptly into fully developed nonzero amplitude oscillation. This pattern of solutions indicates the slow decay of P and oscillations are observed over a large range of time.

.8428407



.0000849

.0032832

.8627064

Fig. 27 X

Fig.27. Phase plane plot of X and Y (P and A) of the system (4.24) for the parametric value  $\lambda = 2 \times 10^{-4}$ . The solution trajectory repels from a point. It is interesting to note the formation of a nest of similar boxes. The minimum of  $(P,A) = (3.2 \times 10^{-3}, 8 \times 10^{-5})$  while the maximum value of  $(P,A) = (8.6 \times 10^{-1}, 8.4 \times 10^{-1})$ .

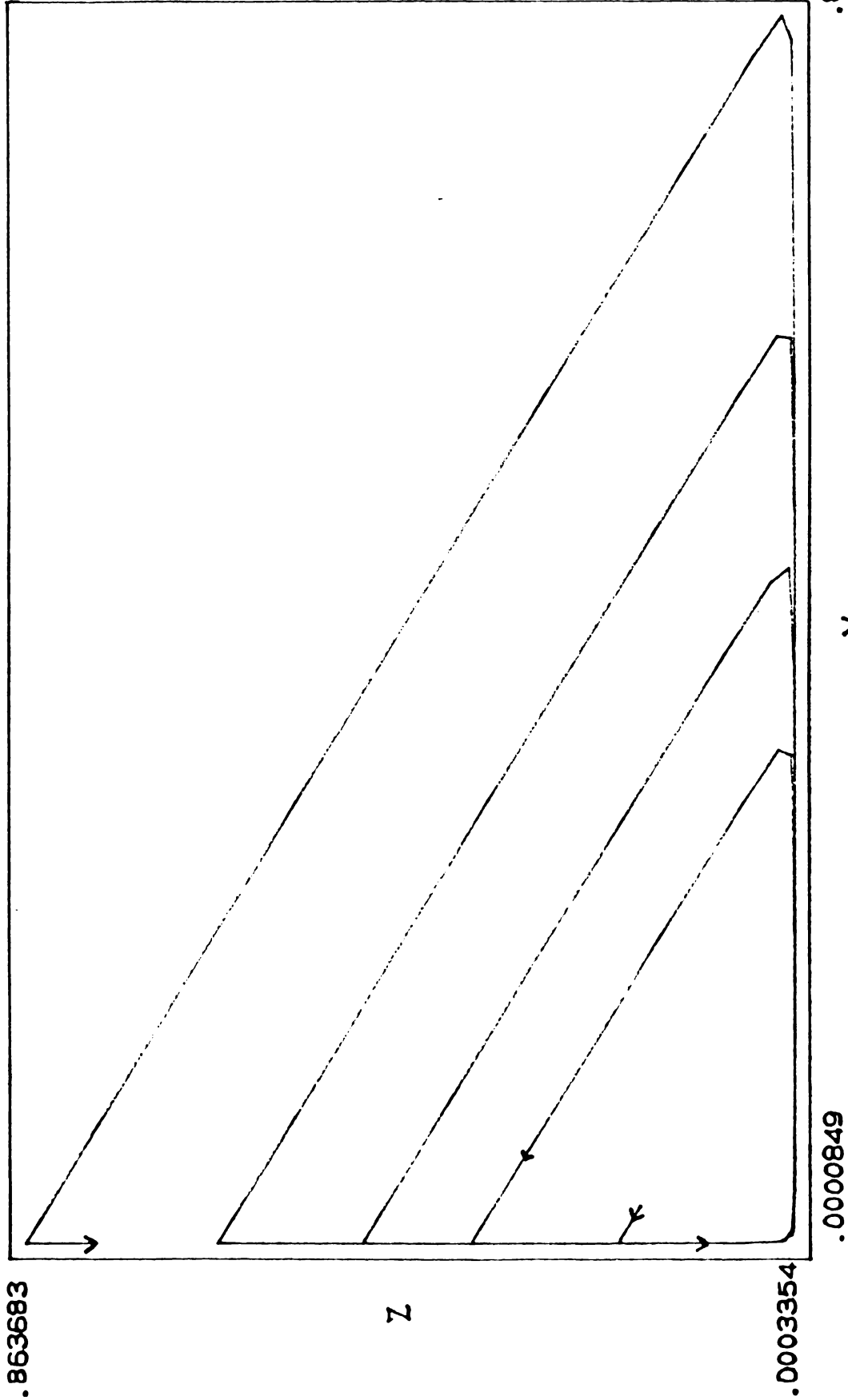


Fig.28.

Fig.28. Phase plane plot of Y and Z (A and B) of the system (4.24) for the parametric value  $\chi = 2 \times 10^{-4}$ . The trajectory repels from the stationary state by forming a nest of similar boxes.  $\text{Min}(A,B) = (8 \times 10^{-5}, 3 \times 10^{-4})$   $\text{Max}(A,B) = (8.4 \times 10^{-1}, 8.6 \times 10^{-1})$ .



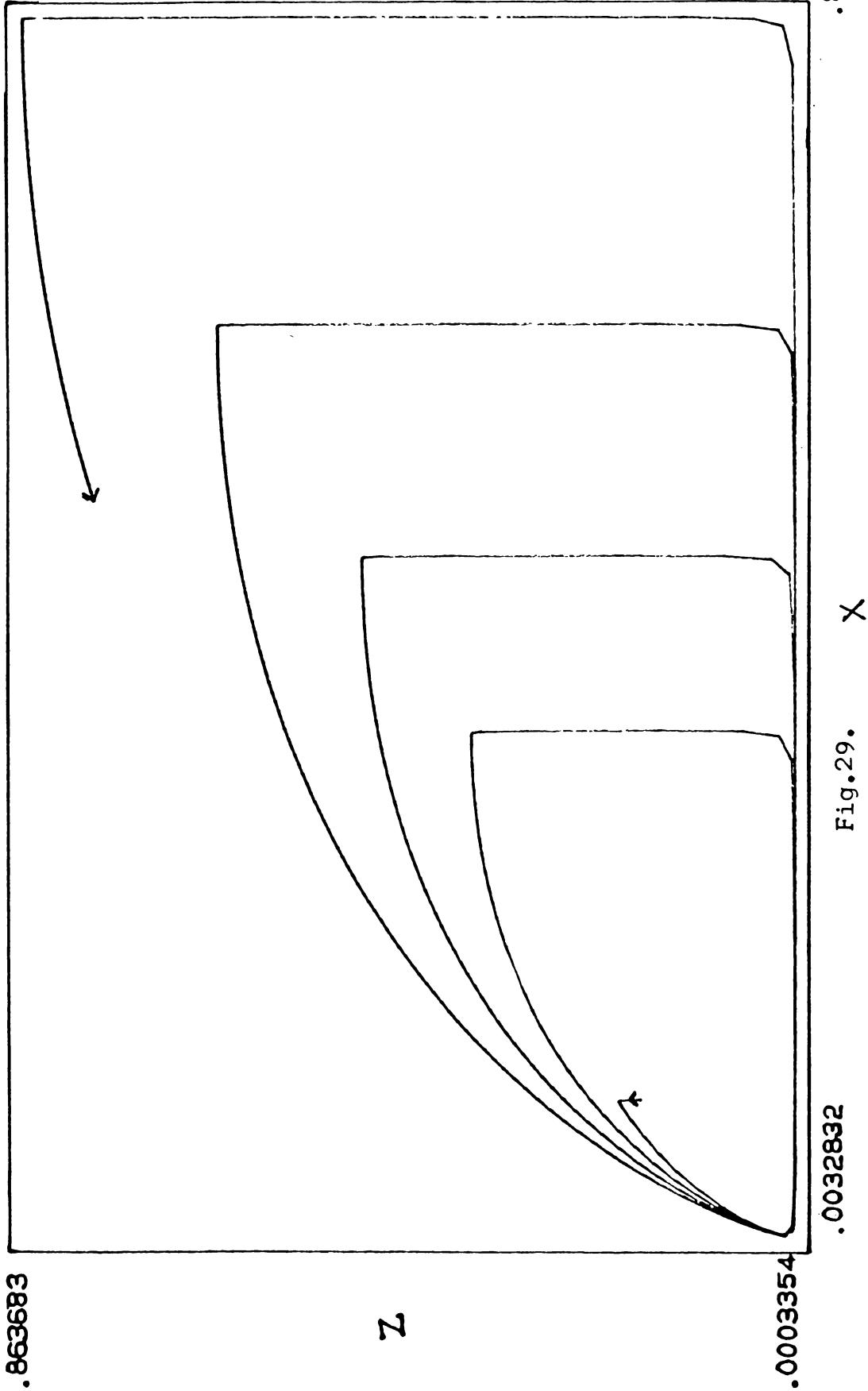


Fig.29.

Fig.29. Phase plane plot of  $X$  and  $Z$  (P and B) of the system (4.24), for the parametric value  $K = 2 \times 10^{-4}$ . The solution trajectory repels from the steady state forming feather like diagram.

## Chapter 5

### CONCLUSIONS

The nonlinear dynamics of certain important reaction systems are discussed and analysed in this thesis. The interest in the theoretical and the experimental studies of chemical reactions showing oscillatory dynamics and associated properties is increasing very rapidly. Many researchers work out mathematical models of such reactions to understand the complex nature of the systems. The oscillatory behaviour and other related characteristics in nonlinear systems far from equilibrium has a highly interesting connection with the organization of the structure of the system [30, 32].

An attempt is made to study some nonlinear phenomena exhibited by the well known chemical oscillator, the Belousov-Zhabotinskii reaction whose mathematical properties are much in common with the properties of biological oscillators. While extremely complex, this reaction is still much simpler than biological systems at least from the modelling point of view. A suitable model [19] for the system is analysed and we have studied the limit cycle behaviour of the system, for different values of the stoichiometric parameter  $f$ , by keeping the value of the reaction rate ( $k_6$ ) fixed at  $k_6 = 1$ . The more complicated three-variable model is stiff in nature.

The arc length continuation method has been used to study the dependence of steady state solutions  $(x_0, y_0, z_0)$  of the model (3.14) on the parameter  $f$ . The values of the parameters in (3.14) other than  $f$  viz.  $s, w$  and  $q$  are fixed as 77.27, 0.161 and  $8.375 \times 10^{-6}$ . The existence of limit cycle behaviour in the three dimensional model is shown analytically and are verified numerically. Among many numerical methods to solve such systems of nonlinear differential equations the Runge-Kutta Method with step doubling is found to be the most suitable one to solve our system. Limit cycle behaviour is observed for the complete model in the  $y$ - $x$  phase plane for  $f = 1.0$  and  $f = 1.1$ , with periods  $\tau = 143.5$  and  $\tau = 148.9$  respectively. The two variable ( $y$ - $z$ ) model, being much easier to handle mathematically, is examined more thoroughly. The oscillatory behaviour of this system is examined for several values of  $f$  lying in the unstable region  $\frac{1}{2} < f < 1 + \sqrt{2}$ . Isolated limit cycles are obtained for  $f = 0.5001, 0.74, 0.9, 1.0, 1.3, 1.4$  and  $1.5$  in the  $y$ - $z$  phase plane. The birth of more than one limit cycle is observed for the system (3.18) at the parametric values  $f = 1.1, 1.2$  and  $1.595288$ . This may be considered as a signal for the excitability property of the reaction model. Many workers [6,14,45,59,65,74,75] predicted and some discussed the excitable behaviour of B-Z reaction system for this range of  $f$ . The solution

trajectory starting from the initial concentration  $(y_0, z_0) = (1.0, 488.8)$  is attracted to another stationary state  $(1.297, 4.355)$  for some parametric values,  $f = 1.6, 1.7, 1.8, 1.9, 2.0, 2.1$  etc. Thus multiple steady states are observed in this region of  $f$ . The experimental results observed in B-Z reaction can be cited in [4,16].

The fact that the autocatalysis is the common feature of almost all oscillators (biological and non-biological) inspired us to study a general cubic autocatalytic system.

We have presented a model analysing the autocatalytic system. The cubic autocatalytic step  $A + 2B \longrightarrow 3B$  lies at the heart of the simplest models for oscillatory and other complex nonlinear behaviour in closed systems, in the CSTR and in reaction coupled with diffusion [57]. General reaction systems containing either quadratic autocatalytic reaction step or cubic autocatalytic step, coupled with autocatalyst decay step which are two dimensional were studied so far [9,27,28,29]. In order to explain the complex phenomena observed in oscillators like aperiodic oscillation, period doubling, etc. a three dimensional model is required. Sustained oscillatory behaviour is observed in the system(4.24). The range of the parameter  $\mathcal{K}$  at which the stationary states are unstable is found analytically. This range is found to be  $\mathcal{K}_{1c} < \mathcal{K} < \mathcal{K}_{2c}$ , where  $\mathcal{K}_{1c} = 0$  and  $\mathcal{K}_{2c} = 0.0003$ . The values

of other parametric values  $\eta'$  and  $\tau_2$  are fixed as  $\eta' = 10^{-4}$  and  $\tau_2 = 10^4$ . The initial value taken for the numerical integration is  $x_0 = y_0 = z_0 = 0.1$ . Limit cycles are obtained for the system in X-Y, Y-Z and Z-X phase planes respectively. The trajectories are attracted to a limit cycle and the unstable critical point inside it acts as an attractor, for the supercritical Hopf bifurcation point  $\mathcal{K}_{2c}$ . When the integration of the system (4.24) is carried out numerically for other parametric values less than  $\mathcal{K} = 0.0003$ , large amplitude waves corresponding to the concentrations of each constituents P, A and B are formed. The trajectories corresponding to the system repel from a fixed point  $(3 \times 10^{-3}, 8 \times 10^{-5}, 3 \times 10^{-4})$ . Thus the numerical result confirms the analytic prediction that, the equilibrium state solution of the system in the region  $\mathcal{K}_{1c} < \mathcal{K} < \mathcal{K}_{2c}$  is an unstable focus. At the critical Hopf bifurcation value,  $\mathcal{K}_{2c} = 0.0003$ , the unstable focus becomes a stable one. The same behaviour of the solutions described above are obtained for some other values of  $\tau_2$ , viz. 9999.0, 10001.0, 10002.0, 10004.0, 10005.0, 10007.0, 10008.0, and 10009.0.

Several interesting phenomena, other than sustained oscillations or damped oscillations, such as bursting, excitability, intermittency, CDO, chaotic structures etc.

are to be examined more elaborately for the oscillators, considered here. In the case of the three-variable Oregonator model, the sustained oscillatory behaviour of the system is to be examined for all other values of  $f$ . Satisfactory models are yet to be developed for explaining some recent experimental results of the B-Z chemical reaction (eg. certain pattern formation). Many attempts to explain some of these phenomena are reported in the literature [18, 22, 44, 71, 76]. The reaction system based on the cubic autocatalytic step has to be subjected to more studies.

## BIBLIOGRAPHY

- [1] Abramowitz, M. and Stegun, I.A., 'Handbook of Mathematical Functions', Dover, New York, 1964.
- [2] Andronov, A.A., Vitt, A.A. and Khaikin, S.E., 'Theory of Oscillations', 2nd Edition, Pergamon Press, New York, 1966.
- [3] Bar Eli, K. and Noyes, R.M., 'Relevance of a Two-variable Oregonator to stable and unstable steady states and Limit Cycles to thresholds of excitability and to Hopf as SNIPER Bifurcations', J.Chem.Phys. Vol.86, No.4, pp. 1927-1937, 1987.
- [4] Bar Eli, K. and Ronkin, J., 'Oscillations and Steady States in the Bromate-Bromide-Cerous System: Comparison of Experimental and Calculated Data of Different Sets of Rate Constants', J.Phys.Chem. Vol.88, pp.2844-2847, 1984.
- [5] Belousov, B.P., 'A Periodic Reaction and Its Mechanism', Ref. Radiants. Med., Medgiz, pp. 145, 1959.
- [6] Britton, N.F., 'Threshold Phenomena and Solitary Travelling Waves in a Class of Reaction-Diffusion Systems', SIAM J. Appl. Math. Vol.42, No.1, pp. 188-217, 1982.
- [7] Busse, H.G., 'A Spatial Periodic Homogeneous Chemical Reaction', J.Phys.Chem., Vol.73, p.750, 1968.
- [8] Coddington, E.A. and Levinson, N., 'Theory of Ordinary Differential Equations', Mc-Graw Hill, N.Y., 1955.

- [9] D'Anna, A., Lignola, P.G. and Scott, S.K., 'The Application of Singularity Theory to Isothermal Autocatalytic Open Systems: the elementary scheme  $A+MB=(M+1)B.$ ', Proc.R.Soc.Lond. A 403, pp. 341-363, 1986.
- [10] Duffy, M.R., Britton, N.F. and Murray, J.D., 'Spiral Wave Solutions of Practical Reaction-Diffusion Systems', SIAM J. Appl. Math. Vol.39, No.1, pp.8-13, 1980.
- [11] Epstein, I.R., 'Complex Dynamical Behaviour in Simple Chemical Systems', J.Phys.Chem., Vol.88, pp.187-198, 1984.
- [12] Ermentrout, G.B., 'Period Doublings and Possible Chaos in Neural Models', SIAM J. Appl. Math., Vol.44, No.1, pp. 80-95, 1984.
- [13] Ermentrout, G.B. and Rinzel, J., 'Waves in a Simple, Excitable or Oscillatory, Reaction-Diffusion Model', J. Math. Biol. Vol.11, pp.269-294, 1981.
- [14] Ermentrout, G.B. and Kopell, N., 'Parabolic Bursting in an Excitable System Coupled with a Slow Oscillation', SIAM J. Appl. Math. Vol.46, No.2, pp. 233-253, 1986.
- [15] Field, R.J., 'Limit Cycle Oscillations in the reversible Oregonator', J.Chem.Phys., Vol.63, pp.2284-2296, 1975.
- [16] Field, R.J., and Boyd, P.M., 'Bromine-Hydrolysis Control in the Cerium Ion-Bromate Ion-Oxalic Acid-Acetone Belousov-Zhabotinskii Oscillator', J.Phys.Chem. Vol.89, pp.3707-3714, 1985.



- [17] Field, R.J., Körös, E. and Noyes, R.M., 'Oscillations in Chemical Systems II. Through Analysis of Temporal Oscillation in the Bromate-Cerium-Malonic Acid System, J.Am. Chem. Soc., Vol.94, No.25, pp. 8649-8664, 1972.
- [18] Field, R.J. and Noyes, R.M., 'Explanation of Spatial Band Propagation in the Belousov Reaction', Nature, Vol. 237, pp. 390-392, 1972.
- [19] Field, R.J. and Noyes, R.M., 'Oscillations in Chemical Systems IV. Limit Cycle Behaviour Model of a real Chemical Reaction', J.Chem.Phys., Vol.60, No.5, pp.1877-1884, 1974 a.
- [20] Field, R.J. and Noyes, R.M., 'Oscillations in Chemical Systems v. Quantitative explanation of band migration in the Belousov-Zhabotinskii reaction', J. Am. Chem. Soc., Vol.96, pp. 2001-2006, 1974 b.
- [21] Field, R.J. and Troy, W.C., 'The Existence of Solitary Travelling Wave Solutions of a Model of the Belousov-Zhabotinskii Reaction', SIAM J. Appl. Math. Vol.37, No.3, pp. 561-587, 1979.
- [22] Fife, P.C., 'Stationary Patterns to Reaction Diffusion Equations', J.Chem.Phys., Vol.64, No.2, pp.554-564, 1976.
- [23] Fife, P.C., 'Mathematical Aspects of Reacting and Diffusing Systems', Lecture Notes in Biomathematics, Vol.28, Springer-Verlag, N.Y. 1979.
- [24] Forsyth, A.R., 'A Treatise on Differential Equations', 6th Ed. London, 1929.

- [25] Gear, C.W., 'Numerical Initial Value Problems in Ordinary Differential Equations', Prentice-Hall, Inc. Englewood Cliffs, N.J. 1971.
- [26] Gibbs, R.G., 'Travelling Waves in the Belousov-Zhabotinskii Reaction, SIAM J. Appl. Math. Vol.38, No.3, pp.422-444, 1980.
- [27] Gray, P. and Scott, S.K.  
Chem. Engg. Sci., Vol.38, pp. 29-43, 1983.
- [28] Gray, P. and Scott, S.K.  
Chem. Engg. Sci., Vol.39, pp.1087-1079, 1984.
- [29] Gray, P. and Scott, S.K., 'Sustained Oscillations and other Exotic Patterns of Behaviour in Isothermal Reactions', J.Phys.Chem., Vol.89, pp.22-32, 1985.
- [30] Guckenheimer and Holmes, P., 'Nonlinear Oscillations, Dynamical Systems and Bifurcations of Vector Fields', Springer Verlag, 1983.
- [31] Hagan, P.S., 'Spiral Waves in Reaction-Diffusion Equations', SIAM J. Appl.Math., Vol.42, pp.762-786, 1982.
- [32] Hale, J.K., 'Oscillations in Nonlinear Systems' Mc-Graw Hill, N.Y., 1963.
- [33] Hale, J.K., 'Ordinary Differential Equations', Wiley-Interscience, N.Y. 1969.
- [34] Hans Degn, 'Oscillating Chemical Reactions in Homogeneous Phase'. J.Chem.Educ.. Vol.49. No.5. pp.302-307. 1972.

- [35] Hassard, B.D., Kazarinoff, N.D. and Wan, V.H., 'Theory and Applications of Hopf Bifurcation', London Mathematical Society, Lecture Notes Series No.41, (Cambridge University), Cambridge, 1981.
- [36] Hastings, S.P. and Murray, J.D., 'The Existence of Oscillatory Solutions in the Field-Noyes Model for the Belousov-Zhabotinskii Reaction', SIAM J. Appl. Math., Vol.28, No.3, pp. 678-688, 1975.
- [37] Howard, L.N., 'Nonlinear Oscillations in Nonlinear Oscillations in Biology', Lecture in Applied Mathematics, Vol.17, American Mathematical Society, Providence, R.I. (1979).
- [38] Hudson, J.L. and Mankin, J.C., 'Chaos in the Belousov-Zhabotinskii Reaction', J. Chem. Phys. Vol. 74, pp. 6171-6177, 1981.
- [39] Iooss, G. and Joseph, D.D., 'Elementary Stability and Bifurcation Theory', Springer-Verlag, N.Y. 1981.
- [40] James P. Keener and Tyson, J.J., 'Spiral Waves in the Belousov-Zhabotinskii Reaction', Physica 21 D, pp. 307-324, 1986.
- [41] Janz, R.D., Vanecek, D.J. and Field, R.J., 'Composite double oscillation in a modified version of the Oregonator model of the Belousov-Zhabotinskii reaction', J.Chem.Phys., Vol.73, No.7, pp.3132-3138, 1980.

- [42] Jepson, A.D. and Keller, H.B., 'Steady State and Periodic Solution Paths: their Bifurcations and Computations', Int. Ser. Num. Math., Vol. 70, pp. 219-246, 1984.
- [43] Klaasen, G.A. and Troy, W.C., 'The Stability of Travelling Wave Front Solutions of a Reaction-Diffusion System', SIAM J. Appl. Math., Vol.41, No.1, pp. 145-187, 1987.
- [44] Kopell, N., 'Target Pattern Solutions to Reaction-Diffusion Equations in the presence of Impurities', Adv. Appl. Maths., Vol.2, pp. 389-399, 1981.
- [45] Kopell, N., 'Forced and Coupled Oscillators in Biological Applications', Proc. Int. Cong. Math. 1983, Warszawa, pp. 1645-1659.
- [46] Kubicek, M., 'Dependence of Solution of Nonlinear Systems on a Parameter', ACM Transactions on Mathematical Software, Vol.2, No.1, pp. 98-107, 1976.
- [47] Kubicek, M., 'Algorithm for evaluation of Complex Bifurcation points in Ordinary Differential Equations', SIAM J. Appl. Math. Vol. 38, No.1, 1980.
- [48] Kubicek, M. and Marek, M., 'Computational Methods in Bifurcation Theory and Dissipative Structures', Springer-Verlag, N.Y. 1983.
- [49] Marsden, J.E. and Mc Cracken, M., 'The Hopf Bifurcation and its Applications', Springer-Verlag, N.Y. 1976.

- [50] Merkin, J.H., Needham, D.J. and Scott, S.K., 'A Simple model for sustained oscillations in iso-thermal branched chain or autocatalytic reactions in a well stirred open system. II. Limit cycles and non-stationary states. Proc.R.Soc.Lond.A. 398, pp.101-116, 1985 a.
- [51] Merkin, J.H., Needham, D.J. and Scott, S.K., 'A Simple model for sustained oscillations in iso-thermal branched chain or autocatalytic reactions in a well stirred open system. I. Stationary states and local stabilities, Proc.R.Soc.Lond.A.398, pp.81-100, 1985 b.
- [52] Merkin, J.H., Needham, D.J. and Scott, S.K., 'Oscillatory Chemical Reactions in Closed Vessels', Proc.R.Soc. Lond.A. 406, pp. 299-323, 1986.
- [53] Minorsky, N., 'Nonlinear Oscillations', Van Nostrand, N.Y., 1962.
- [54] Murray, J.D., 'On a model for temporal oscillations in the Belousov-Zhabotinskii Reaction', J.Chem.Phys., Vol.61, pp.3610-3613, 1974.
- [55] Murray, J.D., 'On a model for concentration waves in the Belousov-Zhabotinskii reaction', J. Theor. Biol. Vol. 56, pp. 329-353, 1976.
- [56] Murray, J.D., 'Lectures on Nonlinear Differential Equation Models in Biology', Oxford University Press, Cambridge, 1977.

- [57] Nicolis, G. and Portnow, J., 'Chemical Oscillations', Chem. Rev., Vol. 73, No.4, pp.365-384, 1973.
- [58] Nicolis, G. and Prigogine, I., 'Self Organisation in Non-equilibrium Systems', Wiley Interscience, New York, 1977.
- [59] Noszticzius, Z., Wittman, M. and Stirling, P., 'Bifurcation from Excitability to Limit Cycle Oscillations at the end of the Induction Period', J.Chem.Phys. Vol.86, No.4, pp.1922-1926, 1987.
- [60] Noyes, R.M., 'An alternative to the Stoichiometric factor in the Oregonator Model', J.Chem.Phys., Vol.80, No.12, pp. 6071-6077, 1984.
- [61] Peggy Marie Wood and John Ross, 'A quantitative Study of Chemical Waves in the Belousov-Zhabotinskii Reaction', J.Chem.Phys., Vol.82, No.4, pp.1924-1936, 1985.
- [62] Pomeau, Y., Roux, J.C., Rossi, A., Bachelart, S. and Vidal, C., 'Intermittent behaviour in the Belousov-Zhabotinskii Reaction', Le Journal de Physique Letters, Vol. 42, pp. 271-273, 1981.
- [63] Prigogine and Lefever, R., 'Symmetry breaking instabilities in dissipative systems-II', J.Chem.Phys. Vol.48, pp. 1695-1700, 1968.
- [64] Rinzel, J. and Keener, J.P., 'Hopf Bifurcation to Repetitive Activity in Nerve', SIAM J.Appl.Math. Vol.43, No.4, pp.907-922, 1983.

- [65] Rinzel, J. and Tray, W.C., 'Bursting Phenomena in a Simplified Oregonator flow system model', J.Chem.Phys., Vol.76, No.4, pp.1775-1789, 1982.
- [66] Roose, D. and Hlavacek, V., 'A direct method for the computation of Hopf bifurcation points', SIAM J. Appl. Math. Vol.45, No.6, pp.879-893, 1985.
- [67] Showalter, K., Noyes, R.M. and Bar-Eli, K., 'A Modified Oregonator Model exhibiting complicated limit cycle behaviour in a flow system', J.Chem.Phys. Vol.69, No.6, pp.2514-2524, 1978.
- [68] Silvia Totaro, 'On a Model for pulse propagation in a nerve', Nonlin. Anal. Theor, Methodic Applications, Vol.6, No.2, pp. 125-137, 1982.
- [69] Struble, R.A., 'Nonlinear Differential Equations', McGraw Hill, TMH Edition, N.Y., 1974.
- [70] Sweeney, B.M., 'Rhythmic Phenomena in Plants', Academic Press, London, 1969.
- [71] Thoenes, D., 'Spatial Oscillations in the Zhabotinskii Reaction', Nature. Phys. Sci., Vol.243, pp.18-21, 1973.
- [72] Turner, J.S., Roux, J.C., Mc Cormick and Swinney, H.L., 'Alternating Periodic and Chaotic Regimes in a Chemical Reaction', Phys. Lett. A., Vol.85, pp. 9-12, 1981.

- [73] Tyson, J.J., 'The Belousov-Zhabotinskii Reaction',  
Lecture Notes in Bio-Mathematics, Vol.10,  
Springer, Berlin, 1976.
- [74] Tyson, J.J., 'Some further studies of nonlinear oscillations in Chemical Systems', J.Chem.Phys., Vol.58, No.9, pp.3919-3930, 1973.
- [75] Tyson, J.J., 'Analytic representation of oscillations, excitability and travelling waves in a realistic model of the Belousov-Zhabotinskii Reaction', J.Chem.Phys., Vol.66, No.3, pp.905-915, 1977.
- [76] Tyson, J.J. and Fife, P.C., 'Target Patterns in a Realistic Model of the B-Z Reaction', J.Chem. Phys., Vol.75, No.5, pp. 2224-2237, 1980.
- [77] Winfree, A.T., 'Spiral Waves of Chemical Activity', Nature, Vol.175, pp.633-635, 1972.
- [78] Winfree, A.T., 'Scroll Shaped Waves of Chemical Activity in three dimensions', Science, Vol.181, pp.937-939, 1978.
- [79] Winfree, A.T., 'Oscillations and Travelling Waves in Chemical Systems', Ed. R.J.Field and M.Burger, Wiley, N.Y. 1985.
- [80] Zaikin, A.N. and Zhabotinskii, A.M., 'Concentration of Wave Propagation in a Two-Dimensional Liquid phase Self-Oscillating System', Nature, Vol. 225, pp.535-537, 1970.
- [81] Zhabotinskii, A.M., 'Periodic Liquid Phase Oxidations' Dokl. Akad. Nauk SSR. Vol.157. pp.362-365. 1964.